2004

Short-term performance of a newly developed connection for use in precast double tee systems.

William D. Tape
University of Windsor

Short-Term Performance of a Newly Developed Connection for Use in Precast Double Tee Systems

by

William D. Tape, M.A.Sc., P.Eng.

A Dissertation
Submitted to the Faculty of Graduate Studies and Research
through The Department of Civil and Environmental Engineering
in Partial Fulfillment of the Requirements for
the Degree of Doctor of Philosophy at the
University of Windsor

Windsor, Ontario, Canada

2004

Your file Votre référence
ISBN: 0-494-00024-4
Our file Notre référence
ISBN: 0-494-00024-4

ABSTRACT

The focus of this work was to investigate the effectiveness of using advanced composite materials to enhance double tee to double tee connections in regions of significant seismic and lateral load. This work stems partly from the unfortunate losses experienced during the 1994 Northridge California earthquake. Moreover, this work was also developed from discussions with a local precasting company, which is concerned about premature failure of the connection due to stress concentrations. The author contends that the current connection method, intermittent welded plates, does result in stress concentrations, which can effect the system's overall performance.

The proposed connection was formed by using a grouting material in conjunction with CFRP (Carbon Fiber Reinforced Polymer) fabrics, placed at +/- 45° from the axis of the joint under consideration. It is believed that this connection will not only enhance the system's diaphragm action and reduce stress concentrations in the connectors currently used, but it will also enhance the system's load distribution mechanisms.

At the University of Windsor a special set of experiments were conducted in the Civil Engineering Structures laboratory. These experiments were conducted at a 1:4 scale based on reviewed, full scale plans from a local precasting company. These experiments involved testing of two connected double tees with various connection designs. The tests conducted included dynamic analysis and ultimate loading. The experimental work was verified using a Finite Element Model.

Overall, the proposed composite connection performed well and has proven itself suitable for repair and new construction works. It should be noted that this connection's performance is only known for the short term, thus long term effects are not yet know. This dissertation includes a discussion of design considerations and recommendations for future work. Also provided is a new connection design that enhances double tee to double tee connections in terms of both gravity and seismic loading.

To my wife Ana and my children for their understanding, love and support

ACKNOWLEDGEMENTS

I would like to extend my most heartfelt thanks and gratitude to my Advisor Dr. J. B. Kennedy and Co-Advisor Dr. M. K.S. Madugula for their invaluable guidance and support throughout my work on this dissertation.

I would also like to offer my thanks to my doctoral committee, Dr. N. Zamani, Dr. B. Budkowska, and Dr. R. Gaspar for their time and support. Special thanks to Dr. Zureick for taking the time to be a part of my committee.

To Mr. Richard Clark and Mr. Lucian Pop I would like to extend my deepest gratitude for all of their assistance during this work. Without their devotion, abilities, professionalism, and support, work of this scale would not have been possible. Furthermore, thanks are extended to Mr. Patrick Seguin for all his hard work in preparing the instrumentation for this work.

I would also like to thank Dr. F. Ghrib and Mr. Colin Novak for their assistance in developing the dynamic test setup and other aspects of the testing procedure. As well, Dr. Hearn is thanked for her help in developing the testing method for determining the CFRP development length.

Thanks are also extended to Mr. Rob Dumouchelle, of the University of Windsor's Technical Support Center, for his contribution to this work. As well, special thanks to Mr. Bruce Durfy, M.A.M.E., for his assistance during the physical testing phase of the work

I would like to offer my thanks to Mr. Rob Mavrinac of the Faculty of Engineering for all his assistance during the FEA modeling.

Thanks are extended to Mr. Vince Aleo, P.Eng. for his assistance in obtaining corporate support for this research. Special thanks are also extended to Dr. S. Wood of the University of Texas in Austin, for her help and the furnishing of figure 7.1.

I would like to extend a special thanks to all the companies and individuals that supported this work through time, materials and special considerations.

- I would like to thank J. Santarossa and Sons Ready Mix Concrete and Mr. Anthony Santarossa (President) for their generous donation of all the concrete materials, a casting area for the specimens, and use of their equipment.
- I would like to extend great thanks for the technical support, relating to the composite materials, the donation of the epoxy materials, and favorable pricing of the composite materials to Sika Canada and Mr. Mark Crozier (Technical Sales Representative).
- I would like to thank WJ Steel and Mr. Robert Rea (Vice President) for the use of their truck as well as the favorable pricing of all steel materials required for the specimens.

- I would like to thank Stelwire and Mr. Nick Muzak (Research Supervisor), for the donation of the prestressing cable used in the experimental phase of the work.
- I would like to extend my appreciation for the donation of equipment rentals during the casting phase of this work to Battlefield Equipment Rentals (Windsor Office) and Jeff Puyda (Rental Manager).
- I would like to extend my thanks to Mr Ezio Tartaro of Gintar Contractors and Mr. Chris Thompson of Windsor Wall Form, for their help in casting the models used during the experimental phase of this work.

The contributions of other companies such as ATI Building Materials of Windsor, Prestressed Systems Inc. of Windsor and Windsor Crane Inc. are also acknowledged.

Financial support from the University of Windsor and the Natural Sciences and Engineering Research Council of Canada were also greatly appreciated.

TABLE OF CONTENTS

LIST OF TABLES

LIST OF FIGURES

LIST OF SYMBOLS

Variable		Unit(s)
b	width	mm
b_{bw}	width of the bottom of the web	mm
b_f	flange width	mm
b_{tw}	width of the top of the web (measured at the flange-web interface)	mm
C	resultant compressive force	N
C_b	compressive force developed in reinforcement bar(s)	N
D	distance between centerlines of webs	mm
D_x	longitudinal flexural rigidity	kN-mm^2
D_{xy}	torsional rigidity	kN-mm^2
d	moment arm	mm or m
d_p	effective depth of prestressing	mm
F_I	inertia force at level I of multi-story structure	N
f_t	tensile strength of concrete material	MPa
f'_c	compressive strength of concrete	MPa
G	distance between adjacent members	mm
H_u	shear developed in shear connection	N
h_f	height of flange	mm
h_w	height of web	mm
K	function defined by Bakht et al.	
K_v	quantity from graph from Bakht et al. 2001	
l *or* L	length of member	mm or m

l'	length of fabric measured along the axis of the fiber	mm
l_{tj}	total length of joint for a given level of a structure	m
l_o	lap length of Carbon Fiber Reinforced Polymer (Fig. 5.1)	mm
M_u	ultimate moment	N-m
N_{DT}	number of double tee members	
N_S	number of parking spaces	
P	average weight per wheel, or applied load	N
P_u	force developed in the plane of the flange	N
R_u	resultant force developed, in the plane of the flange, at a connection	N
S	center to center spacing of shear keys	mm or m
T	resultant tensile force	N
T_b	tensile force developed in reinforcing bar	N
t	thickness of component or element	mm
V_b	shearing force developed at the connection in the plane of the cross-section	N
V_{re}	shearing stress developed due to friction and interlocking at cracks	N
V_u	shearing force, or shear force developed at the joint due to shearing in the plane of the cross-section	N
V_n	nominal shear strength	N
V_y	maximum transverse shear intensity	kN/m
w	width of a given section	mm
w_u	equivalent inertia load (uniformly distributed)	N/m
β	dimensionless quantity used by Bakht et al. 2001	
ε_x	strain along the x axis	mm/mm

ε_y	strain along the y axis	mm/mm
γ_{xy}	shear strain in the xy plane	radian/radian
θ	angle of orientation	degrees

ACRONYMS

ACI	American Concrete Institute
CFRP	Carbon Fiber Reinforced Polymer
CPCI	Canadian Precast Concrete Institute
CSA	Canadian Standards Association
FEA	Finite Element Analysis
FEM	Finite Element Model
FRP	Fiber Reinforced Polymer
LVDT	Linear Voltage Displacement Transducer
NCBC	National Concrete Bridge Council
PCI	Precast Concrete Institute
PRESSS	Precast Seismic Structural Systems

1. Introduction

1.1 General

More structures that are concrete dominate our city skylines each year. Such structures meet the ever-increasing demand for cost-savings during the construction phase, durability, and aesthetics. Unlike most building products, concrete can be easily formed into almost any imagined shape. Concrete has lent itself to meeting the needs of both structural engineers and architects.

While concrete does provide great versatility and strength, it was not the primary building material in North America before the 1950s. In 1955, almost 50 percent of all new bridge construction was structural steel, with less then 40 percent being reinforced concrete (NCBC (2004)). Such a situation can be understood as during this time steel structures could span great distances, compared to their reinforced concrete counterparts. This trend would soon change as new concrete technologies developed.

In the mid 1940s Gustave Magnel came from Belgium to North America, and lectured to US and Canadian Engineers about European Prestressing Technology (CPCI 2004). In addition to his lectures, Magnel introduced his book entitled *Prestressed Concrete*. This book attracted a great deal of interest in the possibilities available to engineers. With this newly found knowledge, the first prestressed concrete bridge was constructed in Philadelphia, PA, USA in 1949. This bridge was the Walnut Lane Bridge. The importance of this project is voiced on the Canadian Precast Prestressed Concrete Institute website, which states:

> *"The successful completion of the first bridge structure in the US with its impressive 160-ft main-span and 74-ft end span precast prestressed concrete girders inspired many engineers on both sides of the border to closely examine the properties, benefits and design methods of prestressed concrete. Over 300 engineers from 17 states and 5 countries witnessed the formal testing to destruction of an identical girder used in the main span of the bridge."* (CPCI (2004))

This project would lead to several more like it and would eventually result in the development of a new industry. The Mosquito Creek Bridge in Vancouver was the first prestressed concrete structure built in Canada, constructed in 1952. This bridge, like the Walnut Lane Bridge, is still in use today; in fact, it has been widened over the years.

The newly discovered prestressing technology provided several advantages. These advantages include limiting of cracks, economics, durability, and ability to provide a reasonable cross-section size over long spans. One of the most significant advantages of prestressing of concrete was its ability to be adapted for precast uses. That is to say the structural members, or architectural features, can be constructed off-site and shipped to the location for quick installation. It is because of these advantages that the ratio of steel to concrete bridges has greatly changed since the 1950's. According to the National Concrete Bridge Council (NCBC), in 1995 approximately 70 per cent of all new bridge construction was comprised of concrete structures, compared to approximately 25 percent in steel over the same year. Figure 1.1 shows a bar chart that compares the percentage of bridges built yearly for concrete, steel, and timber, respectively. Note that concrete, while not always a strong favourite, now holds a great deal of the market. What is also of interest is that of the 475,000 bridges found in the US, concrete bridges comprise the smallest percentage considered being deficient structurally. In fact, according to the

NCBC, only four percent of the prestressed concrete bridges are deficient. This number compares favourably with the 17 percent of steel bridges viewed as being deficient.

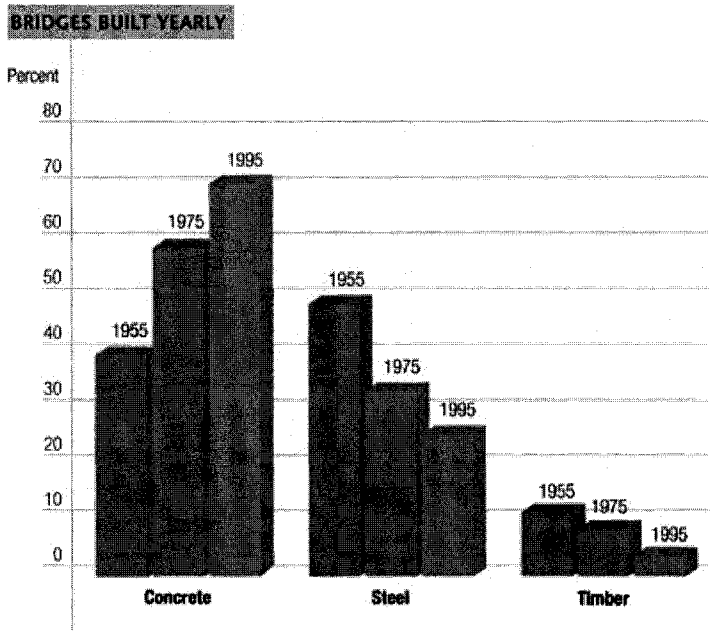

Figure 1.1: Comparison of Bridges Constructed of Concrete, Steel and Timber in 1955, 1975, and 1995 (NCBC 2004)

Precast prestressed concrete has not been restricted to bridge structures. Actually, it is frequently used in other applications. In 1960, the Grosvenor House in Winnipeg Manitoba was constructed completely of precast concrete components. This building, which was originally designed to be a cast-in-place structure, quickly became the tallest "*all-precast building in Canada*" (CPCI 2004). The concept of all precast structures quickly became an acceptable construction methodology. Since that time, several common structures as well as many famous ones, were constructed partly, or completely, of precast prestressed concrete components.

One of the most common applications of precast prestressed elements today is slab systems. Note that by "slab systems" the writer intends to encompass all decking, flooring, and roofing system applications. Actually, these slabs most often tend to act in a larger capacity than simply to provide a gravity load supporting structure. Such a system may be required to demonstrate sufficient strength and stiffness so that it may act as a diaphragm for the translation of lateral forces to the supporting vertical structure. This action is not limited to building structures alone. Such an action can also be anticipated in bridge structures. The specifics of the forces and mechanisms associated with diaphragm action will be discussed in Chapter 3.

Expanded on the concept of precast prestressed slab systems, there are several types available from the various precast manufacturers. Such slab systems/diaphragms are most commonly made using box girders, hollowcore planking, and double tee members (Figure 1.2). The box girder tends only to lend itself to large spans such as bridge structures. Cases in point are the Bear River Bridge of 1972 and Canada's famous Confederation Bridge of 1997. These large cross-section members tend to be less appropriate for building construction as there is little need for the opening found through the cross-section. Considering the hollowcore product, one is also led to the conclusion that its function is application specific. That is to say, while the hollowcore product tends to provide notable strength, its over all span length is limited. As the span increases, the need for intermediate supports increases. Such a product is, therefore, best reserved for application in buildings rather than as a key component in bridge systems. This is not to say that hollowcore cannot be used as a component of a bridge. Rather it is suggested

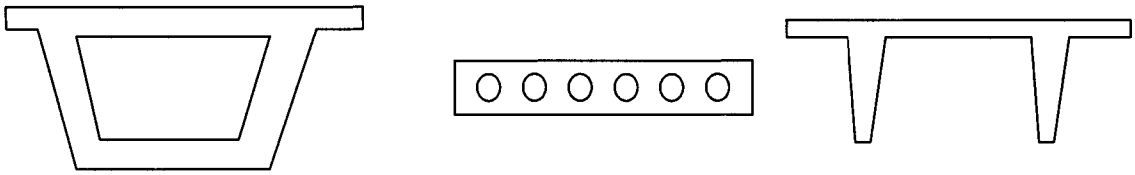

Box Girder Hollowcore Double Tee

Figure 1.2: Cross-section of Common Precast Members Used as Part of a Slab/Diaphragm System.

that it would act in a smaller capacity, compared to its larger cross-section counterparts. Finally, the double tee member tends to provide more versatility, as relates to its application. Like the box girder section, the cross-sectional properties of the double tee allow for large spans while providing an integrated slab. Such a cross-section would tend to be a favourable option for a completely precast bridge structure. An example of this would be the recently constructed Bridge Street Bridge in Southfield, Michigan. Moreover, this cross-section lends itself to several applications in the construction of buildings such as for decking, roofing, and flooring systems. Thus of the slab type precast elements, the double tee appears to provide the most diverse cross-section, as relates to applications in the region of gravity loading and diaphragm action.

The current practice of connecting a series of double tee members to each other, for the purpose of resisting lateral loads during diaphragm action, is to use strategically placed welds along the flanges in contact. The specifics of these welds, including their placement and associated reinforcement, are discussed in detail in Chapter 3. The resulting decking system may then be topped with a layer of concrete, which may or may not be reinforced. Nevertheless, this "topping" is not a standard detail and is application-

specific. Therefore, from a general standpoint, one must assume that all forces associated with gravity loading and diaphragm action are transmitted between the members via the weldments. As these mechanical connections are intermittent along the length of the flange, the development of stress concentrations is not only possible, but is anticipated.

In 1994, the Northridge, California area experienced an earthquake resulting in several catastrophic failures of precast structures. In almost every failure, the structure's ability to respond to the situation in diaphragm action was insufficient. The fact that severe damage had come to relatively new structures, in particular precast structures, tended to place substantial doubt on a precast system's ability to act as a diaphragm. When discussing the resulting damage from this earthquake, Adamo & Associates (2004) noted on their website:

> *"Six parking garages constructed of pre-cast concrete partially collapsed, due to lack of continuity that resulted in inadequate transfer of seismic forces to lateral load carrying components. Inadequate deformation capability of members intended to carry only gravity loads, and vertical ground motion, also contributed to the collapses. A large garage at the Northridge Fashion Center almost completely failed."*
>
> *(Adamo & Associates 2004)*

Figure 1.3 is a photograph of one of the failed precast parking structures. From a subsequent series of investigations into the failed precast structures, it was found that the connection between the members, forming the diaphragm, was limited to a reinforced concrete topping. While no mechanical connections were provided, it is anticipated that had these connections been present, failures would have still occurred, albeit less severe.

From discussions with a local precasting company, who manufactures double tee members, it was suggested that the concrete in and around the mechanical connection tends to fail prematurely. This situation is a point of concern for their company (personal conversation, May 2003). In fact, this situation has also been observed by the company's representatives in areas subject only to gravity loading. Yet the work of Pincheira et al. (1998) suggests that the failure of such a connection would be associated with failure of the reinforcement used to anchor the mechanical connections. Either failure of the anchorage or failure of the surrounding concrete, could result in substantial losses, irrespective of the loading conditions that caused the failure to occur.

Figure 1.3: Photograph of Collapsed Precast Structure in Northridge 1994 (NGDC 2004)

It is suspected that the mechanical connections may not yield sufficient resistance to a large ground excitation or wind load, particularly after long term use of the structure. This suspicion was confirmed by the work of Hofheins et al. (2002), who investigated welded plate connections in precast elements subject to dynamic loading. Long-term use of a structure may also result in the decay of the connectors due to exposure to such

factors as chemicals and weather. Consider, for example, the use of double tee members for parking decks. Such members are subjected to all weather conditions. In colder climates, they may be exposed to de-icing agents such as salt. While the presence of a topping would slow this process, it will not necessarily stop it. Therefore, the efficiency of metal connectors will reduce with time. This same situation may cause a reduction in the member's ability to transfer gravity loads, which may also lead to collapse in the long-term.

Due to the concerns outlined above, it is suggested that a continuous chemical/weather resistant connection be employed along the flanges of adjacent double tees. Such a connection would provide a reduction in localized stresses, and enhance the overall performance of the system in diaphragm action. Introducing a chemical/weather resistant connection affords extra protection from any environmental damage to the remaining welds. Such a connection would also enhance the overall performance of the system such that the limiting factor moves from the connection to the member itself

.

From a review of the recent literature, provided in Section 2.4, it was found that in applications where strengthening of existing concrete members is required, advanced composite materials are being utilized. In particular, most of the research is focused on the use of Fiber Reinforced Polymer (FRP) laminates, specifically using carbon fiber. This material is resistant to most chemicals and environmental conditions. CFRP has been used to repair damaged beams, slabs, and columns. No literature, which examines the use of CFRP along connections, was found.

1.2 Statement of the Problem

As noted earlier, the current connection methods such as a reinforced concrete topping or use of a mechanical connection system can result in connection failure under any loading condition, and loss of continuity in a diaphragm system due to connection failure. These topics will be addressed in detail in Chapter 2.

In order to address these problems a new connection method, using advanced composite materials, was developed during this research. This connection, referring to Figure 1.4, is comprised of a high strength epoxy filler, placed between the members, and the application of two layers of CFRP both on the top and bottom of the flange. The CFRP to be used will be a unidirectional field-manufactured composite wrap system adhearing to the concrete via an adhesive. Both materials will be provided along the entire length of the members being connected. The two layers of CFRP, both on the top and bottom of the joint, will be oriented at a +/- 45^{o} angle with respect to the longitudinal axis of the member. The reasoning for these particular angles will be addressed in Chapter 3.

It is suspected that if this new connection is used by itself or in conjunction with the existing mechanical connection, it will enhance the system's overall performance. The

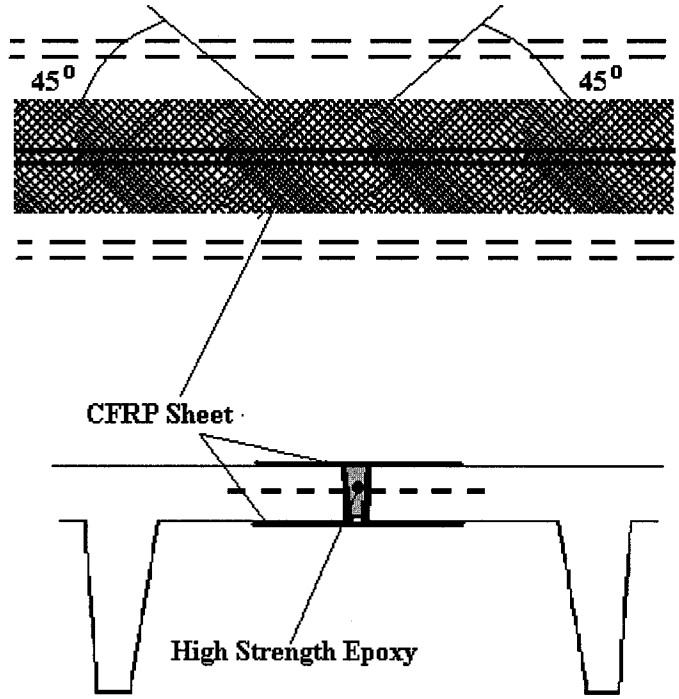

Figure 1.4: Schematic of the Proposed Connection

introduction of this connection is anticipated to create a situation that will ensure a monolithic response of the system under both diaphragm response and gravity loading. As well, this proposed connection is expected to eliminate the stress concentrations that form in the existing system's mechanical connectors.

In summary, it is believed that the proposed connection method can enhance the performance of a double tee system under both gravity, lateral and seismic loading. Such a connection would reduce the risk of premature failure due to gravity loading, as observed by others, and would prevent disastrous consequences as those seen in Northridge. As relates to the situation found in Northridge at the time of the earthquake

Dr. S. Wood of the University of Texas at Austin noted *"a better connection within the diaphragm could have saved the structures"* (e-mail correspondence, July 2004).

1.3 Objectives and Methodology

1. As the current connectors are spaced apart, it is suggested that they can result in high stress concentrations in the flange, in the region of the connector. This is of utmost concern when the member(s) are subjected to large loads, particularly seismic loads. Therefore, this situation will be investigated using both FEA and experimental techniques.
2. It is the purpose of this research to show that the current method of connecting the flanges, which involves only welding at the top flange level, does not allow the slab to act as a true two way slab system. Therefore, the system will not provide the best possible load sharing or load distribution mechanism.
3. During this research, the behaviour of CFRP fabric and high strength joint compound at the connection will be examined. This is anticipated to improve continuity between adjacent members. It is felt that this would improve the two-way action of the system, the diaphragm action, load sharing, and deflection responses between adjacent members.
4. The effect of the introduction of CFRP fabric along the interface to reduce, if not eliminate, stress concentrations in the flange, due to the connection of adjacent members, will be investigated.

For the above purposes, tests were conducted in the laboratory on 1:4 scale models of double tee members. The testing included the following:

(a) testing the existing connection

(b) testing the effects of CFRP and epoxy alone

(c) finally testing of the current connection with the addition of the CFRP and epoxy.

Each test was conducted twice for repeatability. The results of the lab work were compared with the results of a finite element analysis.

1.4 Layout of Dissertation

Chapter 2 contains a review of literature relevant to the topic of this dissertation. This chapter describes the concept and research associated with the current connection, advanced composite materials, and connection-related works.

Chapter 3 discusses the theoretical development of the proposed connection. This chapter discusses the forces associated with double tee to double tee connection, as well as, the current connection practice. A discussion is then provided to suggest the mechanisms behind the proposed system.

Chapter 4 describes the experimental setup. Information concerning the experimental facility that was used in this research, as well as a description of the systems developed specifically for this work are included. This chapter also focuses on the equipment used and the methods used for calibration of the equipment.

Chapter 5 describes, in detail, the experimental tests that were carried out in order to obtain the required data. Locations for all the gauges used to collect data are given. The experimental procedures adopted are also described.

Chapter 6 presents the results of the experimental tests. The discussion of the experimental results is also a part of this chapter.

Chapter 7 provides a cost analysis for the proposed connection. Unit costs are provided in addition to an example of a full structure. This chapter is concluded with a discussion of economic considerations, as relates to the employment of the proposed connection.

Chapter 8 presents the conclusions obtained from this work. Recommendations for future research, and design considerations are also included.

2. Literature Review

This chapter reviews all the pertinent research conducting in the past, which is relevant to this work. Special attention will be paid to the current connection methods, and problems associated with these systems.

2.1 General Work in the area of Tee and Double Tee Members

The initial focus of this review deals with past research relating to prestressed tee and double tee members. It was found that the work related to double tees is limited, compared to the available research relating to single tee members. The single tee has been the focus of work conducted by such researchers as Peterman et al. (2000), Hu and Ye (2001), and Tabsh and Nowak (1991). As the double tee section is a mirror of the single tee, the works associated with single tee members can, generally, be extended to the response of double tee members. This is not to say the double tee by itself has not been the focus of any work. Some of the works relating to double tees were conducted by such researchers as Aswad and Burnley (1991), Aswad et al. (2004), Holmes and Burnley (1997), Arockiasamy et al. (1991), Ghosh (1987), Mohsen (1990), Csagoly et al. (1986), and Savage et al. (1996). These works generally dealt a with specific application, and are thus of limited value when considering the general performance of such members.

The work of Savage et al. (1996) related to the testing of double tees with web openings. It was the intent of this work to develop a design method for these members. To begin this work a linear finite element analysis (FEA) was performed. This analysis

was used to predict areas of stress concentrations, and the effect of the number and position of the prestressing strands. The member's deflection under specific loading conditions was also considered. With the FEA completed, the test specimens were constructed.

The specimens tested were manufactured at Concrete Industries of Lincoln in Nebraska. In total, four single tees were manufactured. Single tees were used as they represent one leg of a double tee. Figure 2.1 provides the dimensions and strand placement for the models. Each member was constructed with five strands, which were 12 mm 1860 MPa low relaxation strands. Four of the strands were depressed at the quarter points, and the fifth was positioned at 600 mm above the bottom of the tee. The concrete's compression strength was 48 MPa. Of the four specimens constructed, one was a solid tee which was used for the purpose of comparison. The other three members were constructed with seven openings along their length. Referring to Figure 2.2, for the three specimens with web openings, the only variable during construction was the amount of reinforcement introduced into the zone around the opening.

The members were tested as a simply supported beam . The authors observed that prior to any loading the members exhibited small cracks, which extended from the corners of the openings. Once in place, the members were tested using large concrete blocks distributed over the member's length. As shown in Figure 2.3, the blocks were placed uniformly and symmetrically on the member. During testing, measurements of the deflection and the strain in the concrete were made. As the member approached

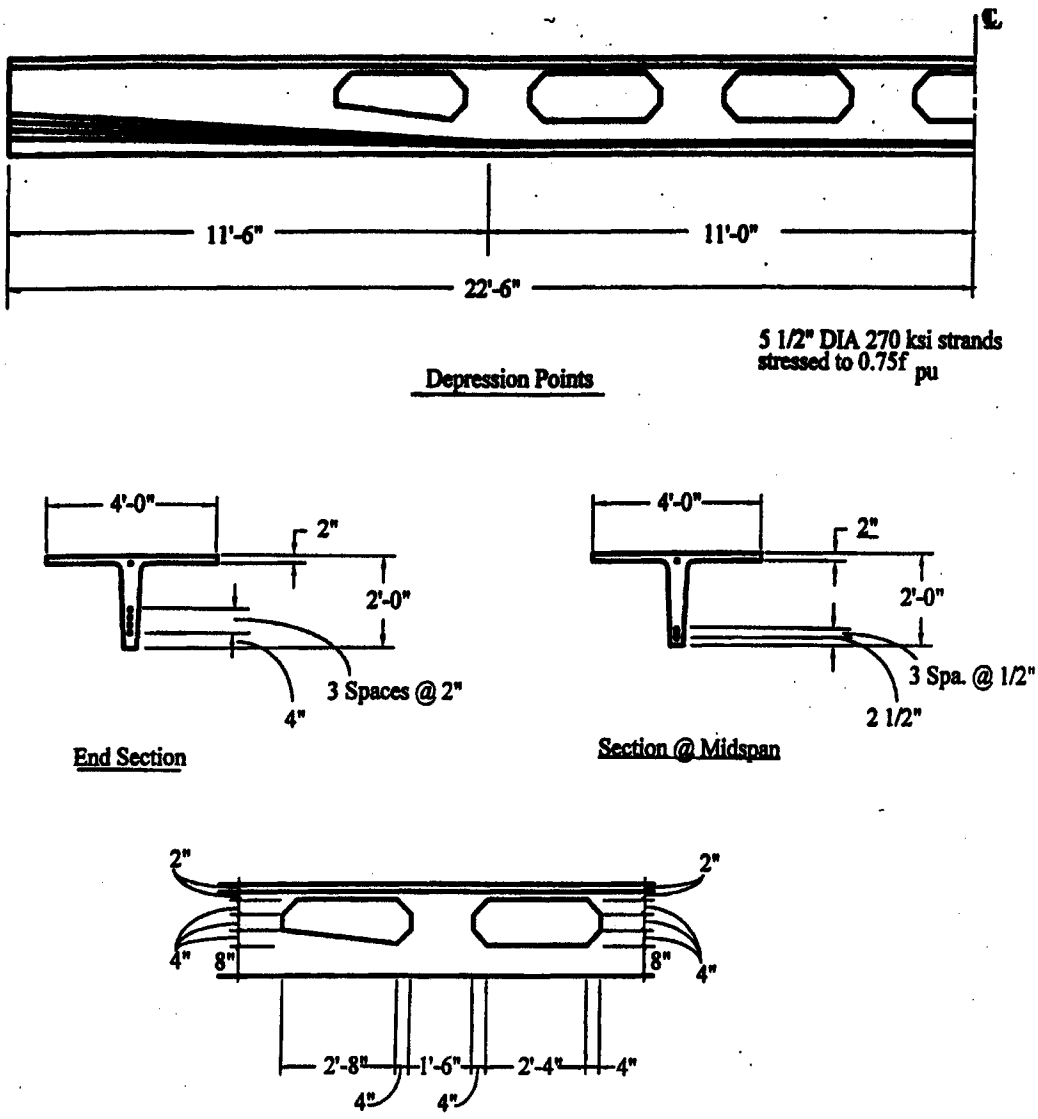

Figure 2.1: Dimensions for Specimens Tested by Savage et al. (1996)

failure, the deflections increased significantly; therefore, a tape measure was used to measure these deflections. Figure 2.4 shows a picture of tee 7G4 after failure.

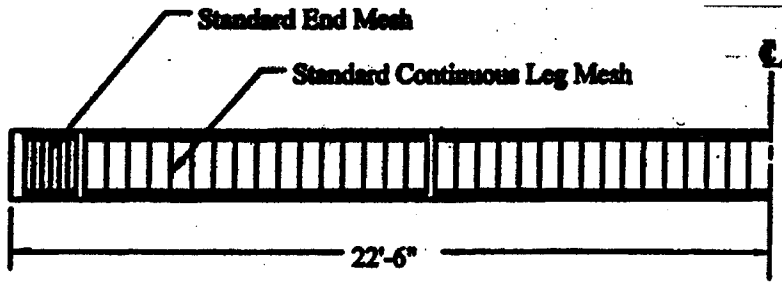

(a) Tee 7G1

Standard Leg Mesh has W2.9 wire vertically @ 7 1/2" O.C.
Standard End Mesh has D7 wire vertically @ 3" O.C.

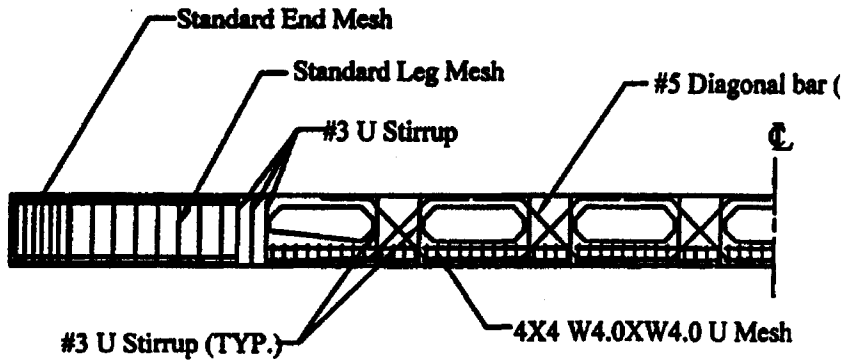

(b) Tee 7G2

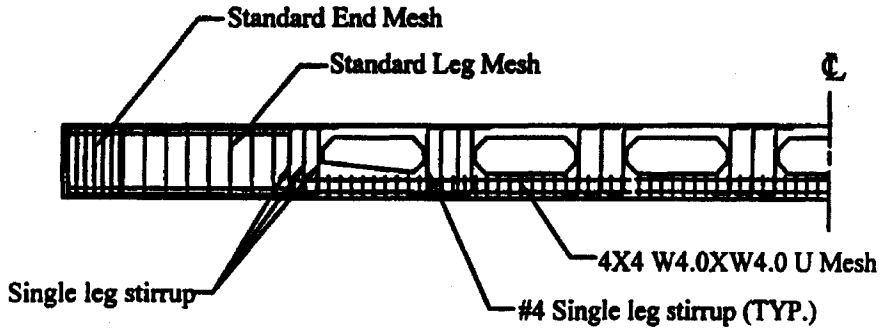

(c) Tees 7G3 and 7G4

Figure 2.2: Reinforcement Details in Tested Members (Savage et al. 1996)

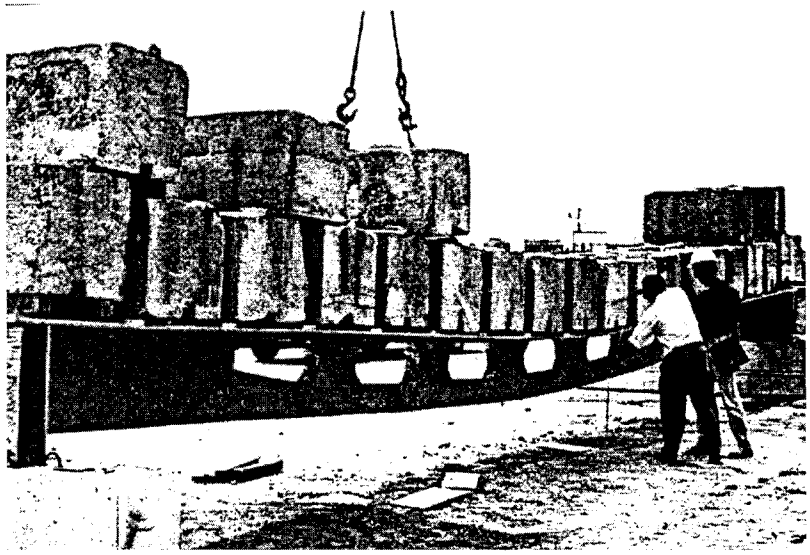

Figure 2.3: Member During Testing (Savage et al. 1996)

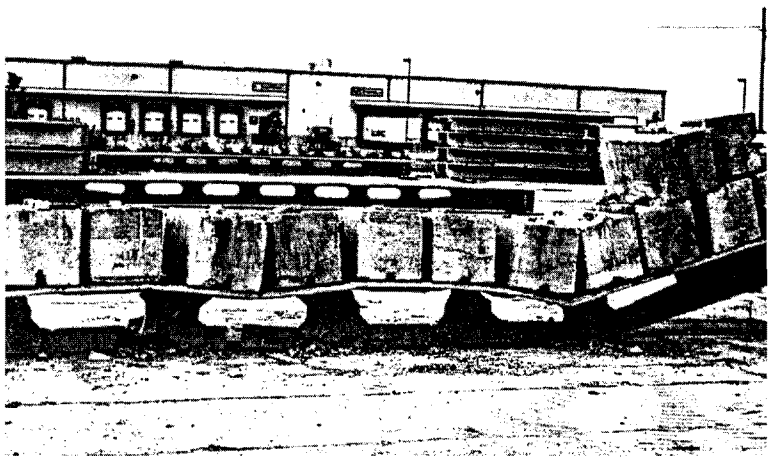

Figure 2.4: Failure of One of the Members (Savage et al. 1996)

The several observations and conclusions were made by the authors. It was found that the introduction of large web openings can be done without any reduction in strength or deflection increase, provided there is proper reinforcing. Furthermore, the results of

the FEA were favorable with respect to the experimental results up to the point of cracking of the section. It was also found that adding a prestressed strand, above the openings, proved effective in preventing localized tensile stress concentrations.

2.2 Continuity Issues in Diaphragms

A review of available literature revealed several papers in the area of diaphragm action. Some papers provided a general discussion of diaphragm action; these papers include Tai and Kulka (1977), and Pantazopoulou and French (2001). Other works found related to the response of these systems due to earthquake loading. Papers by Fleischman et al. (1998), Wood et al. (2000), Ghosh (2000), and Fleischman and Farrow (2003) (a) and (b) discuss the response of such systems.

Only a few papers that relate to diaphragm action in precast structures were available. For example, Elliott and Davies (2001) investigated the response of a hollowcore slab system, which was used as a diaphragm. The work of most interest was that of Wood et al. (2000), and Iverson and Hawkins (1994). These works, discussed in detail below, are related to the response of precast double tee diaphragm construction during the 1994 Northridge earthquake. Northridge was selected as it is an excellent example of the problems associated with weak connections. As will be discussed, joints in precast diaphragms failed, resulting in a loss of continuity in a series of diaphragm systems.

The work of Wood et al. (2000) focused solely on the response of double tee parking structures during the 1994 Northridge earthquake. The authors noted that the common failures in these structures related to buckling of the chords of the diaphragms, and development of cracks across the entire width of the diaphragm systems. These situations were accompanied by damage to the gravity load resisting systems. The authors therefore acknowledged that, had the duration of the earthquake been longer, more catastrophic failures would have been observed. They also noted that the placement of the structural walls, and the diaphragm reinforcement, influenced the seismic response of the system.

The authors made some initial observations relating to the damaged precast structures. The most common form of construction of this type involved the placement of a reinforced concrete topping over the double tee decking. It should be noted that the only connection that existed between adjacent double tees was the concrete topping; no mechanical fastening systems were employed. It was noted that before the earthquake, the topping had cracked as a result of temperature and shrinkage. As no members bridged these cracks, they increased in size during the seismic event. The reinforcement used in the topping was found to be inadequent to develop the strains required to bridge the cracks. Once this reinforcement failed, the shear strength of the diaphragm was drastically decreased.

The focus of the research program conducted by Wood et al. was to determine if precast parking structures tended to be more susceptible, with respect to other concrete

construction methods, to damage as a result of earthquakes. The authors noted that the structures in question did not perform according to the 1989 ACI Building Code assumptions. They also stated that:

> *"while it is necessary for the topping slab and precast floor members to act together to resist gravity loading, this composite action had an unintended influence on the response of the diaphragm when subjected to lateral forces."* (Wood et al. (2000))

The cracking patterns that developed were significantly different than those observed or expected of the system. They further mentioned that due to this inconsistency, the method used to determine the system's capacity was incorrect. With this knowledge, the authors conducted a parametric study of a series of idealized buildings. This study involved the variation of the overall width (33.5 m, 50.3 m, and 67.1 m), and overall length (varying from 45.7 m to 101 m, in increments of 9.15 m). Figure 2.5 shows a schematic of one of the structures considered. It should also be noted that the effects of the ramps were ignored in the analysis, as it was felt that they played no role in the vulnerabilities of the structure.

Referring to Figure 2.6, during the analysis, each of the diaphragms was idealized as a simply supported system. The maximum shear and maximum moment in each system was taken as:

$$V_u = \frac{w_u l}{2} = \frac{F_i}{2} \text{ (maximum shear)} \qquad [2.1]$$

$$M_u = \frac{w_u l^2}{8} = \frac{F_i l}{8} \text{ (maximum moment)} \qquad [2.2]$$

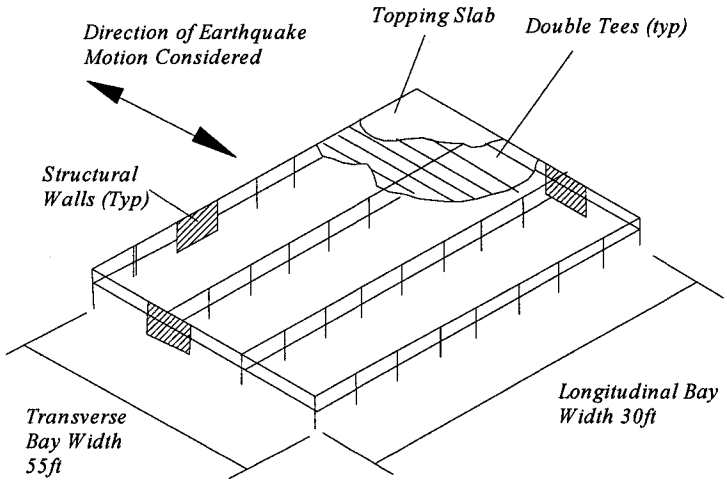

Figure 2.5 Schematic of Structure Used by Wood et al. (2000)

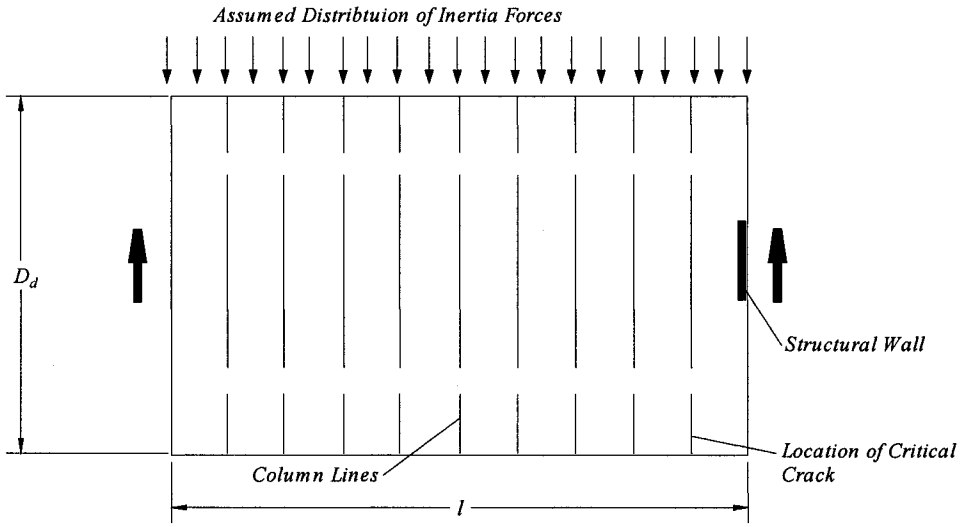

Figure 2.6: Distribution of Forces in Diaphragm Used by Wood et al. (2000)

where F_i is the inertia force at level i and w_u is the uniformly distributed equivalent inertia load. With these values, the diaphragms were designed, assuming that the diaphragm was comprised of only the topping. In the design, the contribution of the flanges of the double tees was ignored, and the strength of the concrete was assumed to be 28 MPa. Figures 2.7, 2.8 and 2.9 provide some insight into the design of the systems.

Figure 2.7 suggests that, at the ends of the diaphragms, the shear reinforcement carried none of the shear until a length of approximately 60 m was achieved. Figure 2.8 shows that for all the considered systems, the required temperature and shrinkage reinforcement was greater than that required to satisfy shear strength requirements. Finally, Figure 2.9 indicates that the shear capacity (according to ACI 318-89) at the end of the diaphragm as more than sufficient for all cases considered.

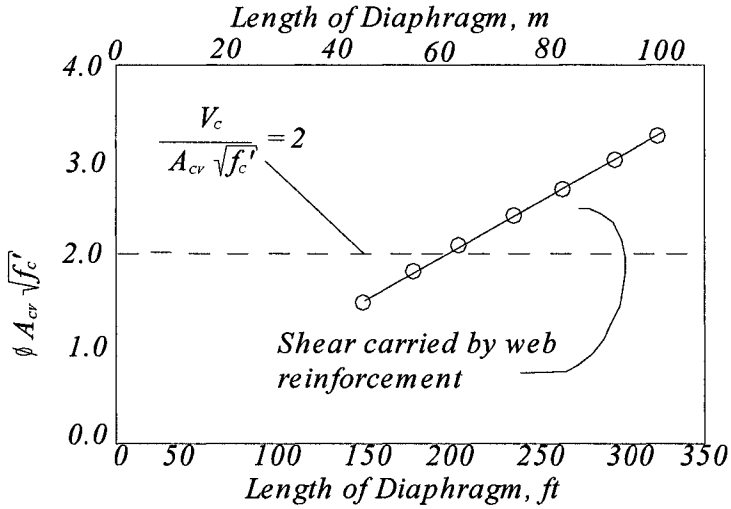

Figure 2.7 Shear Stresses Developed at the Ends of the Diaphragms (Wood et al. 2000)

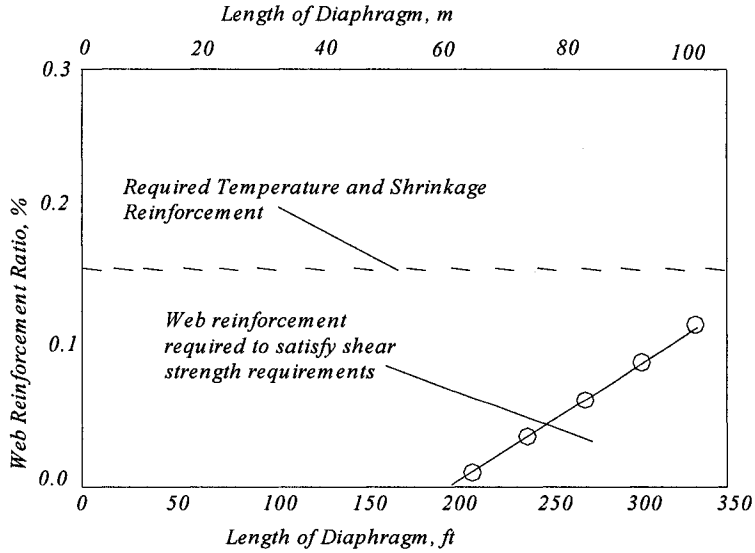

Figure 2.8 Required Area of steel for Diaphragm as Prescribed by ACI 318-89 (Wood . 2000)

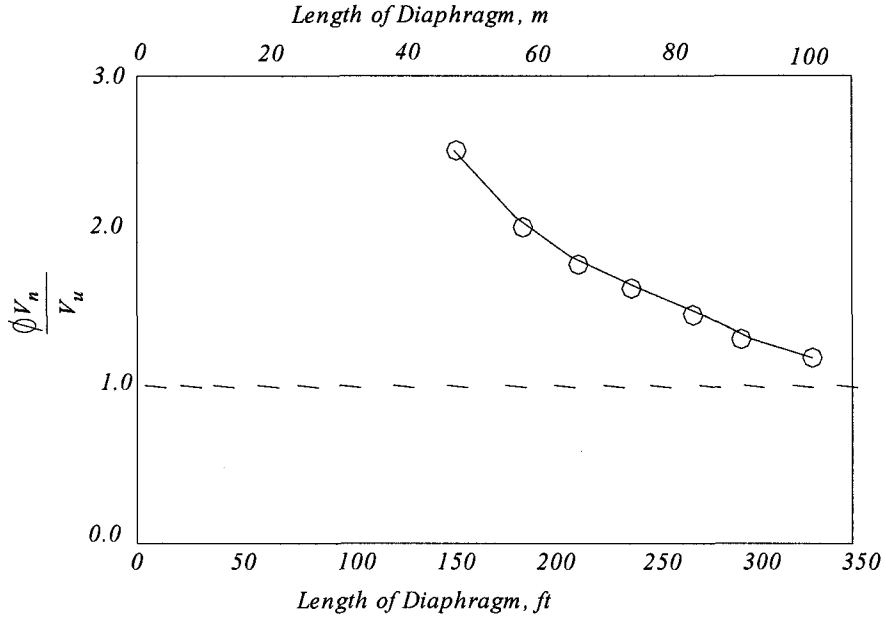

Figure 2.9: Relationship Between ACI 318-89 Shear Capacity and Design Shear in Diaphragms (Wood et al. 2000)

During a comparison of the designs, and associated failed systems, the inconsistencies were significant. Of most importance to the authors was the significant differences between the expected and observed cracking patterns. From the failures, it was observed that cracks tended to develop over the double tee to double tee joints. Yet, the expressions used to determine the shear capacity of the system assumed a significantly different cracking pattern. In particular, the codes used, at the time these structures were designed, employed an expression for shear that assumed the formation of an inclined crack. While discussing this inconsistency they noted:

> *"The transverse reinforcement in beams crosses these cracks and remains essentially unstrained until the inclined cracks have formed. However, inclined cracks did not develop in the diaphragms because the underlying precast members influenced the paths along which the cracks formed in the topping slabs."* (Wood et al. (2000))

They further mentioned that reinforcement in the diaphragm (perpendicular to the chords) did not cross the cracks that formed. Therefore, the tooled joints in the topping slab tended to open during the earthquake as no precast elements crossed at these locations. With this knowledge, the authors employed a shear-friction design method, which they felt was more appropriate to the situation.

The final stage of this work was to compare the designs given by the 1989 code, to the 1999 ACI 318 code. In the 1999 code, the definition of the nominal shear capacity of such systems had been changed, due partly to the events at Northridge. In addition, a requirement for mechanical connectors had been incorporated into the new code. Therefore, the systems were redesigned following the procedure outline in ACI 318-99. The resulting shear requirements are provided in Figure 2.10.

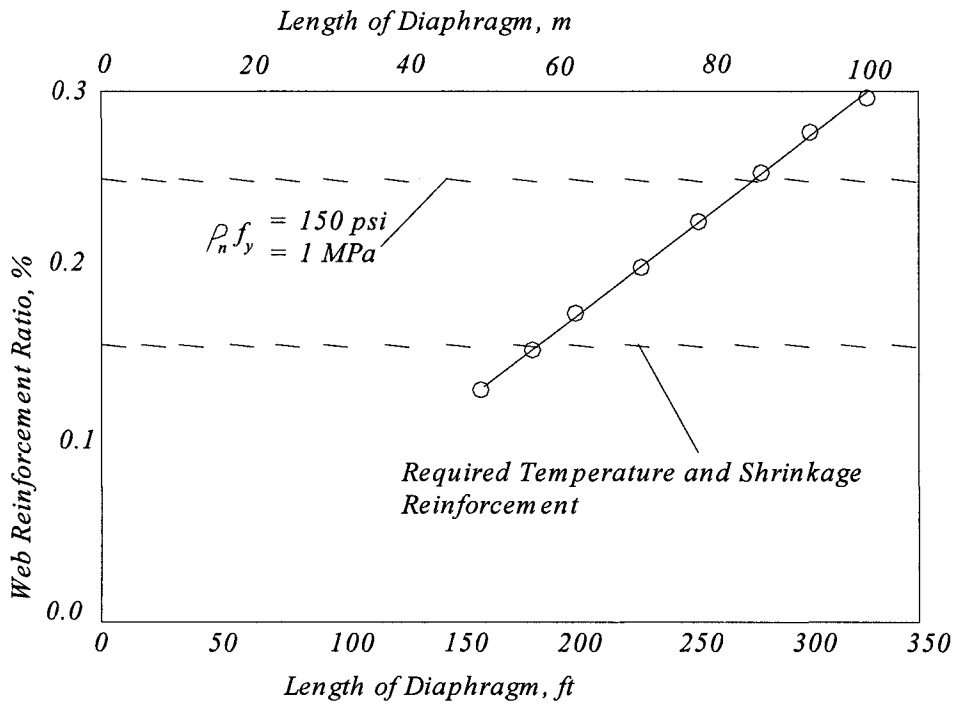

Figure 2.10 Required Area of Steel as Prescribed by ACI 318-99 (Wood et al. 2000)

Wood et al. (2000) concluded that the inconsistency between the anticipated failure and the observed failure was the main cause of the disastrous results. They also noted that the reinforcement provided did not allow for sufficient strength in order to bridge the cracks that developed.

The work of Wood et al. (2000) was not the only investigation to define diaphragm failure as a key factor in the Northridge disaster. In fact, the Northridge earthquake has been subject to several investigations, relating to the precast parking structure failures, over the past decade. These investigations were conducted by researchers such as Iverson and Hawkins (1994), Wood et al. (1996), and Fleischman et al (1998) to name a few. In all of these publications a resounding statement was made, particularly that the failures were associated with a lack of connection between the prestressed members (i.e., double tee to double tee). This conclusion is derived from a series of detailed field investigations conducted after the earthquake. Thus, the key issue as it relates to Northridge, is a lack of continuity in the system that resulted from connection failures.

The work of Iverson and Hawkins (1994) discussed their findings from a field investigation conducted within weeks of the earthquake. This investigation involved site visits to 30 parking structures in the region around Northridge, where the authors were able to enter the structures and review the damage. From this review, like other researchers/investigators (i.e., Wood et. al. (2000), Wood et al. (1996) and Fleischman et al. (1998)) noted that:

> *"one characteristic feature of several of the prefabricated and site precast garages that collapsed was an apparent lack of adequate ties connected precast floor elements to one another and to their lateral load resisting system. In at least three of the garages, it appeared that failure of the inadequate ties permitted precast members to fall from the upper levels causing collapse of the lower levels."* (Iverson and Hawkins (1994))

A similar sentiment was echoed by Adamo & Associates (2004) (refer to Section 1.1 for exact quote). Table 2.1 provides a list of load resistance system, number of stories and their corresponding damage of seven of the 30 parking structures examined. In each of these seven structures the only connection between the double tee members was a reinforced concrete topping. Iverson and Hawkins suggested that the large plan size of these parking structures, compared to other types of structures, and location with respect to the epicenter, were also factors in the collapses.

Table 2.1: List of collapsed Northridge precast parking structures (after Iverson and Hawkins (1994))

Location	**Load Resistance system**	**Stories**	**Damage**
Northridge Fashion Center South	shear walls and double tees	2	extensive collapse
Northridge Fashion Center North	same as south	2	-collapse north-east quadrant -column sheared at south end
Glendale Fashion Center	columns, shear walls and double tees	2.5	-fracture of diaphragm connections -slip of second floor
Glendale Civic Center	columns, shear walls and double tees	3	-collapse of end of fourth floor to grade - failure of top diaphragm
Coldwell Banker	shear walls, double tees	4	-displaced panels -cracks
Devon Industries	shear walls, columns, double tees	1	double tees dropped
Hamer Toyota	shear walls, columns and double tees	3	collapse of top floor

It should be noted that not all precast structures collapsed during the earthquake. In fact, Iverson and Hawkins (1994) observed that at least in six cases these systems did not collapse. These particular structures exhibited a much better performance, in terms of diaphragm response, due to the connection between the double tee members. The connections consisted of more than a reinforced concrete cover; however, it was not possible to obtain more details about these connections. It is assumed that mechanical connectors were employed in these structures, as this connection type was available and being utilised during the years spanning the construction of the structures. While all these systems did exhibit some damage, their distance from the epicentre is not known and may have played a factor in the absence of more severe damage.

The work of Iverson and Hawkins (1994) connected with the work of others led to the observation (as noted in the discussion relating to the work of Wood et al. (2000)) that the lack of connection, and inadequacies of the current design code, were the key to the failures. These problems allowed the diaphragms to fail at the connections. Once continuity in the system was lost, large inter-story drift resulted, causing failure of supporting structural elements. Pincheira et al. (1998), and Zheng and Oliva (2003), to name a few, also supported these observations and conclusions. It was these conclusions that lead to a review, and eventual changes, to the ACI design code, which now requires mechanical connection of such systems (Wood et al. (2000)) as a solution to these continuity concerns.

2.3 Investigations into the Current Connection Method

As noted in Section 2.2, the current design codes now require the use of mechanical connectors because of the Northridge earthquake. Due to this situation, these connectors have become a focus point for some researchers. Pincheira et al. (1998), Strigel et al. (2000), and Hofheins et al. (2002) have conducted work in this area. One mechanical connection investigation found dated back to 1970, and was conducted by Venuti (1970). The following section will review the results of these works. Specifically, the focus will rest on the connection's ability to reach its full potential.

The work of Pincheira et al. (1998) is of interest as it relates to the testing of double tee flange connectors. In particular, this work focused on monotonic and cyclic loading of these connections. This work was presented because of the Northridge earthquake in 1994. As shown in Figure 2.11, the connectors tested for this work consisted of a steel plate welded to reinforcing bars.

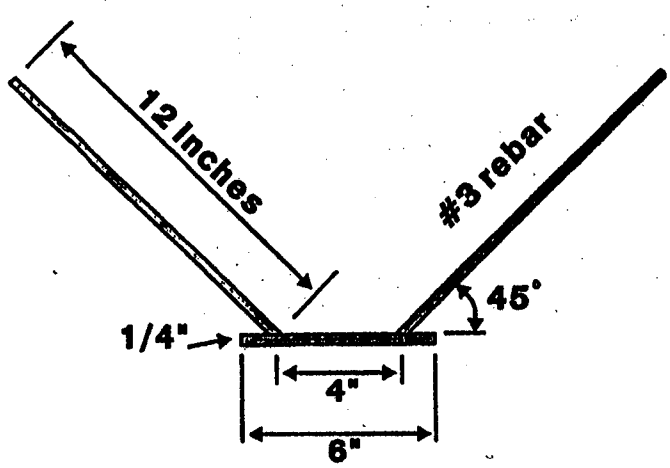

Figure 2.11 Schematic of Connector Utilized by Pincheira et al. (1998)

Referring to Figure 2.12, all the specimens used for this work consisted of a 50.8 mm (2 in.) flange, made with 35 MPa strength concrete. The connectors where embedded into the concrete with a 100 mm x 100 mm wire mesh (area of cross-section of wire = 25.8 mm^2). To connect two specimens together, a 25 mm diameter round bar was welded between two adjacent connectors. The connections where then tested.

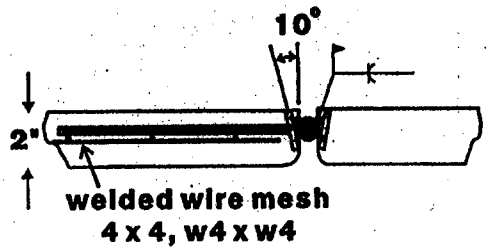

Figure 2.12: Specimen used by Pincheira et al. (1998)

The testing of the connectors involved three different loading conditions, all associated with diaphragm action. In particular, tests were conducted to investigate tension, shear, and a combination of shear and tension at a 1:1 ratio. Figure 2.13 shows a schematic of the testing. These tests were run under either monotonic or reversed cyclic loading. For the monotonic loading, the load was applied incrementally up to 75 percent of the estimated strength of the connector. After this load was reached, the specimen was subjected to given displacements until failure occurred. For the cyclic tests, the experimental conditions conformed to that prescribed by the technical committee of the PRESSS (Precast Seismic Structural Systems) program. In addition to the ultimate load being investigated, referring to Figure 2.14, measurements of relative displacement of the slabs, parallel and normal to the connector, were taken using LVDTs. The tests conducted and specimen designations are given in Table 2.2.

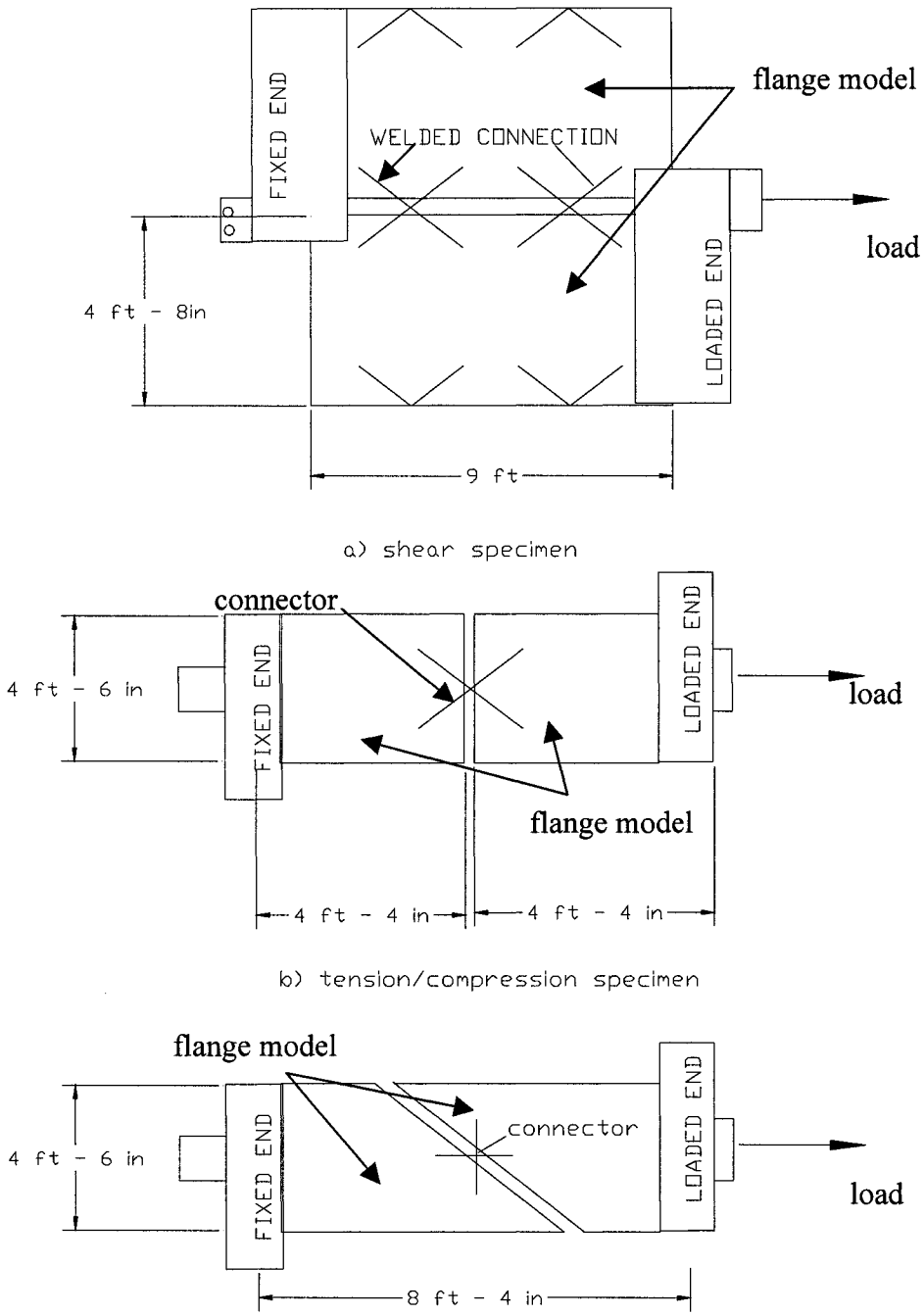

Figure 2.13 Test Setup used by Pincheira et al. (1998)

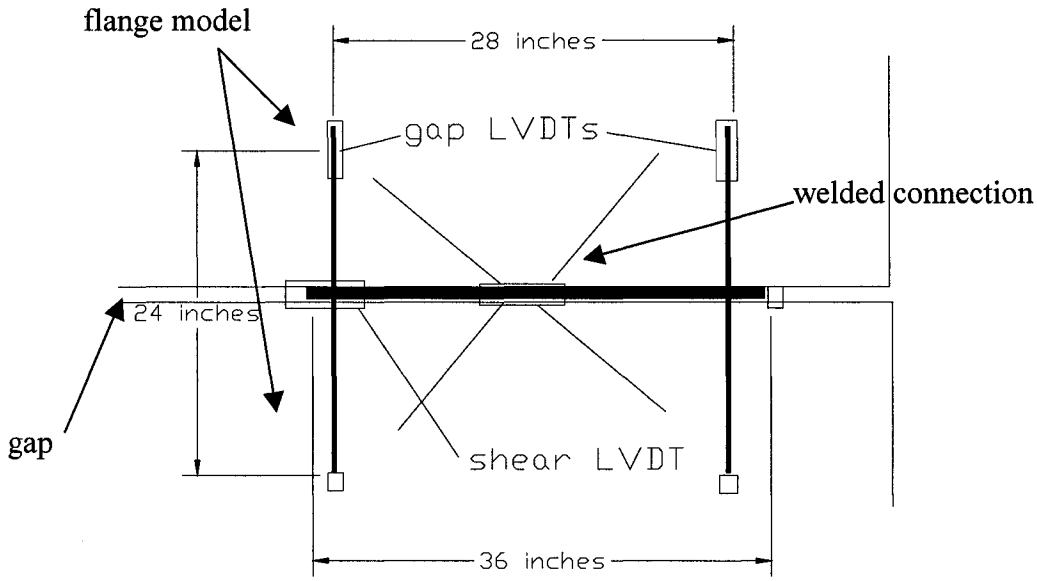

Figure 2.14: Location of LVDTs for Deformation Measurements (after Pincheira et al. 1998)

Table 2.2: Details of Tests Conducted (after Pincheira et al. 1998)

Load condition		Specimen Designation
Shear	Monotonic	MV1 MV2 MV3 MV4
	Cyclic	CV1
Tension	Monotonic	MT1
Alternating Tension and Compression	Cyclic	CT1 CT2
Shear and Tension	Monotonic	MVT1
Shear and Alternating Tension and Compression	Cyclic	CVT1

With very few exceptions, most failures were associated with fracture of the reinforcing bar on the connector. From the results obtained, the authors determined the stiffness of the system and the bond-splitting crack strength. From observations made during the testing, they also noted that cracks developed along the reinforcing bars in all specimens tested.

To investigate the performance of the welds in more detail, the authors conducted four more tensile tests under monotonic loading. Only one of these specimens failed at the weld. The remaining specimens failed due to fracture of the reinforcing bar. From these tests, the authors identified the mechanisms behind the three loading cases, shown in Figure 2.15. For the case of pure shear, refer to Figure 2.15(a). Part of the strength comes from bearing of the plate against the surrounding concrete. In addition, the reinforcing bars resisted the developed forces through shearing and flexure of the bars. Referring to Figure 2.15(b), for the case of pure tension, the reinforcement was subjected to a tensile load. This situation required the bars to develop bearing against the surrounding concrete. Finally, referring to Figure 2.15(c), for the case of combined shear and tension, the test results suggest that most of the connection's strength came from the anchorage of the bars.

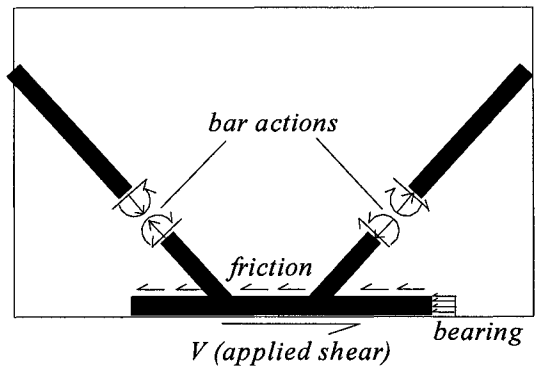

A

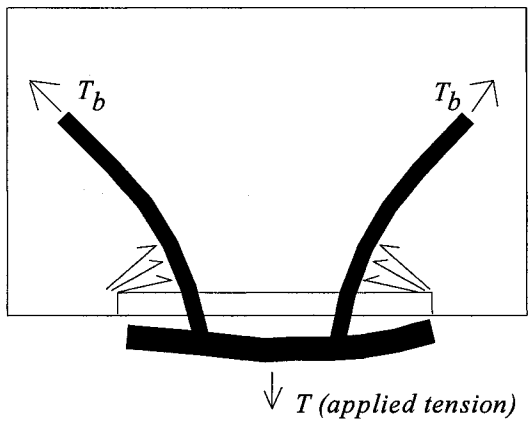

B

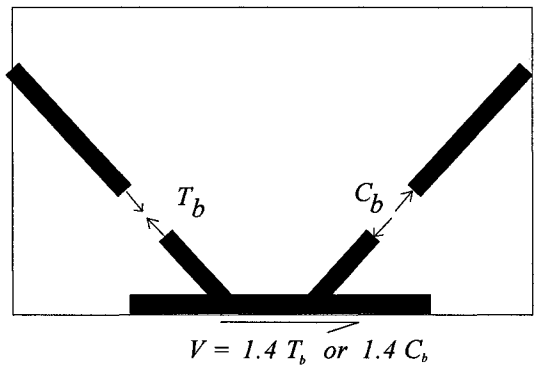

C

Figure 2.15: Mechanisms Formed to Carry Loading (Pincheira et al. 1998)

The authors concluded that under load, the regions around the connection would tend to crack along the path of the reinforcing bars. They did add that this does not seem to affect the strength of the connection. They also concluded that the deformation ductility in shear is sufficient to allow for force redistribution. This allows the connections to reach their full strength. The authors noted that further research is required to determine the effect of out-of-plane contributions. In addition, they felt that the cyclic loading cases required further investigation.

The work of Pincheira et al. (1998) suggested that for failure to occur, and thus loss of continuity in the system, the anchoring reinforcement would have to fracture. This was not the observation made by other researchers. The work of Hofheins et al. (2002), which was used as a basis for developing the current research, examined the behavior of welded connections in precast panels under seismic loading. The objectives of this work were to:

(1) identify the performance of the connection (in terms of force-deflection and ductility)

(2) check the validity of design values for such connection types. These objectives were met by use of both experimental and numerical investigation.

For the experimental work, ten wall panel assemblies were tested. The typical hollow-core precast panel used was 2440 mm (8 ft) wide and 3660 mm to 7320 mm (12 ft to 24 ft) high, with a common thickness of 200 mm (8 in.). These specimens were connected in sets of three, using two angle assemblies and a loose plate (typical detail for this type of structure, and similar to the double tee to double tee connection), between each set of panels. The loose plate was placed between the angle assemblies and welded

in place. For testing purposes, the top of the panel system was attached to a rigid member, which was attached to a dynamic actuator (capable of developing 667 kN of force in tension or compression). The bottom of the panel was pin connected. Once in place, the force was applied in a quasi-static manner, at a rate of 4.5 kN per second. Once a load of 44.5 kN was reached, the load was applied in steps of 22.2 kN until the welded connections failed. Each loading step included cyclic loading increments (to simulate the earthquake effect).

From the laboratory experiments, and supported by numerical analysis (FEA), it was observed that the connection could resist high shear loads. It was also noted that the connections provided little ductile capacity. It was found that near the 89 kN loading point, cracking started due to the embedded angle compressing the concrete. As the concrete started to crumble, the deformed anchors (reinforcing bars) on the back of the assembly failed at their welds. In fact, once the concrete in the region of the connection completely spalled off, the bearing capacity of the anchoring bars was immensely decreased, and thus the load carry capacity was lost. Moreover, from the hysteresis loops, it was noted that the system was still stable until the sudden failure of the connection, thus no ductility in the system was observed.

From both the experimental and theoretical portions of the work, the authors recommended that the connection be improved by increasing the size of the bearing area. They also suggested minimizing the eccentricity of the loads that act on the anchors. The authors concluded that the current connection type does not provide for seismic regions; therefore, the design must be improved. Furthermore, this connection type will result in failure, under cyclic/seismic loading, of the anchoring bar-plate welds. Therefore, from

this work it was determined that the welded connection method, currently employed, tends be the weakest point in the system.

The work of Strigel et al. (2000) came from the premature failure of several welds, at the connections, between adjacent double tee members. This work focused on the welding of two adjacent connectors. To stress the importance of preventing failures at the welds, the authors stated:

> *"It is important that the fracture of the bar-to-plate or slug-to-plate welds by prevented, because weld failures occur with little or no warning and because it is difficult to predict the strength of welds with a high degree of confidence."* (Strigel et al. (2000))

The preliminary study conducted by the authors investigated 36 stud-welded deformed bar anchors (DBAs). These specimens consisted of a 300 mm long # 3 deformed bar (3/8 in. dia.) welded perpendicular to a 75 mm x 100 mm x 6.25 mm steel plate. A steel plate of 75 mm x 75 mm x 6.25 mm was then welded to the back of this plate to form a tee. For testing purposes, two separate precasting companies were asked to fabricate six more specimens each. This was done to ensure a common response between those connections prepared in industry and those prepared by the authors.

The specimens, once completed ,were tested in tension in accordance with ASTM A370. These tests resulted in two different failure modes:

(1) failure of the anchor (as suggested by the work of Pincheira et al. (1998))

(2) failure of the weld at the bar plate connection (as suggested by Hofheins et al. (2002)). From these results, the authors made some recommendations about welding procedure and improved quality control, to ensure that failure did not occur at the weld location.

The much earlier work of Venuti (1970) was carried out due to concern over "*structural integrity of the diaphragm shear connectors between flanges of single- and double tees in resisting seismic shearing forces*". As noted by the author, at the time of this publication, these connectors were placed, as a rule, at 1220 mm (4 ft) spacing. For this work, experimental measurements were carried out on full scale flange specimens to determine the shear capacity of the connection.

The full scale specimens used were 406 mm wide and 762 mm to 1067 mm long, which was consistent with dimensions of a common precast tee/double tee at the time. For the connection, two methods were examined:

(1) the welding of the connecting bar (section of bar used to connect the two specimens) directly to the anchoring reinforcement (no plate is provided)

(2) welding the connecting bar to weldable steel plates (these plates were welded to the anchoring bars embedded into the concrete).

For the testing phase of the work, one side of the slab was attached to a loading head, while the other side was connected to a stationary connection. During the test, the load and relative displacement of the flanges were monitored. The specimens were loaded until failure.

From this work, the author concluded that failure of the connection was a result of yielding of the embedded bars and crushing of the concrete (because of bearing). He also concluded that the bars should not pull out if the bar is clean and the concrete has experienced sufficient vibration. Furthermore, from this work it was noted that a

substantial amount of concrete surrounding the connection failed, resulting in the exposure of the reinforcement (as noted by Hofheins et al. 2002).

Each of the above works suggest a different possibility for failure of the connection. The works of Pincheira et al. (1998) and Venuti (1970) suggest that the anchorage will fail. Yet, the works of Hofheins et al. (2002) and Strigel et al. (2000) suggest that the weld and/or surrounding concrete will fail. The observations of the latter two researchers suggest that the concrete itself may control the connection strength. If consideration is given to the observations of Venuti (1970), the possibility of the concrete failing, prior to the anchorage, is most certainly evident. The failure of the concrete hints that the current connection method results in localized stress concentrations in these regions. The presence of stress concentrations in these regions was observed by Bakht et al. (2001) and Bakht and Mufti (2001), as discussed below.

The work of Bakht and Mufti (2001) is a two-part work with Bakht et al. (2001) being the second part. As a result, these two works are presented together here. Both works focused on the performance of shear-connected precast concrete plank bridges. Such structures are commonly employed in British Columbia, Canada for use by the forestry industry. These bridges are simply supported spans of 6 to 14 m, with welded shear keys spaced at about 2 m centers.

The initial work of Bakht and Mufti (2001) focused on the load distribution on these bridge structures. As stated by the authors "*transverse load distribution in the plank bridges under consideration takes place entirely through the shear forces in the*

shear keys, which have negligible flexural stiffness themselves." (Bakht and Mufti (2001)). It is due to this situation that concern over the fatigue resistance of the shear keys was warranted. To determine the system's performance, the Ministry of Forests of British Columbia desired to obtain information about the magnitude of the shear forces that form in the shear keys. This information was obtained by testing two existing bridges. The main purpose of this testing was to determine the stress levels that develop in the welds at the shear keys.

The bridges tested in this work were the Harris Creek Bridge and East Lens Bridge. Both bridges, heavily used by the logging industry, were tested by employing a three axle dump truck. This truck was selected because it was felt that it best represented the typical logging truck. Specifics of this truck are given in Table 2.3.

Table 2.3: Specifications Relating to Truck Load

Base Length	6,735 mm
Spacing of axles in rear	1,395 mm
Front axle wheel spread	2,430 mm
Rear axles wheel spread	2,398 mm
Mass (front/back)	8,255 kg/ 20,070 kg

During the testing of each of the bridges, the truck was moved to specific location on each of the spans. Once in position, the transverse deflection profiles were observed using high precision deflection transducers. The truck's positions on both bridges are shown in Figures 2.16 and 2.17.

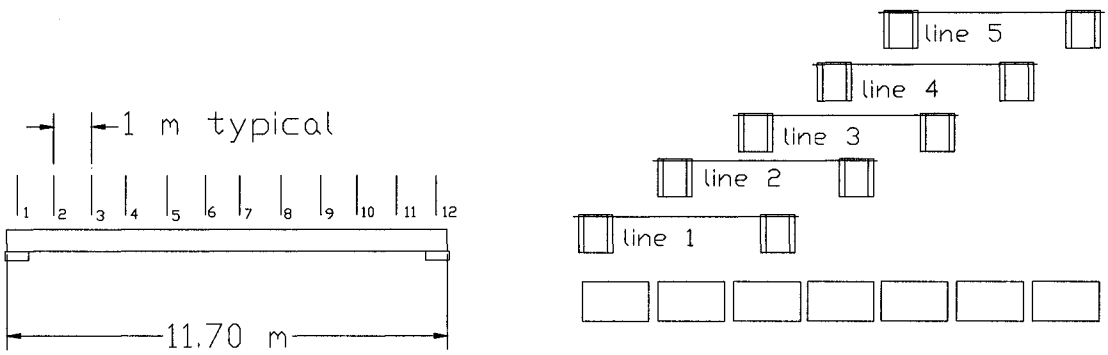

Figure 2.16: Position of the Truck on the Harris Creek Bridge (after Bakht & Mufti 2001)

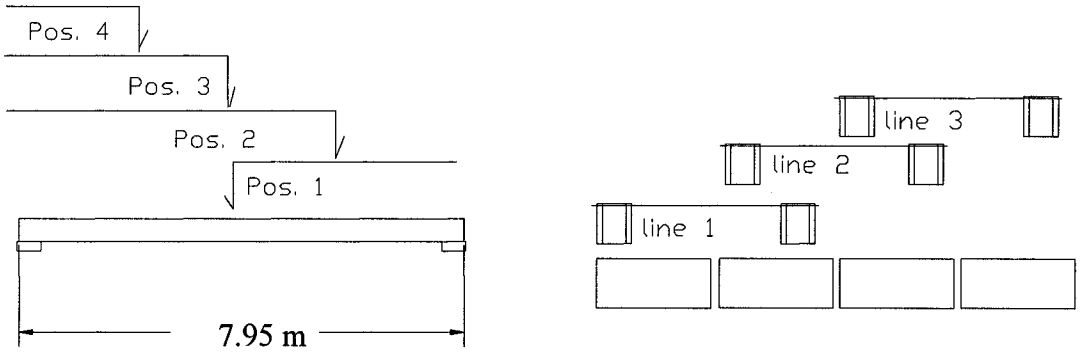

Figure 2.17: Position of the Truck on the East Lens Bridge (after Bakht & Mufti 2001)

After the testing of the Harris Creek Bridge, the transverse position versus the mid-span deflections are plotted, as shown in Figure 2.18. As can be seen in the Figure, the resulting profiles tended to provide some inconsistent behaviour. As noted by the

authors, lines one and five should have been mirror images of each other; however, this was not the case. Moreover, the profile for line 3 should be symmetric, as this position is associated with the load in the center of the cross-section. Irrespective of these inconsistencies, the authors collected ample data for verifying the results of an analytical model. It was also noted that the response of the East Lens Bridge was similar to that seen when testing the Harris Creek Bridge.

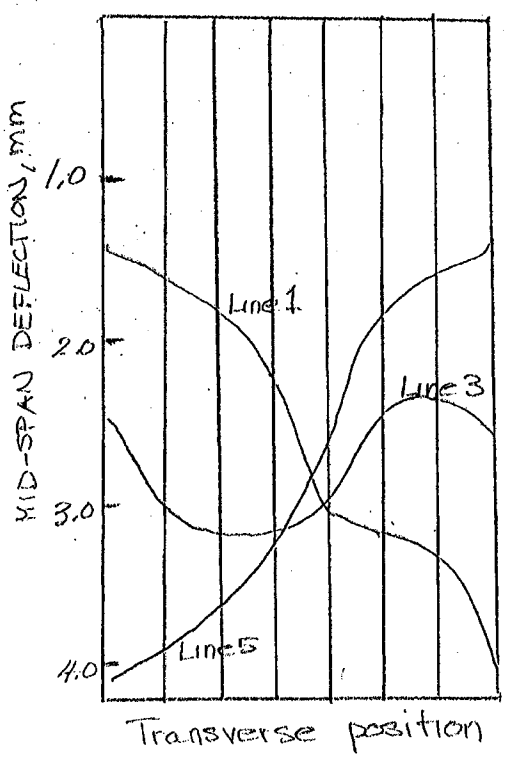

Figure 2.18: Maximum Deflection Observed on the Harris Creek Bridge (Bakht et al. 2001)

The results of the field investigation were compared with analytical models developed by the authors. These models were developed using a finite element software. In addition, another model was developed in a computer program called PLATO. The

PLATO software was selected as it is easy to use, and it is a model type used by others for the design and analysis of these types of structures. For the purpose of analysis, two loading conditions were tested. The first was associated with a single eccentric load of 81 kN, while the other was associated with the same load acting at the center of the cross-section. Figure 2.19 shows the predicted results from both models. It can be seen that the finite element software and the PLATO software agree.

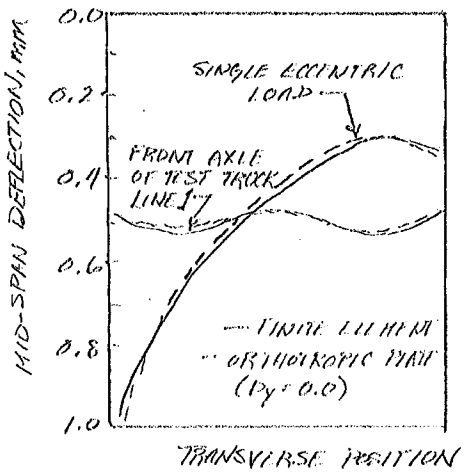

Figure 2.19: Comparison of Mid-span Deflection from Model Results
(from Bakht et al. 2001)

For the East Lens Bridge, the effect of the longitudinal torsional rigidity (D_{xy}) on mid-span deflection was compared with the observed data. Figure 2.20 shows a comparison of the observed data and computed data for line 1 and line 2 (refer to Figure

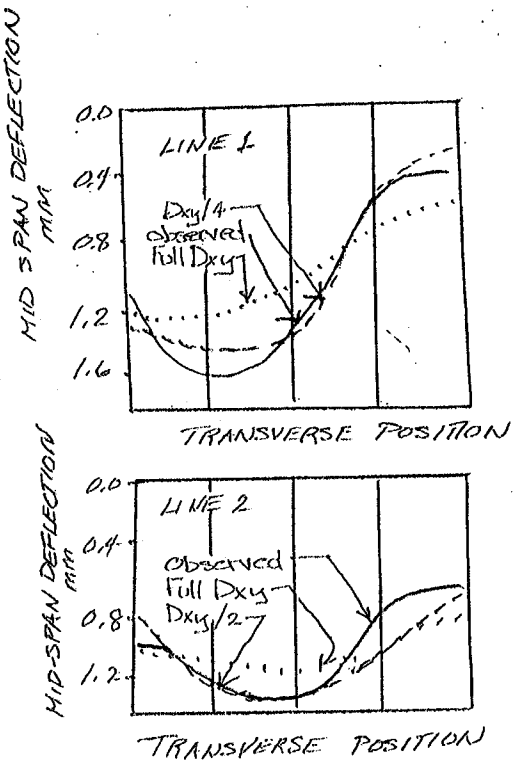

Figure 2.20 Midspan Deflection Results Comparison for East Lens Bridge (Bakht et al. 2001)

2.17). Along line 1, the model associated with $D_{xy}/4$ tends to agree favorably with the results of the physical testing; however, for line 2, the model associated with $D_{xy}/2$ tends to be more appropriate. From these comparisons, the authors felt that using half D_{xy} in a plate idealization tended to be a safe estimate.

The main focus of the work was to evaluate the welds at the shear keys for any particular bridge of this type. This phase was presented in Bakht et al. (2001). The first step for the authors was to classify the bridges into groups based on span length and number of planks. Using this grouping system, one bridge of each type was then

analyzed in order to determine the critical transverse shear. This categorization was done using a non-dimensional parameter β, which is defined as (Bakht et al 2001)

$$\beta = \pi\left(\frac{2b}{L}\right)\left(\frac{D_x}{D_{xy}}\right)^{0.5} \tag{2.3}$$

where D_x and D_{xy} are longitudinal flexural and torsional rigidity per unit width, respectively. This expression was simplified further by the authors, to give

$$\beta = \pi\left(\frac{2b}{L}\right)\left(\frac{0.383}{K}\right)^{0.5} \tag{2.4}$$

$$\text{where} \quad K = 0.333 - 0.21t/w \tag{2.5}$$

Using these expressions six plate types were identified.

For each of the six plates, a model using PLATO was developed. Each model was subjected to a load from an L-75 Truck. From these models, the critical longitudinal section, associated with the maximum transverse shear intensity (V_y), was identified. Figure 2.21 shows the value of V_y with respect to distance from the left abutment. From these analyses, the location of the maximum V_y for each case was determined. Figure 2.22 shows the distribution of V_y for two plate types. The highlighted area under the curve is associated with the force developed in the shear key, where each case assumes a shear key spacing of 1.6 m.

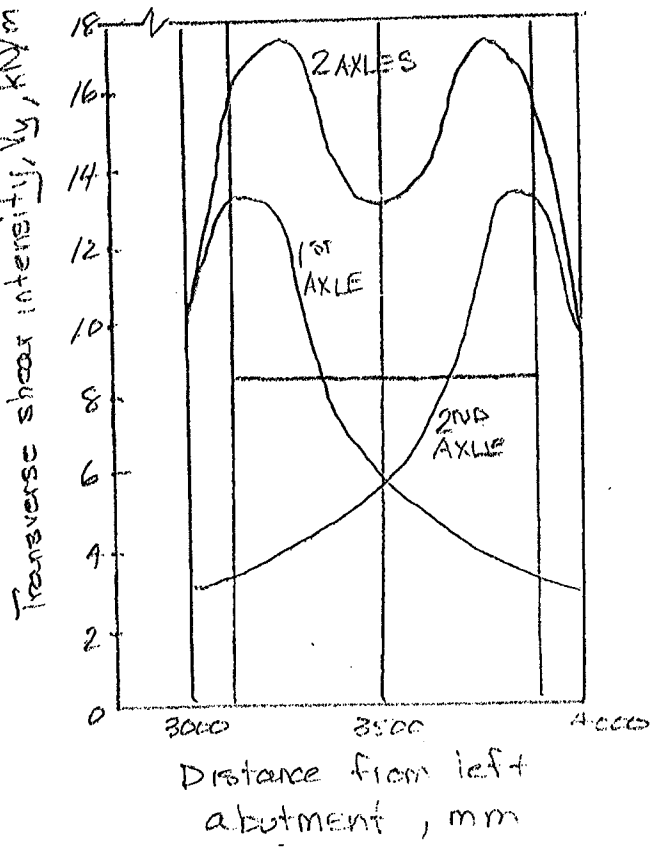

Figure 2.21: Distribution of V_y Based on the Critical Location in Plate No. 1 (Bakht et al. 2001)

From the results of the PLATO models, the authors developed a simplified method for calculating the maximum shear value. This simplified method employs the chart found in Figure 2.23 and the following expression:

$$V = S \times P \times K_V / 1.6 \qquad (2.6)$$

where V is the maximum shear, S is the center to center spacing of the shear keys in mm, P is the average weight carried by each wheel in kN, and K_v is taken from Figure 2.23.

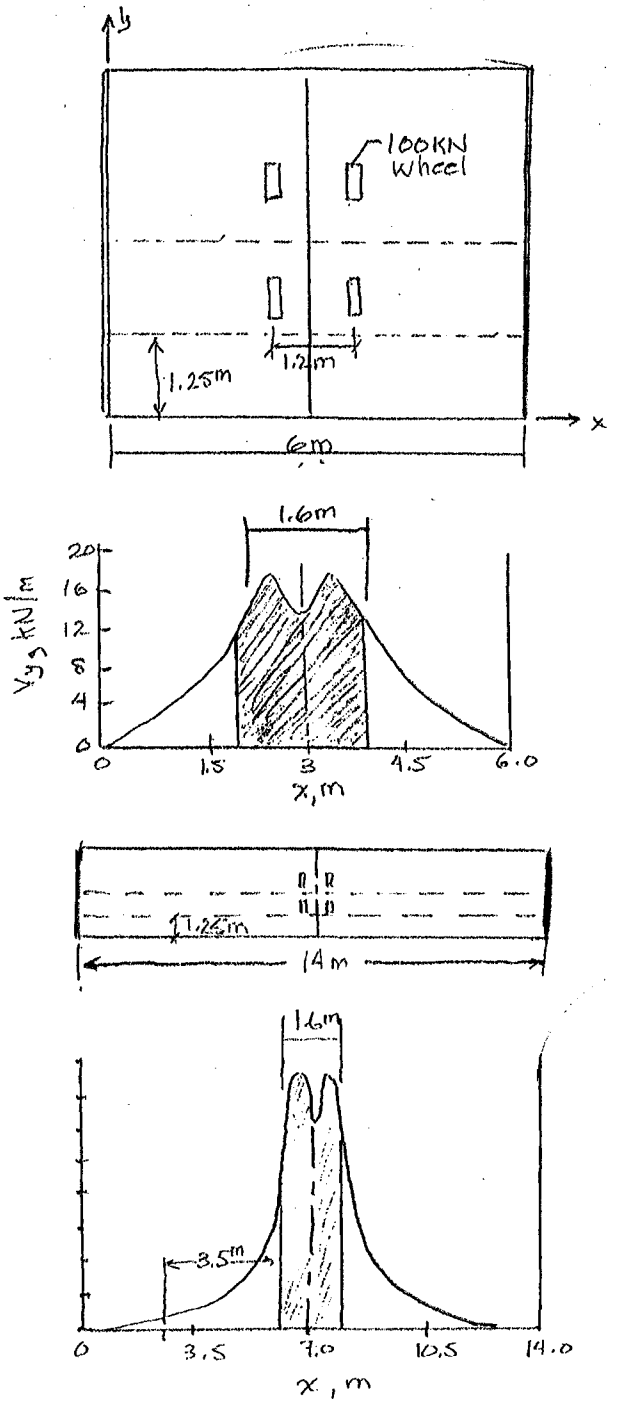

Figure 2.22: Distribution of V_y for Two Plates Examined
(Bakht et al. 2001)

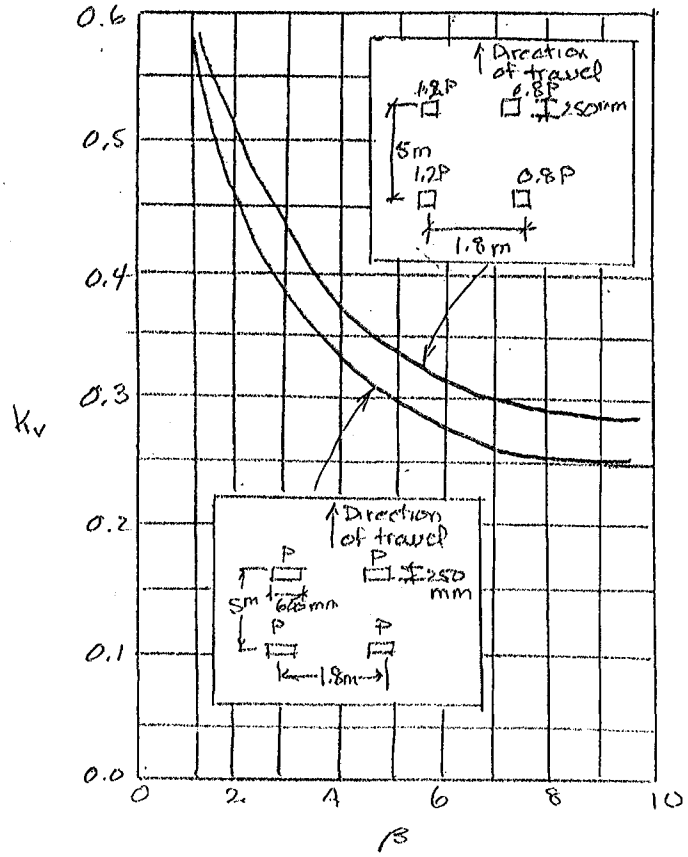

Figure 2.23: Plot of K_v vs β (Bakht et al. 2001)

Having completed the development of the simplified method, which was verified against the results of the bridge tests from Bakht and Mufti (2001), the authors concluded that the welds associated with the shear keys are not over-stressed by the logging traffic.

From all the above works it can be concluded that stress concentrations develop at the current connection locations. It can also be stated that, while not the case in Bakht et al. (2001), and Bakht and Mufti (2001), these concentrations can result in localized failure of the connection whether by failure of the anchorage or surrounding concrete.

The case of a failure occurring in the surrounding concrete, which leads to anchorage failure (Hofheins et al. (2002)), could result in loss of continuity as seen in Northridge.

2.4 Alternative Connection Methods

Some researchers have focused specifically on alternative precast connections. These investigations were conducted by Issa et al. (2003) and Arockiasamy et al. (1991), to name a few. The work of Arockiasamy et al. (1991), discussed below, was of utmost interest concerning the current work.

The work of Arockiasamy et al. (1991) is of great interest as it focused on experiments conducted on 1:3.5 scale model of transversely and longitudinally post-tensioned continuous double tee beams. The focus of this work was to determine the feasibility of using precast prestressed double tee systems for bridges with spans of up to 24.4 m. There were two objectives to this work:

(1) to study the behaviour of bridge models comprising of three double tees, joined to each other by means of a longitudinal V joint

(2) to examine the effect of the strand profile on the ductility of the member.

The members tested by Arockiasamy et al. (1991) were designed to form a two-span continuous bridge deck, which was to hold the live load of a scaled HS 20-44 truck. It was determined that the scaled truck would correspond with a load of approximately 7.41 kips (33 kN); this value included an impact factor. Because of this, the model was designed to carry a load of 35.6 kN (8000 lb). Figure 2.24 shows the strand profile used for the double tees.

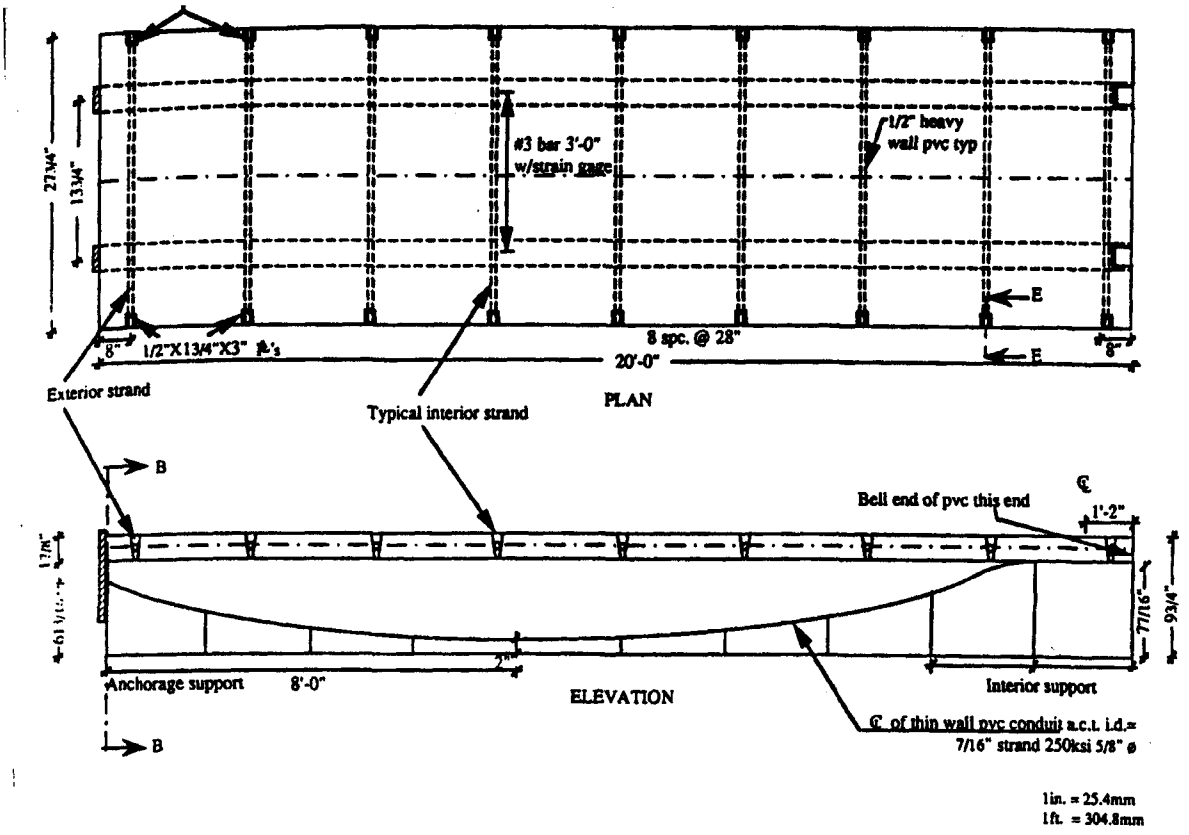

Figure 2.24: Strand Profile (Arockiasamy et al. (1991))

The compressive strength of the concrete was 35 MPa. PVC pipes were installed to provide a location to pass the longitudinal tendon through. After assembly of the bridge model, the transverse joint was grouted. It should be mentioned that the transverse joint rested over a mid-support.

The test setup used by Arockiasamy et al. (1991) can be seen in Figure 2.25. For each load position tested, shown in Figure 2.26, the model was subjected to a cyclic load at a frequency which varied between 3.2 and 4 Hz, for two million cycles. The

maximum and minimum loads that the member experienced were 35.6 kN (8000 lb) and 2.22 kN (500 lb), respectively. Measurements of the deflection were recorded during various cycles at each loading position. The members where then subjected to a static loading of up to 35.6 kN (8000 lb) at each loading location. Deflections were measured at each loading increment during the static testing. After the member had been subjected to eight million cycles of fatigue loading (two million per loading position), the ultimate load test was carried. Referring to Figure 2.27, during this final test the deflection and crack width were noted. Finally, the experimental collapse load was compared with a predicted value.

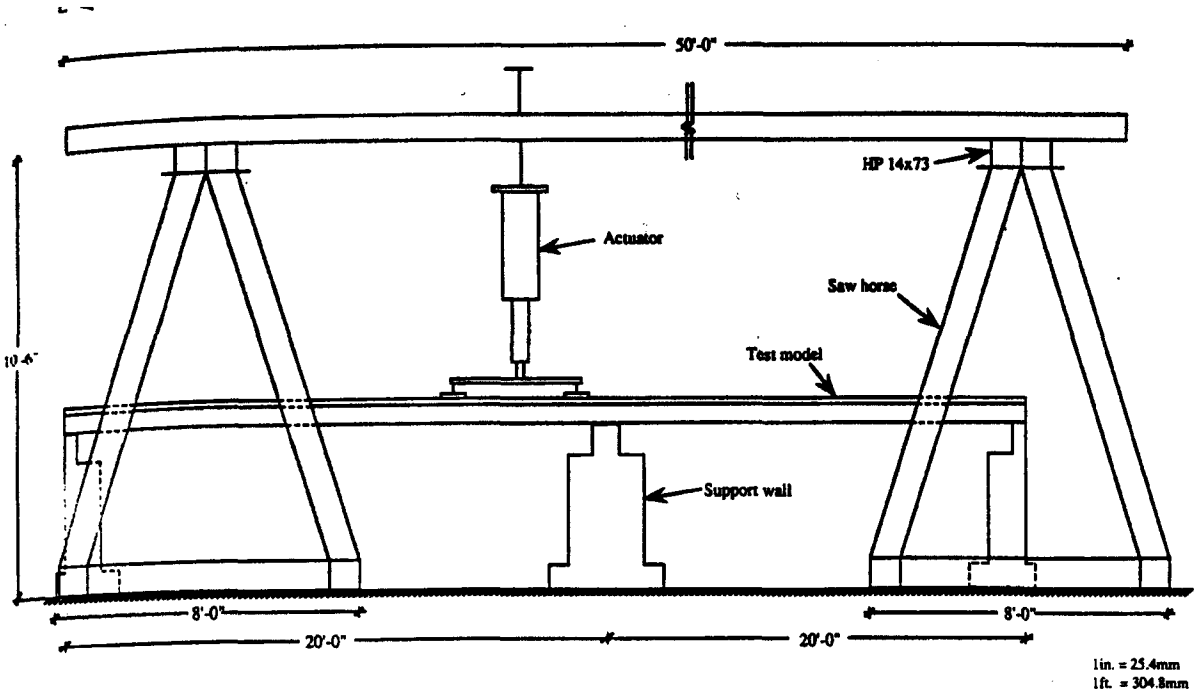

Figure 2.25: Test Setup Used by Arockiasamy et al. (1991)

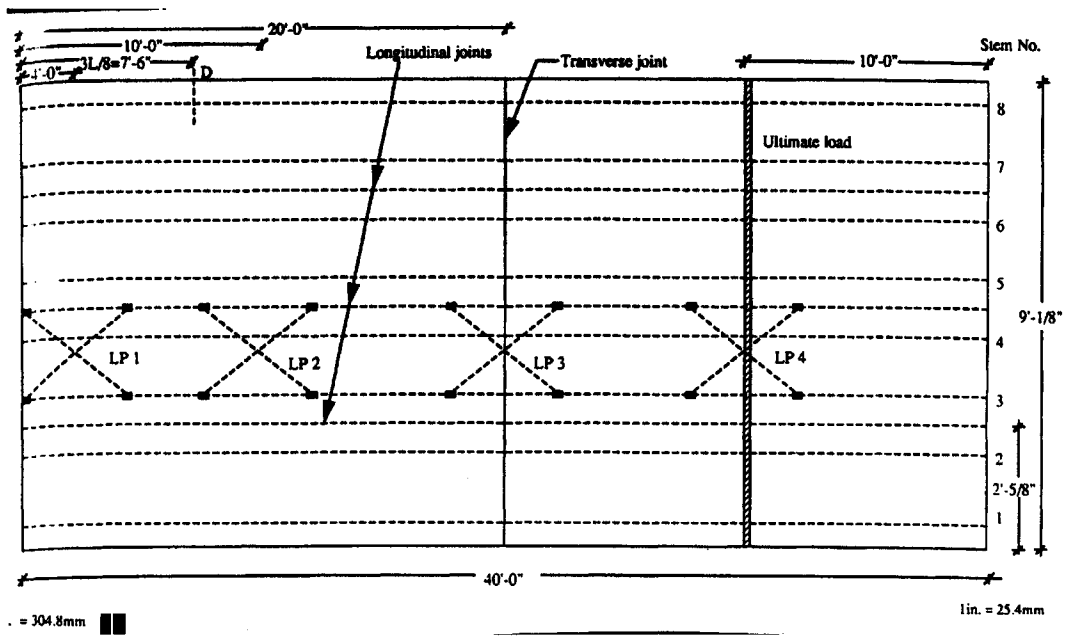

Figure 2.26:Loading Locations during Experimental Work (Arockiasamy et al. (1991))

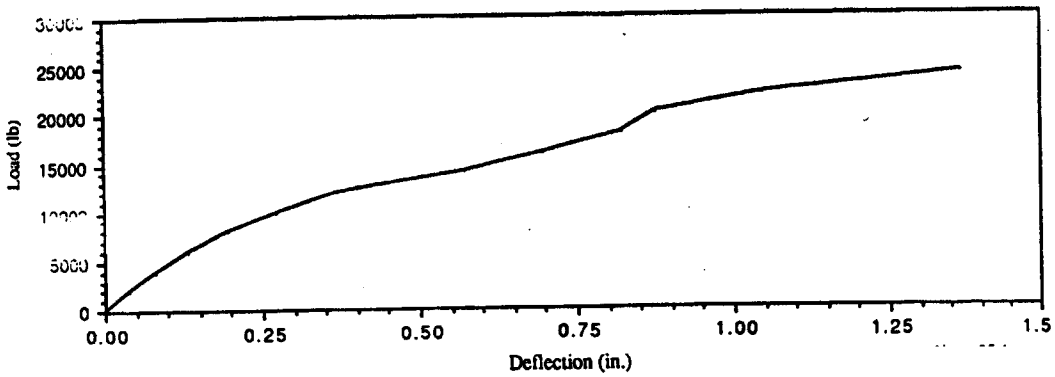

Figure 2.27: Load-Deflection Relationship (Arockiasamy et al. (1991))

The following conclusions were made from this work. It was found that a double tee bridge system assembled with post-tensioning, in both the transverse and longitudinal direction, will exhibit a monolithic behaviour under static and cyclic loading. It was also observed that after eight million cycles, there was no significant crack propagation and no

notable increases in strand stresses. Furthermore, there was no sign of any punching shear failure under any of the simulated wheel loads. The recorded deflection measurements at various stems were compared with the results of a computer model. These analytical results compared favourably with the measured values. Figure 2.28 shows the analytical and experimental results for stem 4 under load at position 4. Note that the x-axis of the graph is the distance in inches measured with respect to the center support.

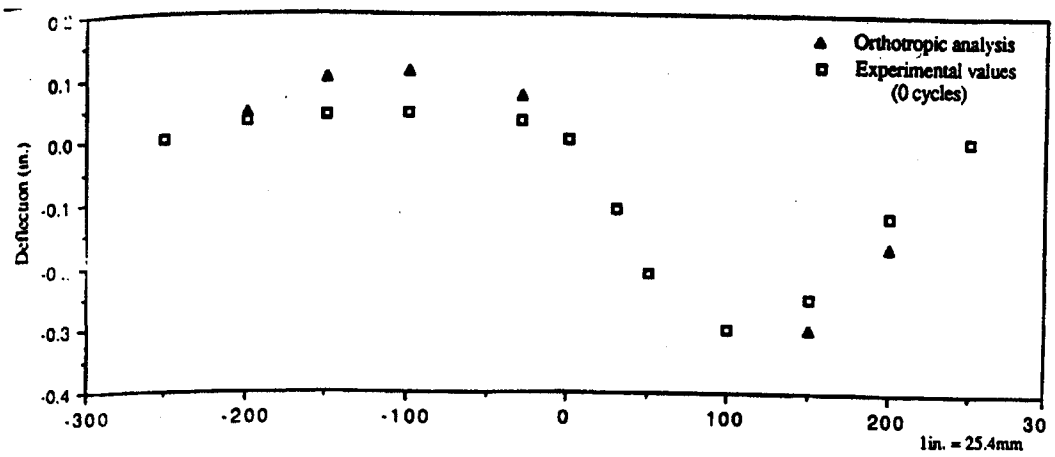

Figure 2.28: Computer and Experimental Results from Stem 4
(Arockiasamy et al. (1991))

2.5 Application of Carbon Fiber Reinforced Polymers

As fiber reinforced polymers (FRP) is the focus of the current work, a more detailed investigation into the available literature provided a number of papers relating to the use of composites in prestressed tee and double tee members. It was observed that the bulk of available literature relates to FRP bars and FRP prestressing tendons. The focus of these recent works appears to be related more to new construction. Some of the recent papers in this area are by such researchers as Zureick et al. (2003), Soudki et al. (1997),

Grace (2000), Grace and Abdel-Sayed (1996), Shahawy et al. (1996), Campbell et al. (2000) and Hamada and Fukute (1992). Unfortunately, these works are of limited value to the current investigation as they relate solely to new construction. Yet, the behaviour of FRP in reinforced concrete (RC) can be drawn from these works.

A further review of available literature relating to CFRP sheeting/laminates was undertaken. The general focus of all these research topics related to investigating the performance change of RC members/systems, by introducing additional reinforcement in the form of FRP, most specifically CFRP. Some of the most recent works are by Abdelrahman (2001), Kanakudo et al. (2001), Tan (2000), Shehata et al. (2001) and Teng et al. (2001). Some of these works are discussed below.

The work of Abdelrahman (2001) closely relates to the investigation currently being undertaken, in that it relates to modification of an existing slab system by employing CFRP. Specifically, this paper detailed the procedure and analysis used to retrofit a flat slab in an existing multi-storey building using CFRP plate. The building was originally designed for residential use only and now required modification of two floors for commercial purposes. In this case, the flexural capacity of the slab needed to be increased by 35 percent.

An initial investigation found that the punching shear capacity of the slab was sufficient for the new loading; therefore, no strengthening methods were required for shear. From the initial investigation, CFRP plates of 1.2 mm in thickness and 50 mm in

width were selected. These plates had a fiber volumetric content of 68 percent, a tensile strength of 2.8 GPa, and a modulus of elasticity of 165 GPa. The specific design procedure followed was in conformity with both ACI code 318-99, and ACI committee 440. The design also allowed for the strain in the existing steel to reach 0.005, at failure, allowing for tension-controlled sections. These criteria, in conjunction with others, led to a maximum spacing between plates of not more than five times the slab thickness, but not less than 100 mm.

During the design phase, a problem was found in the region where the plates were bonded perpendicular to the edges of the top surface of the slab. The required development length in this region was not available, and a mechanical anchor was developed. The anchor was designed to develop 30 percent of the maximum strength of the CFRP plate, while providing a factor of safety of two against anchorage failure. Another problem was found at the column slab interface. Due to the presence of the column, there was a region of up to 1.5 m in length, corresponding to the maximum negative bending moment, that did not have reinforcing other than the existing steel. CFRP could not be added to this region because of the lack of bonding length, as the fibre would have to immediately reach its maximum strength value before any bond could develop. To determine if this situation was critical, a finite element analysis was conducted. Results of the FEA showed that bonded plates in the longitudinal and transverse directions, with respect to the columns long side, as shown in Figure 2.29, reduced the stresses in the steel bars by 9 to 28 percent, thereby preventing flexural failure in this region.

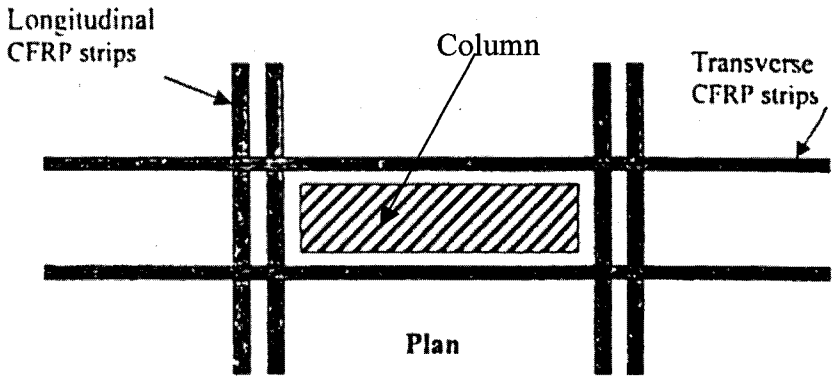

Figure 2.29: FRP Detail at Columns (Abdelrahman 2001)

After construction, a load test was conducted by placing sandbags uniformly over the largest two-bay slab. The load added was equivalent to 9.0 kN/m^2, which corresponded to 1.5 times the expected service live load, and the weight of the finishing materials. The load was allowed to deflect the slab for 24 hours resulting in a maximum deflection of 6 mm at mid-span. After unloading, it was observed that the residual deflection was 0.4 mm.

The work of Shahawy et al. (1996) relates to the present work as it investigated the rehabilitation of prestressed slab systems. It was the objective of this study to determine the amount of CFRP materials required to retrofit a slab in such a way as to provide the slab with its original undamaged strength. To achieve this objective, a series of experimental tests were conducted. For this purpose, two slab types were made in accordance with the Prestressed Concrete Institute (PCI) specifications (1996). Cross-sectional drawings of these members are shown schematically in Figure 2.30. This work involved the testing of a rectangular solid slab 4.4 m in length, and a rectangular voided slab 6.6 m in length, both of which were simply supported at the ends. The voided

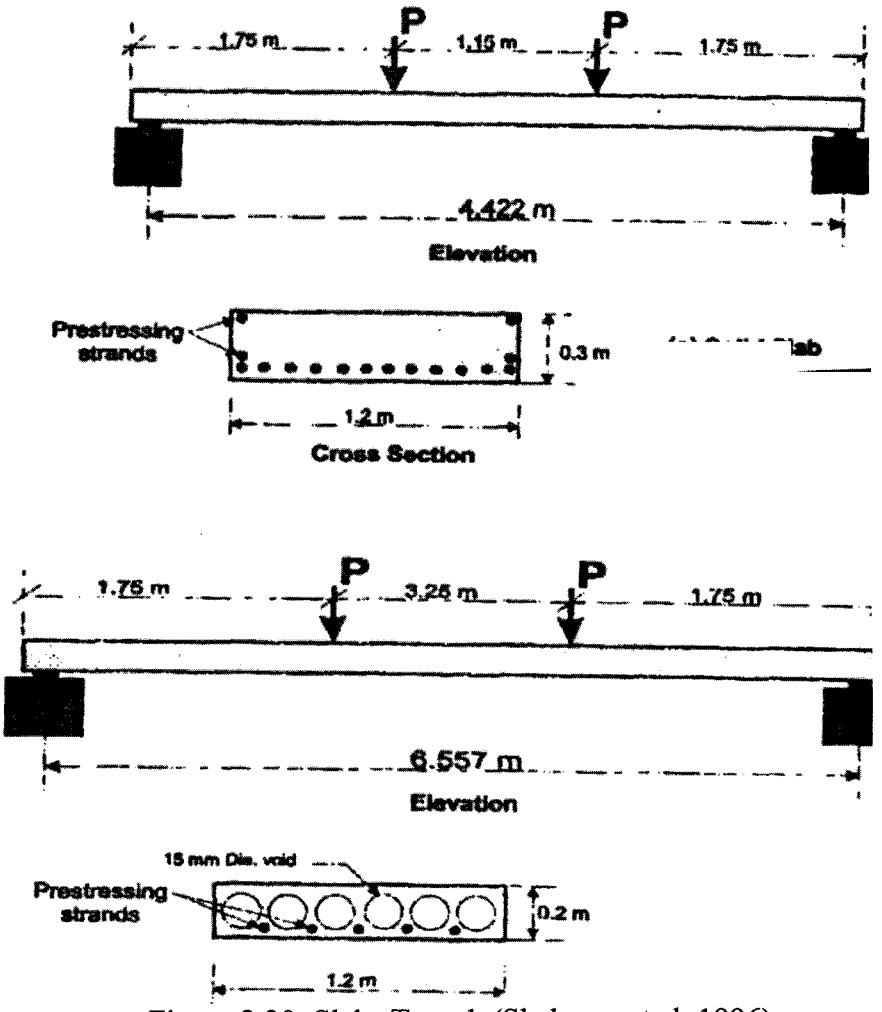

Figure 2.30: Slabs Tested (Shahawy et al. 1996)

slab was the commonly used hollowcore slab. For all tests, LVDTs were used to measure vertical displacement along the member's length, and strain gauges were strategically located. For the purpose of the tests, concentrated loads, distributed over an area, were used. The load was applied incrementally until the member reached its ultimate capacity. These members where then retrofitted with CFRP laminates (see Figure 2.31 for location of CFRP) and, once cured, these slabs were tested again in a similar manner to the original test.

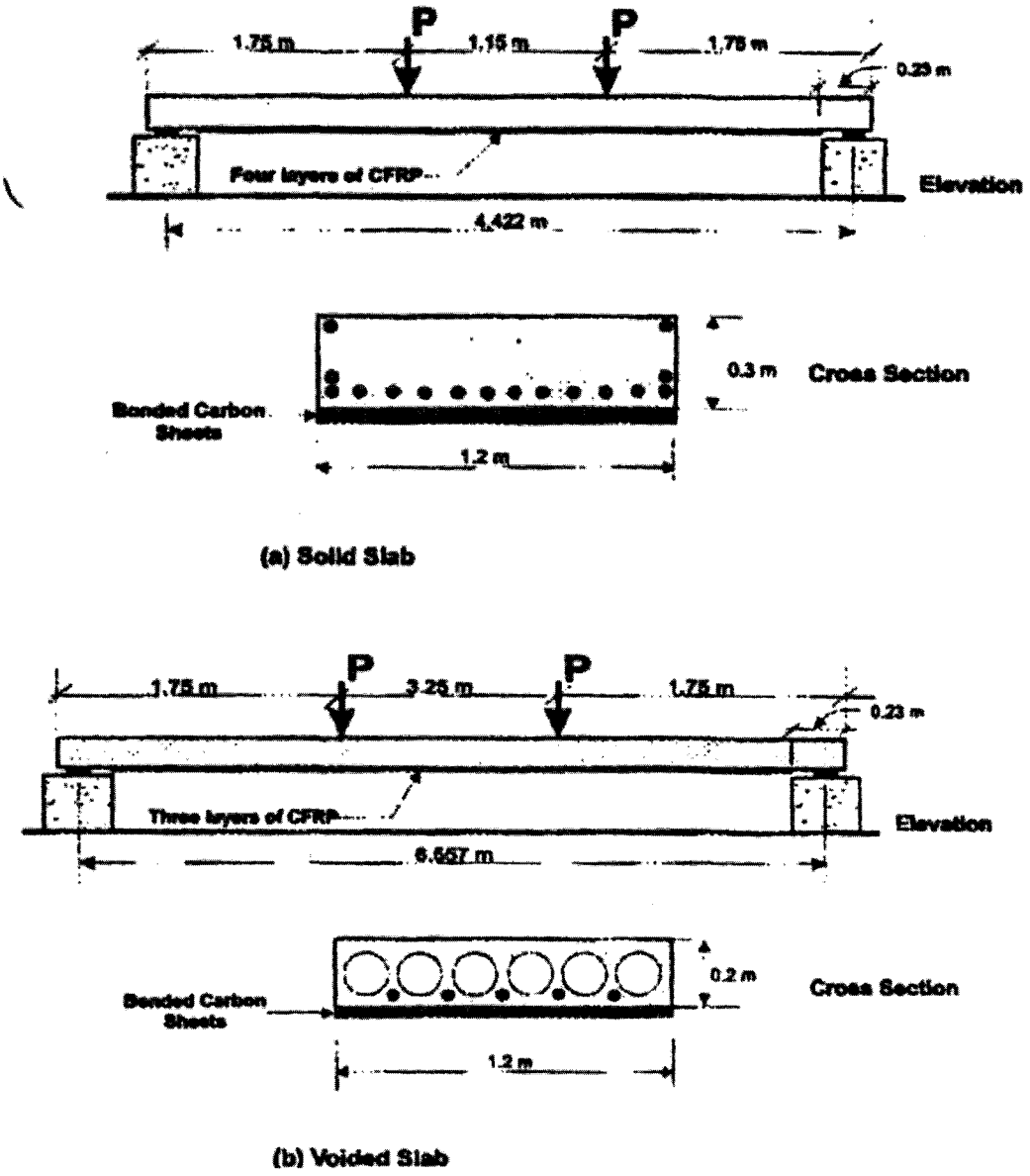

Figure 2.31: Retrofitted Slabs (Shahawy et al. 1996)

The following observations were made by Shahawy et al. (1996). It was noted that the precracked solid slab, which had been retrofitted, failed due to concrete crushing. It was also observed that the retrofitted slab recovered almost 90% of its original ultimate

moment. The retrofitted voided section exhibited an ultimate load equal to approximately 178% of the original. Furthermore, in the case of both slabs, the deflection of the retrofitted member closely resembled that of the original member. Finally, the following conclusions were made from the results:

- The failure modes of the retrofitted slab differed from the original failure mode due to the effectiveness of the repair method.
- The retrofitting of severely damaged slabs using CFRP greatly enhanced the flexural capacity of the member.
- The maximum deflection of the retrofitted slab was approximately the same as that of the original slab.

The above works can be associated with systems similar to that being investigated in the current investigation. Yet, all these works are limited to strengthening of concrete systems themselves. No research was found relating to the use of composites at precast connection locations for the purpose of strengthening the system, or reducing stress concentrations. However, the work of Antonopolos et al. 2001 and Prota et al 2001 did suggest an advantage to using composites to enhance joint strength at reinforced concrete beam-column interfaces.

3. Theoretical Development of the Connection

This chapter outlines the theoretical formulation of the proposed connection. The mechanisms behind the current mechanical connection and the proposed connection will be reviewed.

3.1 General

Frequently, floor and roof systems are required to exhibit sufficient strength and stiffness to transmit lateral forces, such as seismic and wind loadings. The system response required of the slab, termed diaphragm action, requires the system to act in a similar fashion to a deep beam. In fact, this is best stated by MacGregor and Bartlett (2000) who, when discussing this action, stated ".. *they act as deep flexural members lying in horizontal planes*".

The general assumption of diaphragm action is that the flexural resistance is provided by the chords, located at the extremes of the system. These chords can be beams, or in some cases, extra reinforcement in the slab. It can be shown that for many slab systems, the forces developed in the chords are generally low, as the moment arm between the compressive and tensile chords is large. The slab located between the chords is associated with transfer of shear forces. This situation is very similar to the design of a plate girder in structural steel design. Figure 3.1 shows schematically the general principles associated with diaphragm action.

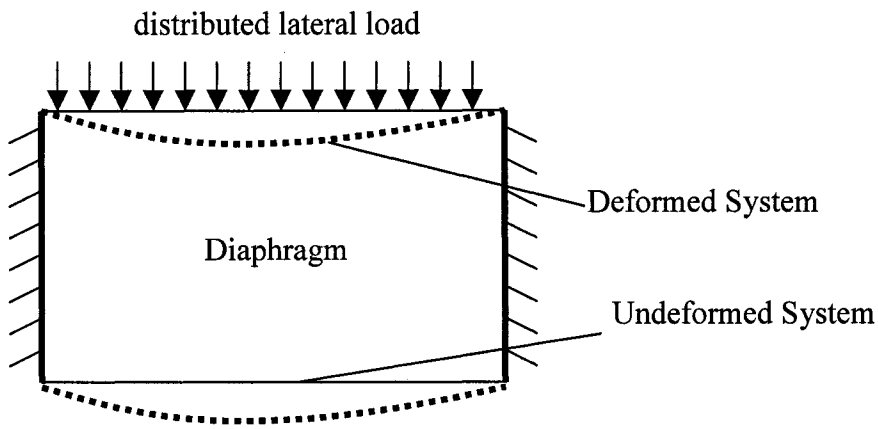

Figure 3.1: Diaphragm Action of Semi-Rigid Diaphragm

In a cast-in-place slab system, the transfer of shear between the chords is relatively simple, based on the continuity in the system. In precast structures, such as the elements being investigated in this work, the slab system is not initially continuous. This lack of continuity prevents the transfer of shear through the diaphragm. Thus, the system must be connected in some fashion to facilitate this force transfer.

3.2 Current Connection Practices

The method employed to connect the precast members must be able to resist the forces developed during the case of lateral load application. Figure 3.2 shows schematically the forces developed in a precast diaphragm system. As shown in Figure 3.2, based on the orientation of the precast members, the element to element joint must transfer the developed shear force in the same manner as a beam. This shear transfer is performed by one of the following methods:

1. A topping of reinforced concrete is cast over the newly formed slab.

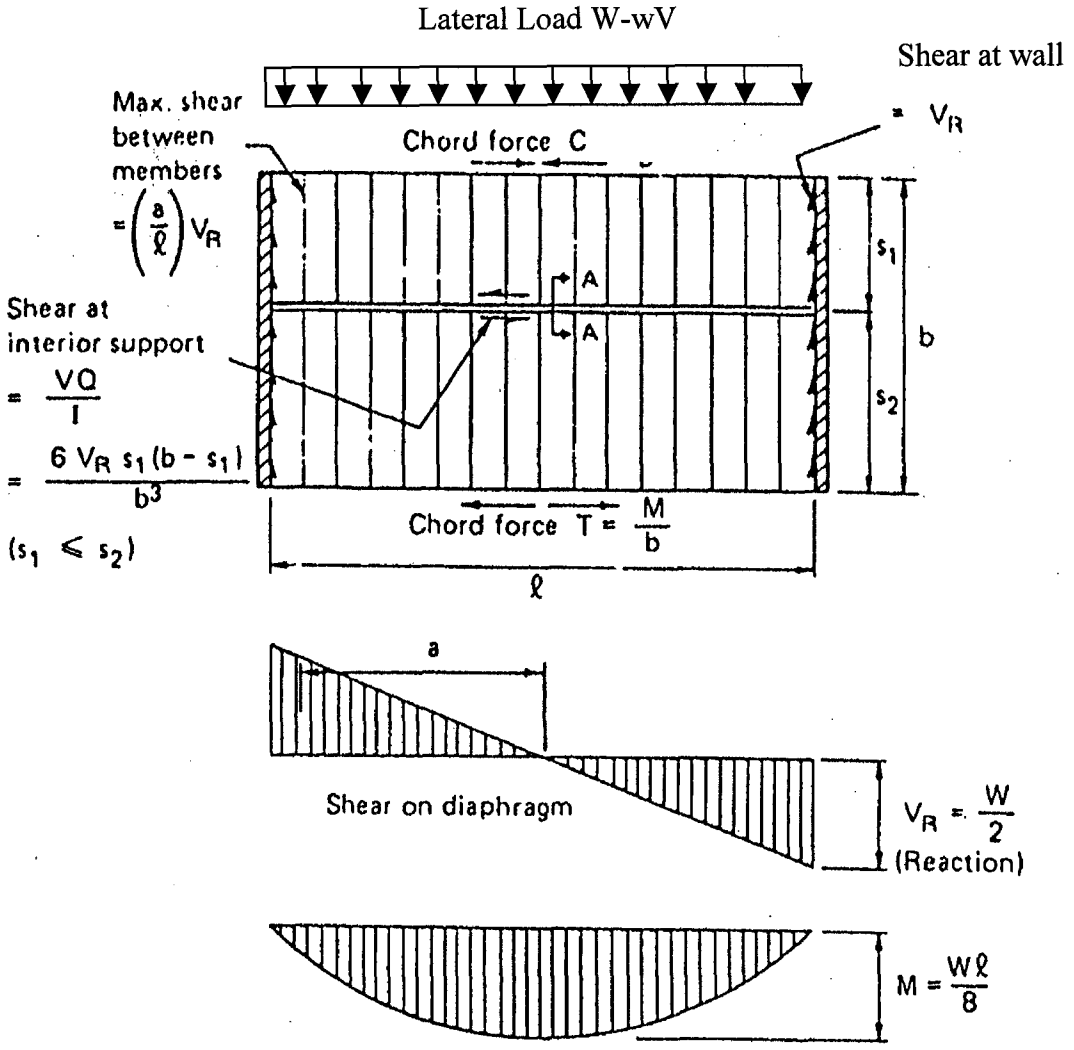

Figure 3.2: Diaphragm Action In Precast Structures (Tai and Kulka 1977)

2. Mechanical anchorage

3. A combination of the topping and mechanical anchorage.

4. Grouted keyways

Once one of the above methods is employed, the system is assumed to act as a diaphragm. The writer wishes to point out that grouting, in terms of double tee members, is not currently employed.

The first method outlined above, casting of a topping, failed to provide adequate resistance against earthquake loads during the 1994 Northridge earthquake. In fact, as mentioned earlier, Wood et al. discussed in detail the failures that developed as a result of this connection type. These failures were attributed to the inability of the topping to maintain continuity.

The second connection method, the mechanical anchorages, are commonly employed. This connection is the focus of several papers by such researchers as Hofheins et al. (2002), Pincheira et al. (1998), and Bakht and Mufti (2001). Mechanical anchorages involve the use of several "shear connectors" placed along the edge of the flange, in the region where connections are to be made. Figure 3.3 shows a schematic of a shear connector. A steel plate, or section of bar, is placed between two adjacent shear connectors and then welded in place. Once welded, these connectors must be able to resist various forces. These forces are a result of flexure and shear due to deflection of adjacent spans and diaphragm action.

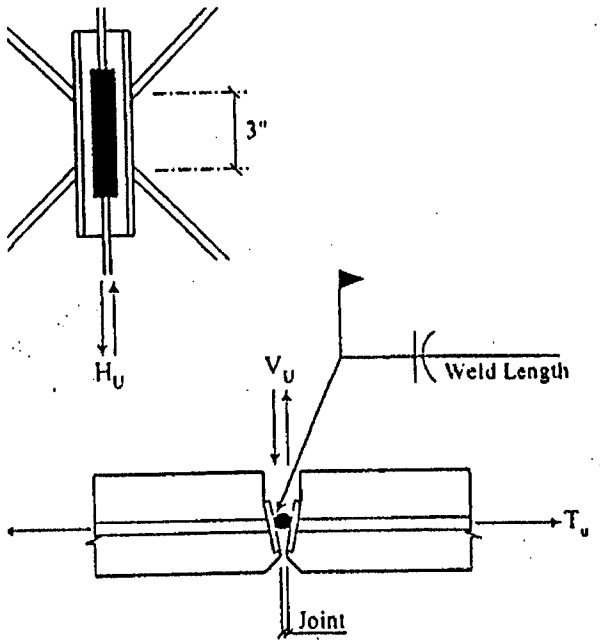

Figure 3.3: Shear Connector for Flange to Flange Connection
(PCI Committee Report 1998)

Consider a flange to flange connection, as shown in Figure 3.4. For this connection, three different forces must be considered. First, consider the forces that develop in the plane of the flange. If the flanges were not connected, the members would move with respect to each other, in the presence of a lateral load. The presence of the shear connector prevents this relative movement, thus a force H_u will develop. This force is associated with the transfer of shear through the diaphragm between the chords. In addition to this shearing force, the double tees will have a tendency to pull apart as the diaphragm begins to deflect. This force will be termed P_u, and represents the tensile resistance of the shear connection. The last force is associated, not with diaphragm action, but with deflection response between adjacent members. Referring to Figure 3.5, consider a load placed on one double tee member. This force will result in the deflection

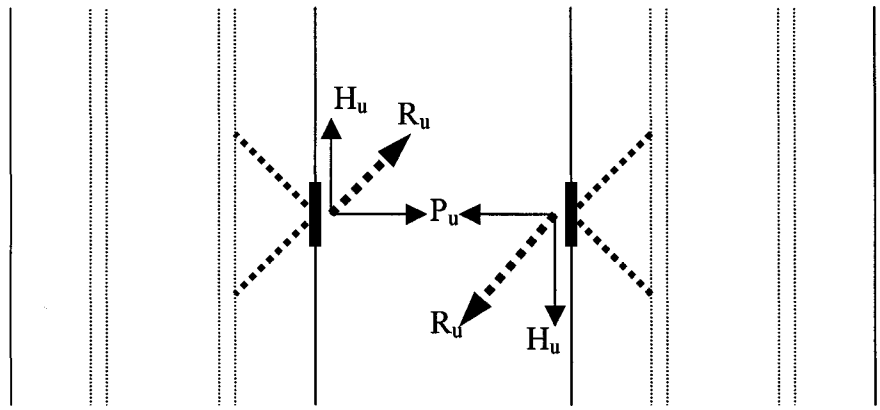

Figure 3.4: Force Development in Flange to Flange Connection
(in the Plane of the Flange)

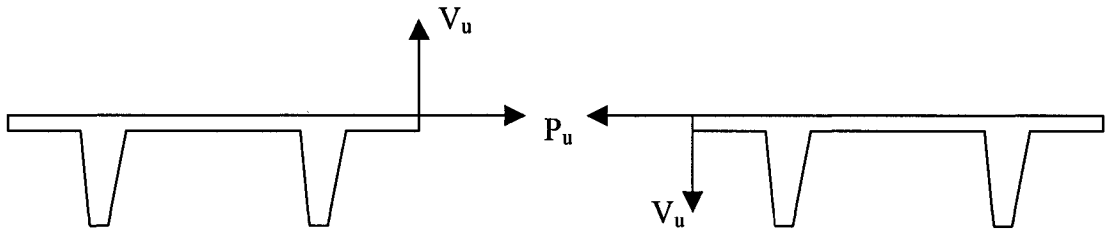

Figure 3.5: Force Development in Flange to Flange Connection
(in the Plane of the Cross-section)

of that member. Due to the presence of the mechanical connection, the adjacent double tee will resist the deflection of the loaded member. This action will result in a shearing of the connection, in the plane of the cross-section; the associated force will be termed V_u. All these forces are resisted by the enbedment of reinforcement into the flange of the member, as shown in Figure 3.3. The development of H_u and P_u in perpendicular directions is dealt with by placing the anchoring reinforcement at an angle θ, where θ is

in general equal to 45°, which is measured to the face of the flange. Each of these connectors is, therefore, able to resist the forces H_u, P_u and V_u.

The writer is of the opinion that the forces outlined above tend to result in high force levels in the flange, in the region of the shear connector. These concentrated forces can, therefore, result in premature failure of the concrete in the region of the connection. In particular, these stress levels may approach their critical values during ground excitation.

3.3 Proposed Connection Method

In recent years, the use of CFRP to repair and reinforce concrete structures has been the focus of a substantial volume of work (see Chapter 2). The current work proposes that this material, in conjunction with a high strength epoxy grout, can enhance the connection, and thus improve its response under seismic loads. This method is also suggested as a retrofit to the existing connections. Consequently, it is proposed for use in conjunction with the mechanical shear connection in sensitive areas.

Firstly, consider the mechanical properties associated with the CFRP fabric. This fabric is comprised of a high strength uniaxial carbon fiber. It provides a high tensile strength (discussed in more detail in Chapter 4); however, the fabric can be considered to have no compressive or shear resistance properties. Thus, it is best utilized when orientated in the direction of the principal tensile load.

Once again, consider a flange to flange connection of two double tee members. It has been shown that forces P_u and H_u develop as a result of diaphragm action. As shown in Figure 3.4, an equivalent resultant force Ru can replace these two forces. This R_u, is the force resisted by the reinforcing in the shear connection. Therefore, if additional reinforcement can be introduced, at the same orientation, the developed forces can experience improved distribution over the length of the flange. This may reduce the chance of premature failure of the concrete in the flange. Referring to Figure 3.6, if a CFRP fabric is placed at a +/- 45° orientation (consistent with the current design of the shear connection reinforcement), the force R_u is now distributed over a length of the flange thereby reducing the stresses that develop as a result of a localized connection. As the fabric is effective in tension, and not in compression, it is provided at +/- 45° orientations; therefore, it can resist these forces irrespective of the direction of the load application.

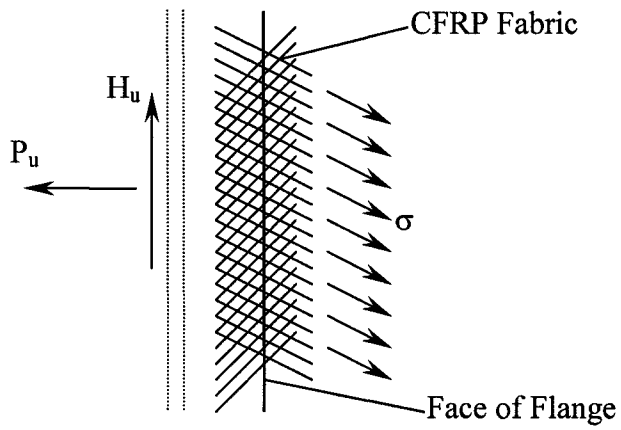

Figure 3.6: Distribution of Forces after Introduction of CFRP Fabric

The introduction of the CFRP, by itself, does seem to address the need for improved force distribution in the plane of the flange. Yet, it fails to address the need for

resistance of the V_u force in the plane of any given cross-section. In fact, when installing two adjacent double tee members, a space is left between them. This spacing prevents any contact that would resist V_u. To improve the distribution of this force, it is suggested that a high strength epoxy joint compound be introduced. By high strength, it is meant that the compressive resistance of the epoxy is greater than that of the concrete materials. The epoxy is placed between the flanges, as it will introduce an artificial bond between the members. This addition is not new; in fact, it is commonly employed during the installation of hollowcore planks. Furthermore, when this method of grouting is currently applied, it utilizes a concrete material rather than a high strength grout. In the current recommendation, the epoxy is suggested as it provides an excellent bond with the parent concrete. Moreover, it ensures that the weakest point is outside the joint itself. It is anticipated that the epoxy will eventually crack, as a result of repetitive loading. While the epoxy would no longer act as a solid link between flanges, the force V_u would be resisted by the development of friction across the crack, as shown in Figure 3.7.

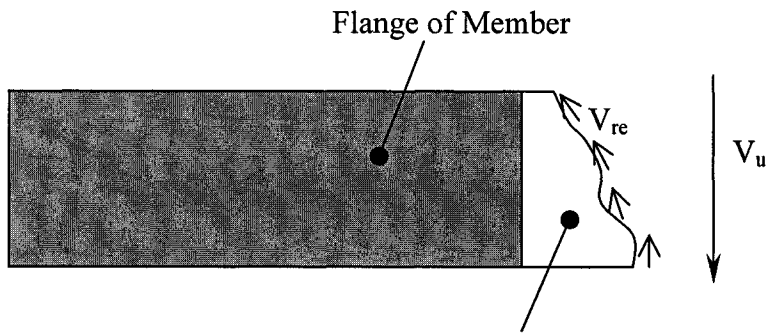

Figure 3.7: Transfer of V_u across Cracks in the Grouting Material

If the CFRP and epoxy systems are employed together, the resulting joint will introduce two-way action and thus, an apparent monolithic action of the attached members. Referring to Figure 3.8, the presence of the CFRP across the top and bottom of the joint will act as tensile reinforcement, depending on the developed moment. The epoxy will act to resist the associated compressive forces developed in bending of the joint. This system will have a higher flexural resistance than the flange; therefore, failure of the joint should not govern the design. This situation should be checked with every design.

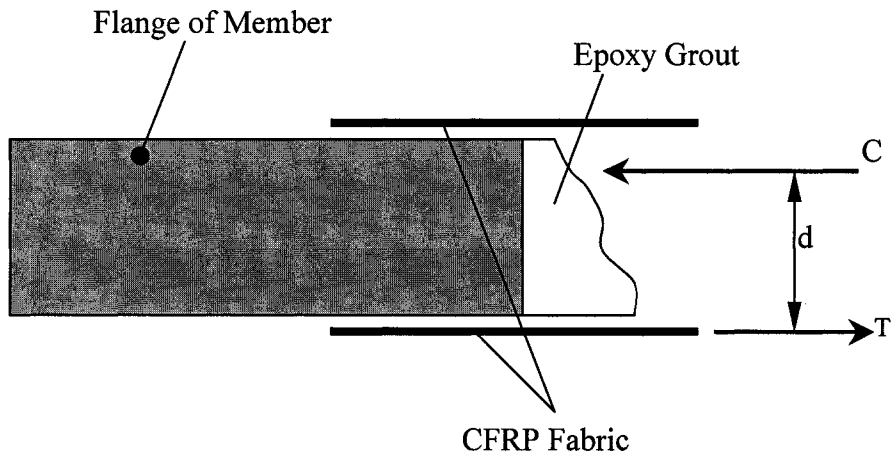

Figure 3.8: Developed Two-Way Action Due to Composite Joint System

It is believed that the associated monolithic joint will improve the serviceability of the system, and load sharing/distribution. Moreover, it is believed that the joint will better distribute the stress along the flange and thus, resist seismic excitation without concern of failure.

4. Experimental Setup and Equipment

The following sections outlines the specifics relating to the physical-testing portion of the current work. A description of the equipment used is also provided.

4. 1 Materials

4.1.1 Concrete

This section details the specifications placed on the concrete materials used for all test specimens.

For the double tee specimens, and lap length specimens (discussed in detail later in Sections 4.2 and 4.3, respectively), the concrete materials were provided by J. Santarossa & Sons Ready Mix Concrete, Windsor, Ontario. The 28-day compressive strength was specified to be 40 MPa. Further specifications included a maximum aggregate size of 10 mm, a 200 mm slump, addition of a super plasitizer, and an accelerator additive. The accelerator was added to provide a high early strength of at least 30 MPa, within seven days. The 30 MPa strength is associated with the minimum strength required for the transfer of prestressing force. All other concrete materials used are specified, where appropriate, later.

4.1.2 General Reinforcement

All reinforcing bars, excluding prestressing wire, had a yield strength of 400 MPa. All plates, structural sections, and welded wire fabrics were made of steel with a 300 MPa yield strength.

4.1.3 Prestressing Wire

For the purpose of prestressing the double tee specimens, a single prestressing strand (wire) was used. The wire was manufactured, and provided, by Stelwire of Hamilton, Ontario. The wire had a nominal diameter of 5 mm, and a cross-sectional area of 19.9 mm^2. The wire was specified by the manufacturer to have an ultimate tensile strength of 1970 MPa.

As shown in Figure 4.1, the mechanical properties of the prestressing wire were determined, via tensile tests that were conducted on two sections of wire. Referring to Figure 4.2, the results from the two tests compared favourably with each other. The results of the tests can be found in Table 4.1.

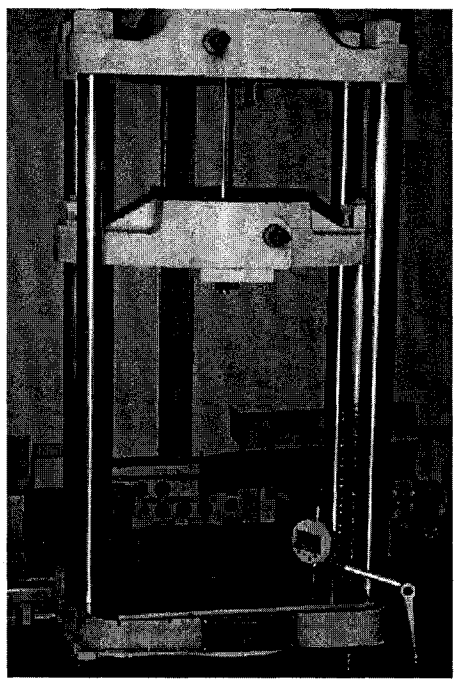

Figure 4.1: Photograph of the Tensile Test of the Prestressing Wire

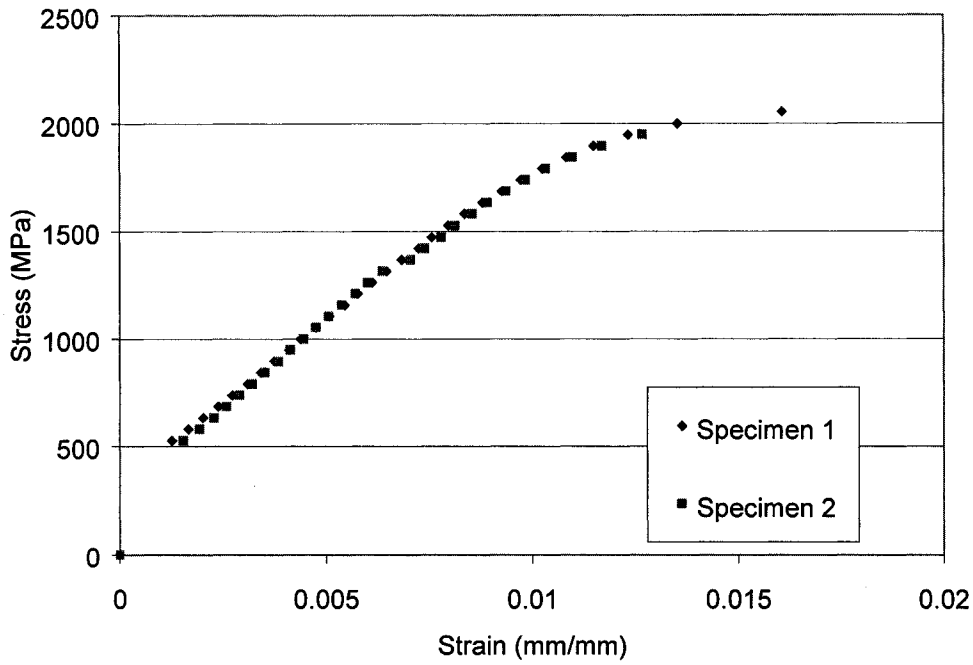

Figure 4.2: Experimentally determined Stress-Strain curve for Prestressing Wire

Table 4.1: Mechanical Properties of Prestressing Wire

Property	Value
Ultimate Tensile Strength (MPa)	1970
Modulus of Elasticity (GPa)	190

4.1.4 CFRP Fabric

The CFRP fabric used for this work consisted of a series of small carbon fibers aligned in a uniaxial direction. Tables 4.2 and 4.3 provide the material properties of the individual carbon fibers and the unidirectional fabric, respectively.

Table 4.2 : Material Properties of Carbon Fibers (after Sika 2003)

Properties	Value
Fiber Direction	Unidirectional (0^o)
Tensile Strength	3.8 GPa
Tensile Modulus	235 GPa
Area Weight	610 g/m^2
Elongation at failure	1.5 %

Table 4.3: Material Properties of CFRP Fabric (after Sika 2003)

Properties	Average Value MPa	Design Value MPa
Tensile Strength	849	717
Tensile Modulus in the fiber direct.	70 600	65 100
Compressive Strength	779	715
Modulus perpendicular to the fiber	67 000	61 500
Shear Strength +/-45° in plane	52	46
Shear Modulus +/-45° in plane	2500	2390
Ply Thickness (mm)	1.016	
Tensile % Elongation at Failure	1.12	0.98

The fabric was adhered to the specimens by means of an epoxy resin, designated Sikadur HEX 330, manufactured and provided by Sika Canada. The HEX 330 epoxy resin system consists of two components that were mixed in a predetermined ratio just prior to application. Table 4.4 provides the properties of the resulting epoxy resin.

Table 4.4: Epoxy Resin Properties (after Sika 2003)

Properties	Value
Tensile Strength	30 MPa
Elongation at Break	1.5 %
Glass Transition Temp.	53° C after 7 days of curing
Modulus of Resinp	3.45 GPa
Mix Ratio	A:B = 4:1

The procedure adopted for the use of the Sikadur 330 was in conformity with the guidelines suggested by Sika and their representative. It should be noted that, from a strength and elongation standpoint this resin proved to be sufficient. Considering now the glass transition temperature, or heat deflection point, as defined by Sika; this value is associated with the resin changing from a glassy state to a rubbery state at which time the mechanical properties of the material are greatly affected. As noted by Zureick and Kahn

(2001) this value is also affect by moisture levels. Moreover, these authors suggested that the temperature on the structure is notably higher than the air temperature, as a general rule. Sika currently uses the Sikadur 330 system in a number of their construction projects and contends that given the regional conditions this value is more than sufficient; however, the resin used should be selected based on the environmental conditions (e.g. highest temperature) to avoid unforeseen negative effects.

4.1.5 Epoxy Filler (PowerFix 3)

As will be discussed in Section 5.2.2, the space between two connected specimens was filled with a two-part epoxy filler. This filler is designated PowerFix 3, and is manufactured by Sika Canada. Table 4.5 provides the properties of the filler material.

Table 4.5: PowerFix 3.0 Material Properties (after Sika 2003)

Properties	Value
Compressive Strength	81 MPa (at 3 days/23°C)
Tensile Strength	24 MPa
Elongation at Break	0.95%
Flexural Strength	42 MPa
Tangent Modulus of Elasticity	7.22 GPa
Shear Strength	19 MPa
Bond Strength (2 days)	28 MPa

4.2 Double Tee Specimens

4.2.1 General Design Specifications

The general design of the double tee specimens was based on a review of the design of several full sized members produced by a local precast company. The general specifications for the specimens will be given below.

The specimens were designed (using simlitude) to represent a 1:4 scaling of the typical double tee members reviewed. This scaling factor was selected based on a review of fabrication, shipping, and testing constraints. Table 4.6 compares the general dimensions of the typical full size member, and the test specimens. As can be found in Table 4.6, certain dimensions of the specimen marked with an asterisk " * " exceeded the 1:4 scaling factor. These dimensions were modified to ensure sufficient concrete cover to the reinforcement and/or to ensure proper placement of the concrete.

Table 4.6: Comparison of Full Sized Members to Test Specimens

Dimensions	**Test Specimen**	**Full Size (Avg)**
Flange Width (b_f)	762 mm	3050 mm
Flange Depth (h_f)	51 mm *	102 mm
Web Depth (h_w)	178 mm	711 mm
Bottom Width of Web (b_{bw})	37.5 mm *	102 mm
Top Width of Web (b_{tw})	50 mm *	171 mm
Distance between centers of Webs (D)	375 mm	1,500 mm
Centroidal location of Prestressing (d_p)	150 mm	600 mm
Length of Member (L)	4570 mm	18,300 mm

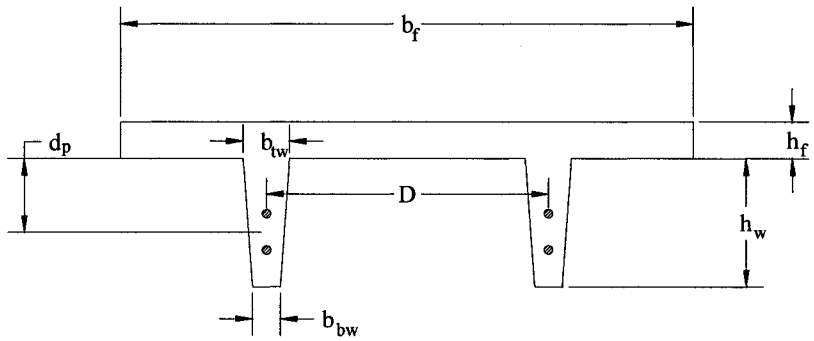

4.2.2 Flexural Reinforcement

Once the specimen's dimensions had been determined, the flexural reinforcement was detailed. In the case of all full size double tee members reviewed, the compression zone was contained within the flange; in addition, all prestressing wires were pulled to 70

percent of their ultimate value. Therefore, the specimens were detailed such that the maximum number of wires, pulled to 70 percent of the ultimate strength, were used while maintaining the compression zone within the flange depth. The effective depth of the prestressing for the specimens also conformed to the 1:4 scaling factor. A detailed analysis of the resulting member was done using the commercially available software Concise Beam 4.01 by Black Mint (2003). The analysis conformed to the conditions put forth by CAN/CSA A23.3-94 (1994). According to the results of the computer analysis, the specimens had an ultimate moment capacity of 16.7 kN-m. Appendix A contains the summary report provided by the software.

4.2.3 Shear Reinforcement

For the purpose of shear reinforcement, a welded wire fabric of 10 gauge wire (diameter of 1.7 mm), at 50 mm x 50 mm spacing, was used along the entire length in both webs. The placement of the shear reinforcement guaranteed that shear failure would not govern under a concentrated load applied at center-of-span. The size/spacing of the reinforcement was based on design requirements and product availability.

4.2.4 Flange Reinforcement

In addition to the reinforcement for shear and flexure, additional reinforcement for the flange was required to prevent punching of the slab during loading. To prevent punching, and to maintain a standard welded wire mesh size, the same reinforcement used for shear was also employed for this purpose.

4.2.5 Shear Connectors

In order to facilitate the connection between two double tee members, shear connectors were introduced into the specimens. These connectors are similar to those currently used by the precast industry. The shear connector for both the test specimen and for actual precast double tee members, consists of anchoring reinforcement attached to a weldable plate. The plates are aligned along the flange edges where the double tee is to connect to another element, or member. The specific spacing tends to differ from member to member.

The shear connector employed for this study, shown in Figure 4.3, consisted of a #3 rebar (dia. of 9.5 mm), bent at 90°, welded at the mid-height of a flat steel plate. The steel plate used was 6.25 mm flat stock cut to a size of 25 mm wide, and 50 mm high. The rebar was cut such that the total length used was 500 mm. This allowed for 250 mm of the bar to project into the flange at angles of +/- 45°. The 250 mm length was selected based on available space in the flange, and the required development length for rebar.

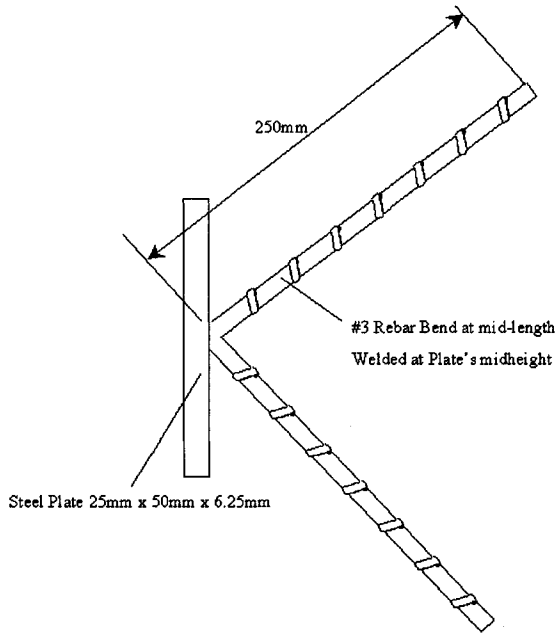

Figure 4.3 :Shear Connector Employed in the Current Study

As previously discussed, the primary purpose of the shear connector is to resist shear forces developed due to diaphragm action. The required number of shear connectors for this purpose is small compared to the number actually provided in industry. From discussions with the engineering department of a local precast concrete company, it was found that the placement of the shear connectors tends to follow a general rule of thumb. Referring to Figure 4.4, this general guideline is that if a load was placed at any point along the web, and it was projected out towards the connecting edge, at least one shear connector should be intercepted within a +/- 45° envelope. From this method it was found that the center to center distance between connections was to be 375 mm. Figure 4.5 shows a photograph of one specimen, prior to casting. The shear connectors can be seen along one side of the member.

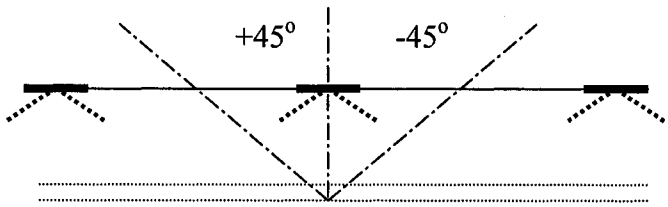

Figure 4.4: Design Envelope for Placement of Shear Connectors

4.2.6 Bearing Plate

Due to the constraints posed by the narrow dimensions of the webs, a special bearing plate design was required. A typical bearing assembly found in a full size double tee, as shown in Figure 4.6, would generally involve reinforcing bars extending from the exposed bearing plate up into the web of the member. Such a connection was

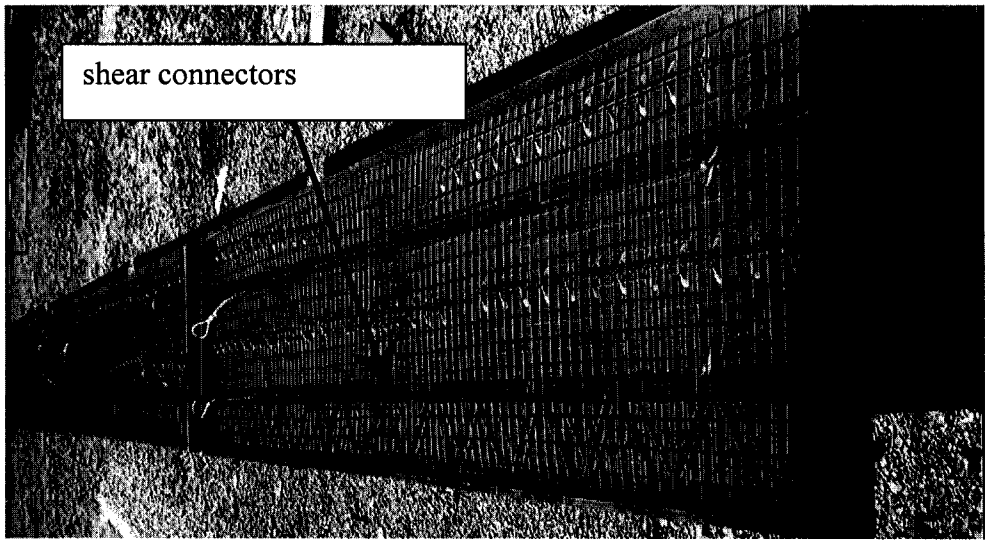

Figure 4.5: Photograph of Model with Shear Connectors (Prior to Casting)

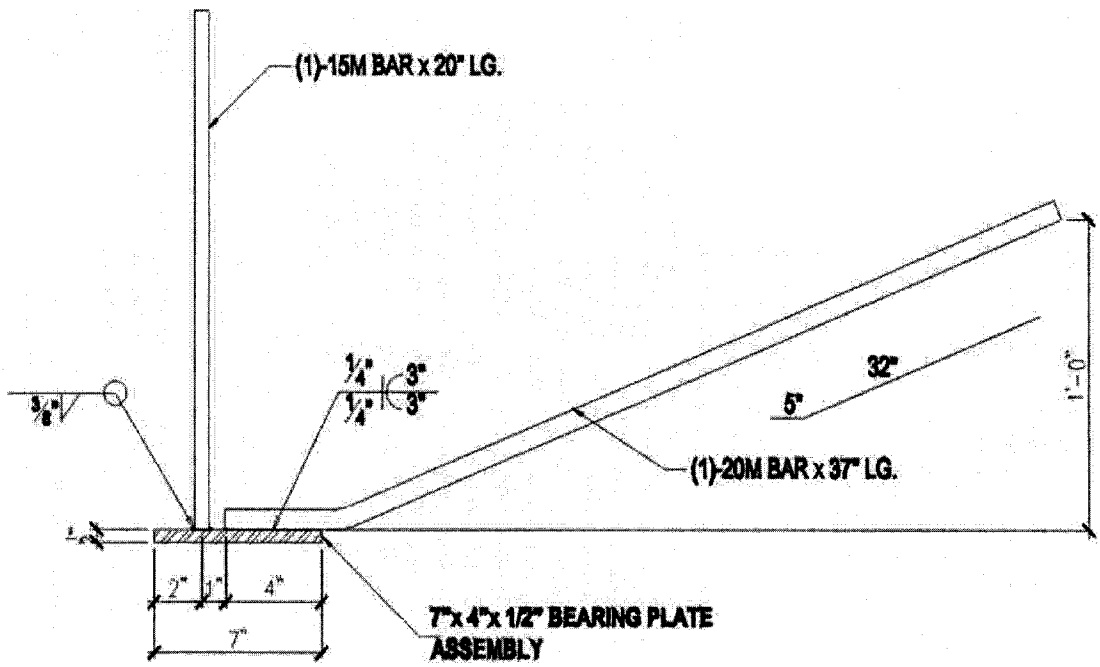

Figure 4.6: Typical Bearing Connection in Full Sized Double Tee Members (PSI 2004)

not possible in the 1:4 scale specimens as the reinforcement would have intercepted the prestressing wire. The overall height of the bearing assembly for the specimen was limited to 50 mm, which corresponded to the location of the first prestressing wire. From this limitation, a new connection was developed and tested. The connection employed was derived from a commonly used connection in structural steel. In structural steel, it is common to connect a steel element to a concrete slab system via steel channel. This application was adapted to the current project, and a 25 mm x 12.5 mm x 3.18 mm channel section was employed.

Prior to finalizing the design of the bearing plate, it was decided to limit the overall length of the plates to 75 mm. In order to determine the appropriate number of channels to attach to each plate and their corresponding orientation, a special set of experiments was performed. Figure 4.7 shows the different configurations of the channel(s) tested. Each of these plates was attached to an arm, refer to Figure 4.8, that was used to pull on the specimen. The channels and plates themselves were cast into a solid concrete block. The dimensions of this block were limited to the width of the web of the specimen, and 250 mm in all other directions. The compressive strength of the concrete was 38.5 MPa based on cylinder tests. Figure 4.9 provides a schematic and photograph of the specimens, and test setup.

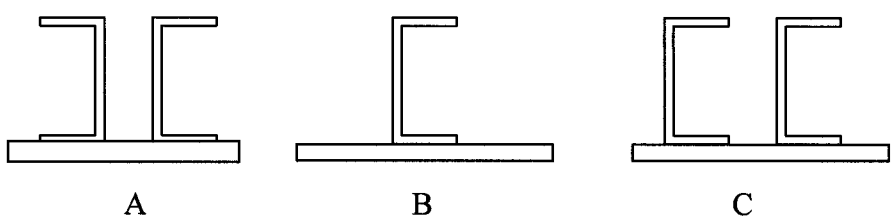

Figure 4.7: Different Support Arrangements Tested

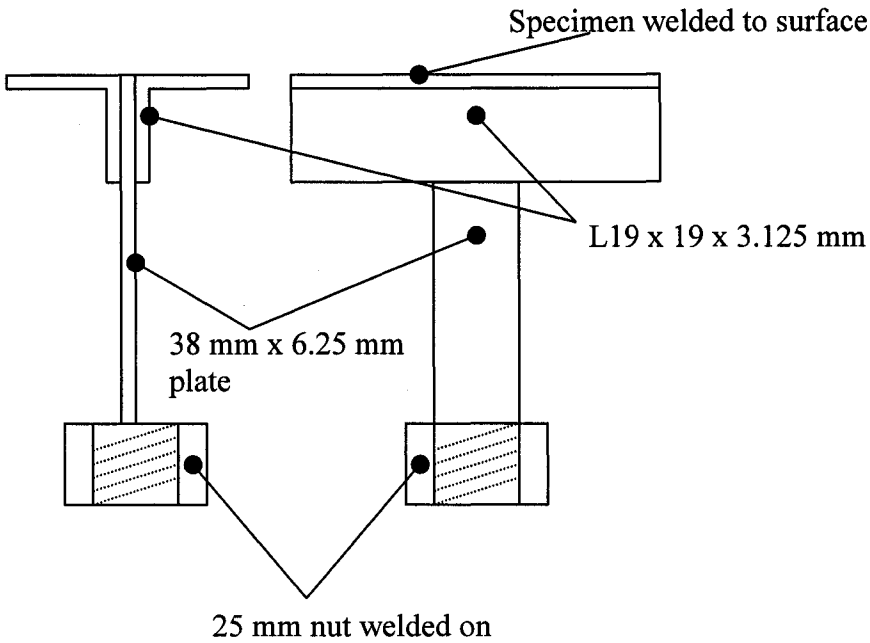

Figure 4.8: Assembly used to pull Bearing Plate in Tension

Two specimens of each of the three arrangements shown in Figure 4.7 were tested to ensure repeatability. From the testing, it was found that the arrangement, labeled A in Figure 4.7, was capable of resisting the greatest tensile load. This particular arrangement resisted 3710 N, before failure of the surrounding concrete. Table 4.7gives the minimum failure loads for the three configurations. Appendix B contains photographs of the test.

Table 4.7: Results of Bearing Plate Tests

Specimen (refer to Figure 4.7)	**Minimum Failure Load (N)**	**Failure Mode**
A	3710	Surrounding Concrete
B	2080	Surrounding Concrete
C	2420	Surrounding Concrete

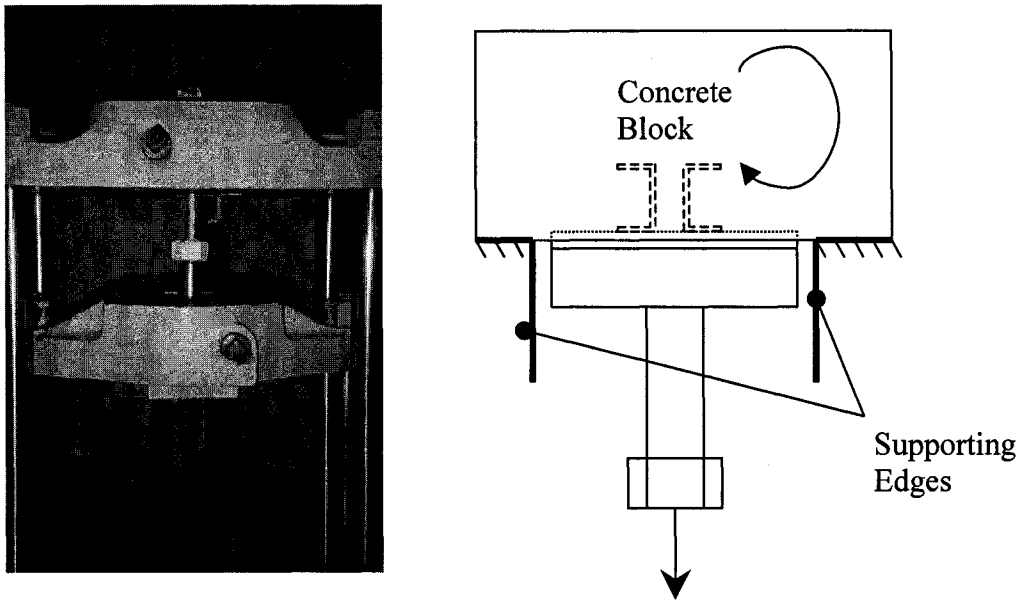

Figure 4.9: Schematic and Photograph of Specimen and Test Setup

4.2.7 Lifting System

Due to the stresses present in the system, as a result of the prestressing forces, the method used to lift the specimens had to minimize any additional stresses. Following the procedure outline by PCI 1996, 6.25 mm x 9 x 17 (¼ in. x9x17) aircraft cable, with a tensile strength of approximately 31 kN, was embedded into each web near the ends of the member. Figure 4.10 provides the details provided by PCI 1996. By placing these cables near the end of the specimens, the resulting moment developed during lifting, counteracted the stresses developed by the prestressing. Therefore, the stresses were maintained well within safe levels.

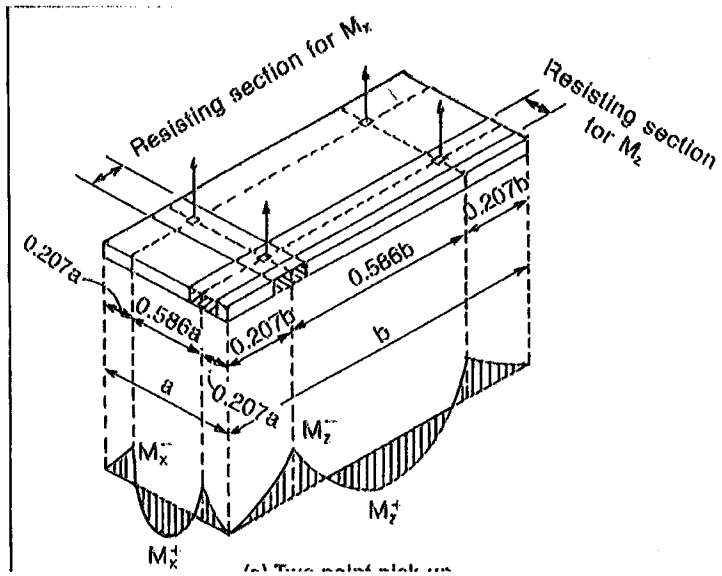

Figure 4.10: Lifting System Specifications (PCI Design Manual 1996)

In order to prevent any additional axial stresses during lifting, as a result of skewing of the lifting cables, a lifting strut was designed. The strut was designed with a factor of safety of three, and was capable of lifting approximately 1140 kg. Figure 4.11 provides a detailed schematic of the lifting strut. Figure 4.12 shows a photograph of the strut lifting one of the specimens.

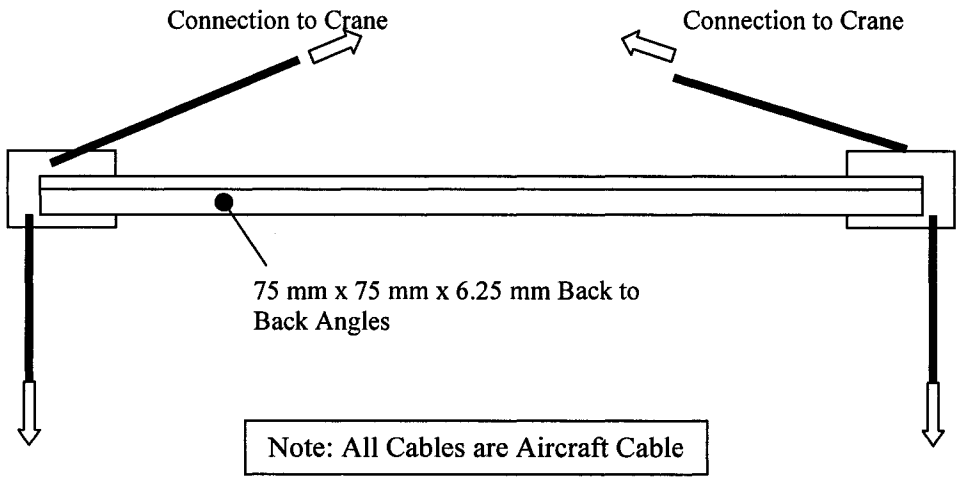

Figure. 4.11: Lifting Strut Details.

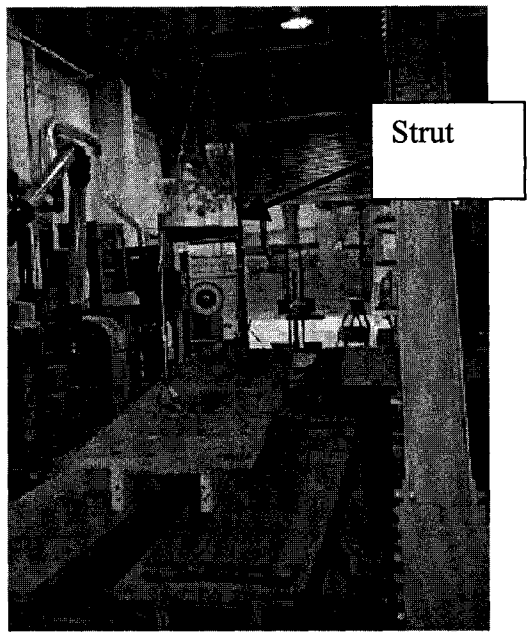

Figure 4.12: Photograph of Lifting Strut in Use.

4.2.8 FABRICATION

In order for the casting of all the specimens to be economical, it was decided that they should be cast in no more then two sets. From this, and in cooperation with J. Santarossa & Sons Ready Mix of Windsor, Ontario, a prestressing bed was designed and constructed. This prestressing bed consisted of two bulkheads welded to isolated on grade concrete footings and a wood frame to support the specimens. The two footings were placed at a distance of approximately 43.9 m (144 ft) from each other. The wood frame used to support the specimens, was then placed between them. In total, nine specimens could be cast at one time. Figure 4.13 provides a photograph of the prestressing bed with the forms in place.

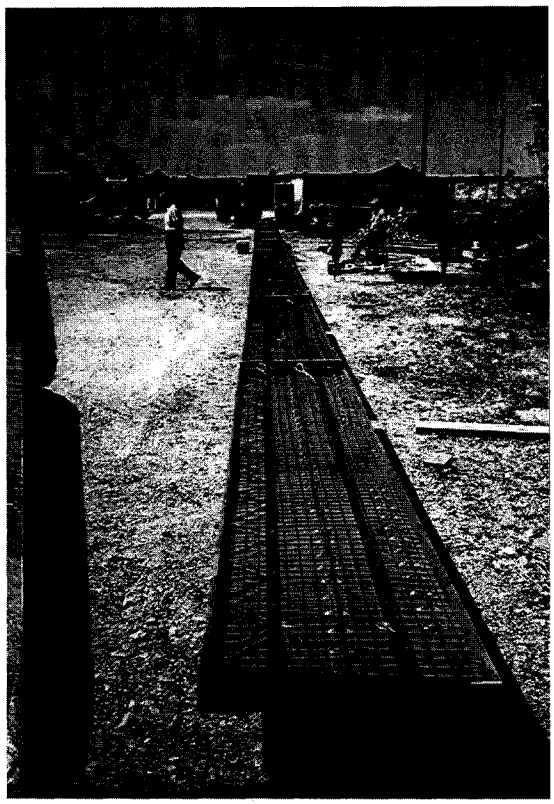

Figure 4.13 Photograph of the Prestressing Bed Prior to Casting

The footings were designed to resist the overturning forces developed by the prestressing. The footings were 1220 mm x 3050 mm x 184 mm. In addition to the weight of the footing, four concrete blocks, each weighing approximately 29 kN, were placed on both of the footings. The total weight of the footings, with the blocks, was sufficient enough to provide a factor of safety of approximately three against overturning, and a factor of safety of about two against sliding. The reinforcement placed in the footing was designed in accordance with CAN/CSA A23.3-94. Figure 4.14 shows schematically the distribution of the reinforcement in the footing. The compressive strength of the concrete used in the footings based on testing was 34.8 MPa.

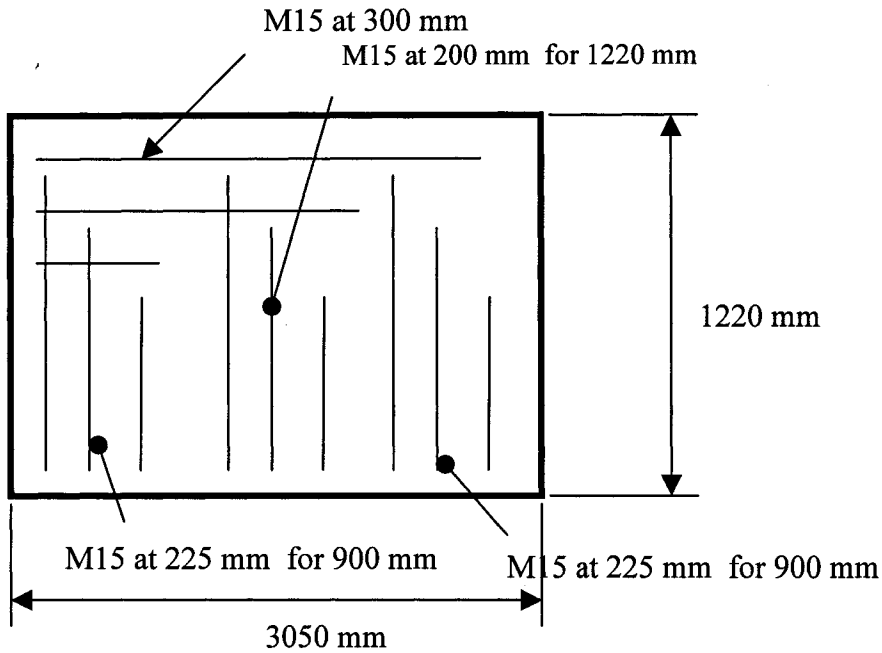

Figure 4.14: Reinforcement of Footings.

To attach the bulkheads to the footing, a special anchoring system was designed. This anchor consisted of a 19 mm steel plate with dimensions of 914 mm x 305 mm, with 175 mm shear studs. The anchors were placed and leveled prior to casting of the footings, as shown in Figure 4.15.

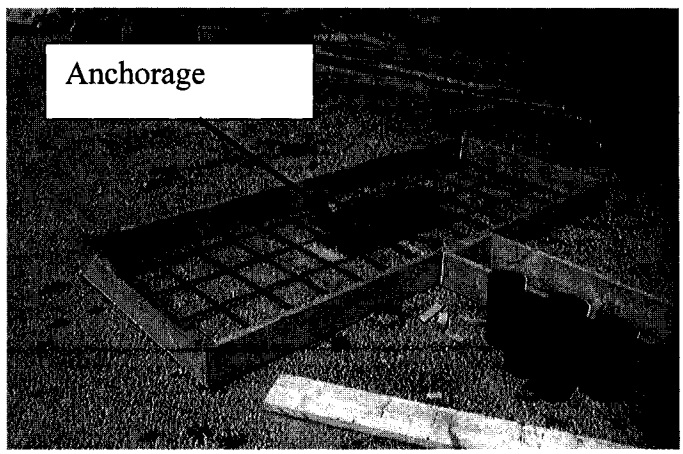

Figure 4.15 Anchoring System for the Bulkhead.

4.3 Lap Length Test Specimens

The following section is concerned with the design of the specimens used to test the development length (lap length) of CFRP required for the flange to flange joint.

These specimens were 498 mm long by 300 mm wide, and were designed to simulate a 300 mm length of the flange of the double tee specimens. Figure 4.16 shows a schematic of the specimen used. As can be noted, the depth of the specimen is not constant over the entire length. The "thin" section of this specimen is an exact copy of the flange found on the double tee specimens. The reinforcement of this flange was identical to the flange reinforcement used.

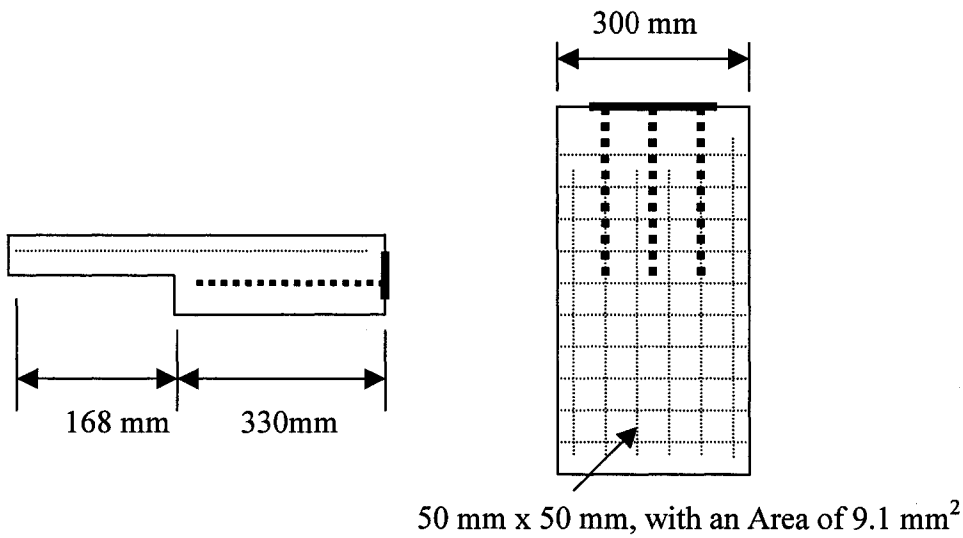

Figure: 4.16: Lap Length Specimen

The flange transforms into a deeper concrete region. The purpose of this thickened region involves the representation of the stiffness and transition associated with the double tee webs. It also provided a region to contain the connection required to test

the specimen. They were, as will be discussed in detail in Section 5.1, pulled in tension. Therefore, a special connection was required. Figure 4.17 shows this connection. As is shown, a steel plate of 12.5 mm x 50 mm x 175 mm was welded to three M10 rebars. The M10 bars had a total length of 300 mm, which corresponded to their full development length. This connection was embedded in the concrete at mid-height of the deep region.

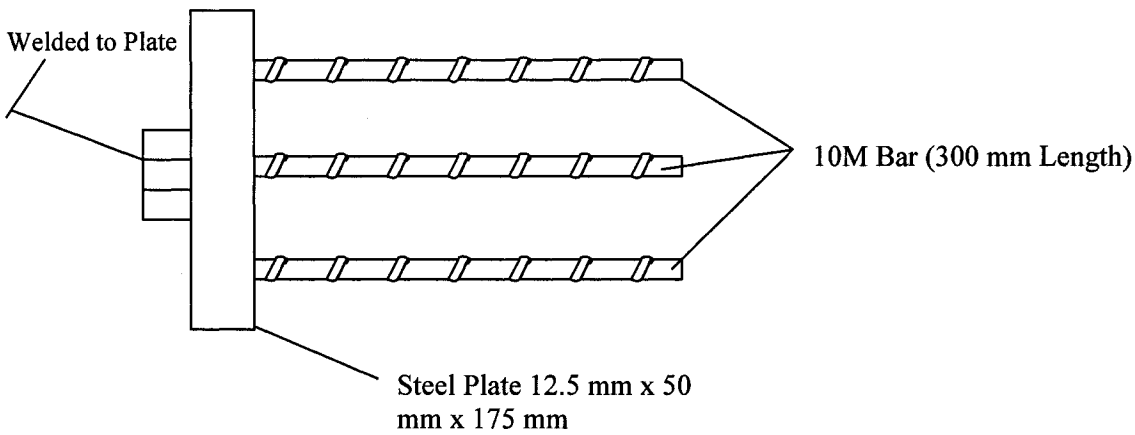

Figure 4.17: Connection for Lap Length Specimen

4.4 Testing Equipment

4.4.1 Load Cells

For this work two types of load cells were used. These included commercially available standard full bridge load cells and specially designed and fabricated quarter bridge load cells. The following section outlines the specifics of these systems.

4.4.1.1 Points of Load Application

At the points where the loads were to be applied, full bridge load cells were used. For all testing conducted, only two load cells were used. These load cells had capacities of 44.5 kN (10 kips) and 222 kN (50 kips), respectively. It should be noted that the 44.5 kN (10 kips) load cell was used for the testing involving the application of a tensile load to the lap length specimens. The 222 kN (50 kips) load cell was used for measure the applied bending loads only.

Prior to testing, both load cells were calibrated using a universal testing machine (Tinius Olsen Serial No. 141478/63418-2), which was calibrated by Cal-Chek Canada just prior to this work. Appendix C provides the calibration factors and the corresponding units.

4.4.1.2 Support Reactions

To obtain the reaction at each support, a special load cell was designed by the writer, and fabricated at the University of Windsor. These load cells were designed to behave elastically to measure loads up to 22.5 kN in tension or compression. Moreover, they were also designed to act as a leveling system for the specimens during testing. Figure 4.18 shows a schematic of the load cell.

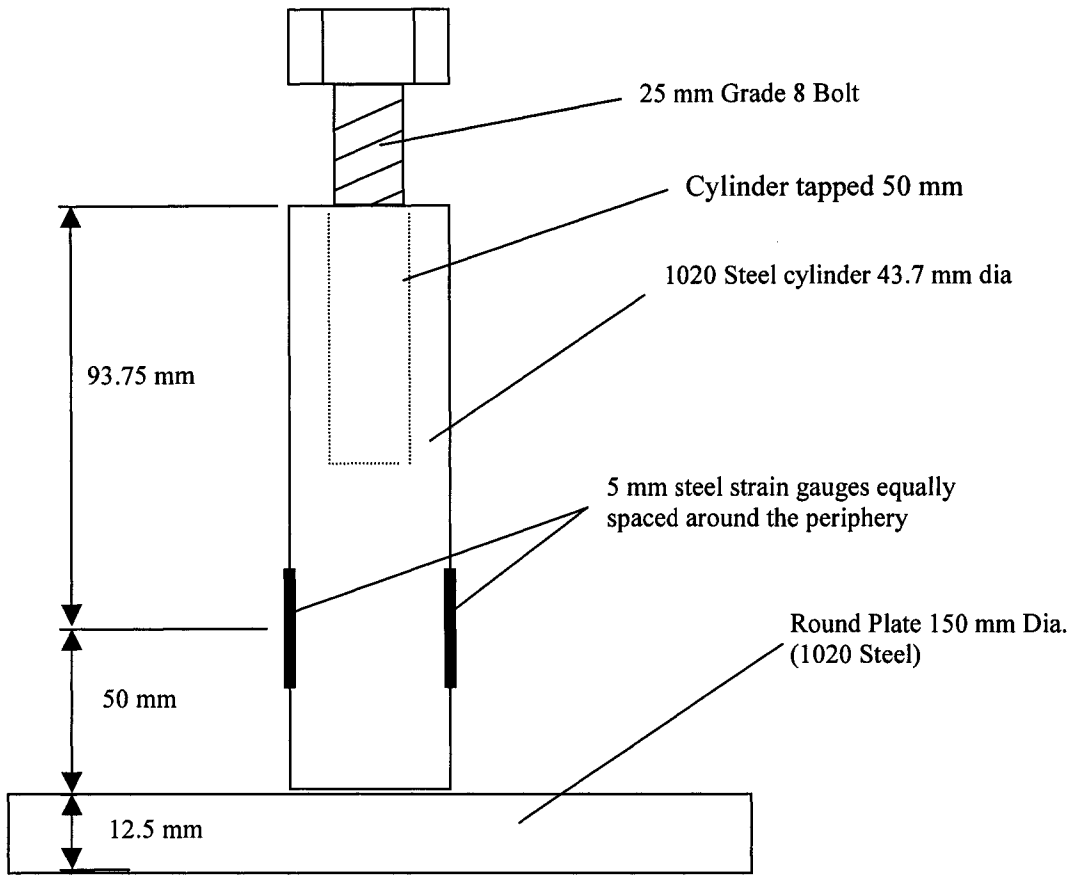

Figure 4.18: Support Load Cell Designed at the University of Windsor

A 50 mm long hole was drilled into the top portion of the cylinder of the load cell and tapped for a bolt, see Figure 4.18. This length allowed for up to 50 mm of height adjustment of the specimen. Once again, referring to Figure 4.18, the plate at the bottom extends out from the base of the cylinder to allow the load cell to be clamped down during testing, in case of the development of an uplift force. The entire body of the load cell was made of 1020 steel and the bolt used was a 25 mm, grade 8 bolt, with the head machined flat for better contact with the specimen.

To measure the strain in the load cell, four 120 ohm - 5 mm strain gauges were placed at 90° to each other, at a height of 50 mm from the base. The placement of the gauges is based on a finite element model of the worst case conditions, and Saint Venant's principle. The gauges were wired in a quarter bridge configuration; Figure 4.19 shows a schematic of the wiring of the gauges with respect to the Wheatstone Bridge. As can be seen, the wiring would provide an average strain value. This averaging is beneficial in case any accidental moment developed.

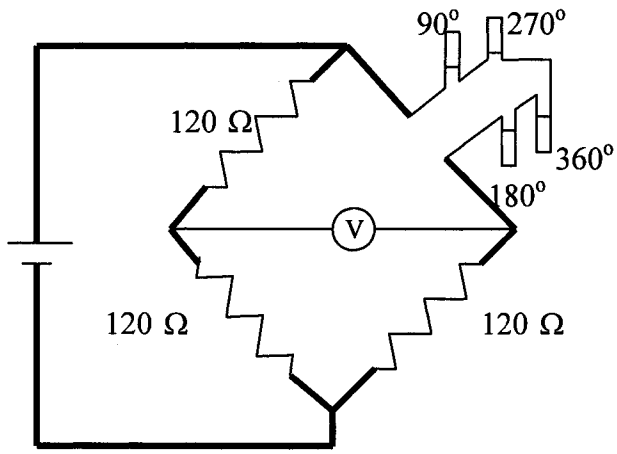

Figure 4.19 Wheatstone Bridge Schematic for Load Cells.

In total, eight of these support load cells were fabricated. All were calibrated using the same universal testing machine as that used to calibrate the other load cells. The calibration factors are provided in Table C.2 of Appendix C.

4.4.2 Data Acquisition

For this work, two separate data acquisition systems were used. Specifically, a different system was used for the static testing than was used for the dynamic testing. This section will provide information about the data acquisition systems.

4.4.2.1 Static Tests

To obtain data from the specimens during the static loading portions of the experiments, a Datascan data acquisition system, from Datascan Technology Ltd. of England, was used. As shown in Figure 4.20, the Datascan consisted of one main module and four expansion modules. Each module contains eight channels; therefore a total of 40 channels were available. The Datascan exported raw data to a laptop though a serial port connection. The data was obtained and interpreted by the Dalite software, also from Datascan Technology Ltd. of England.

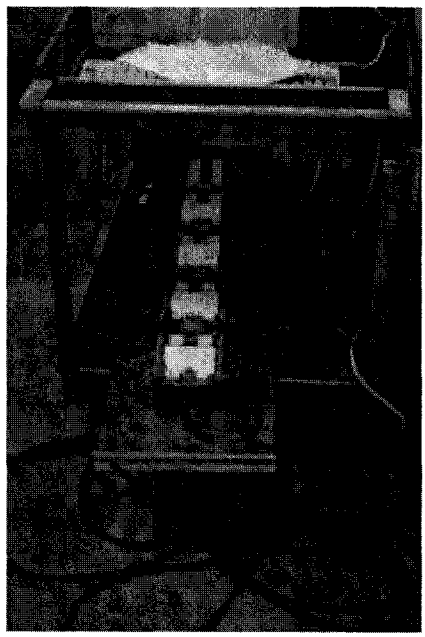

Figure 4.20: Photograph of Datascan System

4.4.2.2 Dynamic Tests

To obtain the data from the dynamic tests, a Megadac data acquisition was used. The Megadac is capable of taking a total of 25,000 readings per second from the connected accelerometers. The Megadac is controlled by, and routes all data to, an attached desktop computer. Figure 4.21 shows a photograph of the computer and Megadac system.

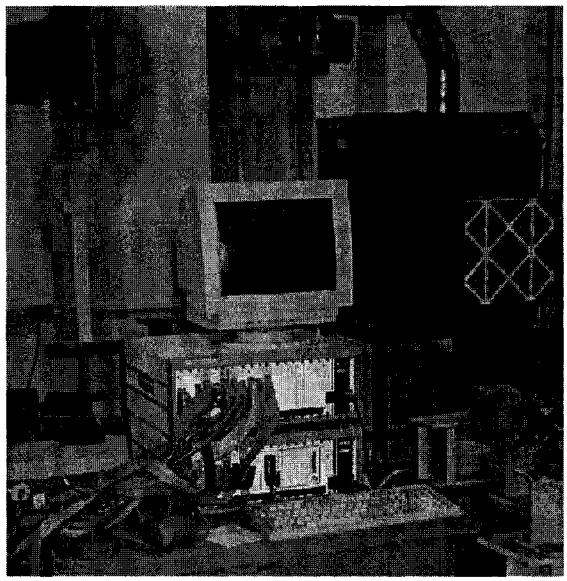

Figure 4.21: Photograph of Megadac and Computer System.

4.4.3 Concrete Strain Gauges

The strain gauges used for measuring the strain in the concrete were 120 ohm gauges of 30 mm length. The length is based on the maximum aggregate size of 10 mm used in the casting of the specimens.

4.4.4 Accelerometers

For this work, four accelerometers were employed. These accelerometers were connected to the Megadac, which took approximately 4900 readings per second from each. Each accelerometer was positioned to measure the acceleration in the vertical direction.

Each accelerometer consisted of a semiconductor acceleration transducer which contained a built-in amplifier. Each was capable of measuring accelerations in the range of ±0.1 to ± 50 g's, with a frequency response of up to 1400 Hz. These accelerometers were 23 mm x 23 mm x 11 mm in size, and can be see in Figure 4.22.

Figure 4.22: Photograph of Accelerometer

Each of the four accelerometers was calibrated using a B&K Calibration Exciter Type 4294, by Bruel & Kjaer of Denmark. The Exciter emitted a RMS (root mean square) acceleration of 10 m/s^2, RMS velocity of 10 mm/s, and a displacement of 10 μm at a frequency of 159.2 Hz. The results of the calibration confirmed that indeed all accelerometers were in working order, and all still performing within the anticipated ranges.

4.4.5 Displacement Measurement

For the purpose of measuring displacement, four LVDTs were employed. Each LVDT, with a travel of 125 mm, was routed to the Datascan data acquisition system and provided an in terms of mV. Table C.3, of Appendix C, contains the calibration values for all four LVDTs.

5. Data Collection and Experimental Runs

The following section addresses the specifics of all tests conducted. Gauge location details will also be provided.

5.1 CFRP Lap Length Tests

Prior to testing of the double tee specimens, with the CFRP connection, the minimum lap length "l_o", refer to Figure 5.1, of CFRP needed to be determined. This minimum lap length was associated with the length of CFRP required to cause ultimate failure of the flange under pure tension. The length l' corresponds to a measurement taken along the length of the fiber.

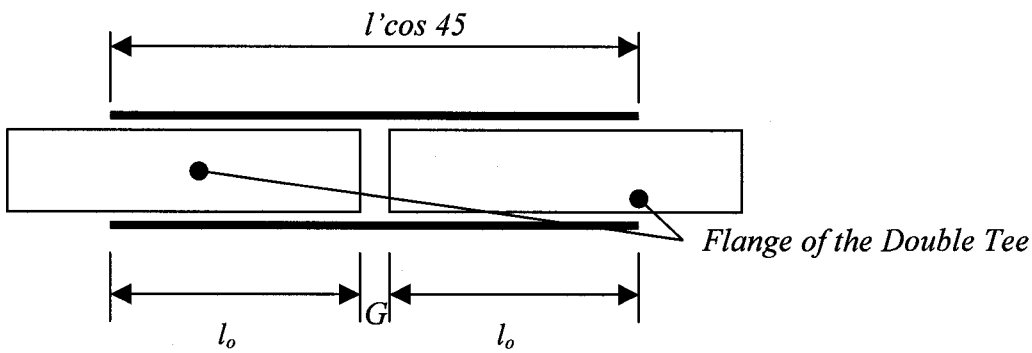

Figure 5.1: Definition of lap length

The specimens used for this test, here forward referred to as pull specimens as they were pulled in tension, were discussed in Section 4.3. These specimens were connected, in sets of two, in the same fashion as the double tee flanges would be. The flanges of the pull specimens were epoxied to each other using the PowerFix 3 by Sika. Once the epoxy dried, two layers of CFRP fabric of length l' were adhered across the top

and bottom, of the joint (see Figure 1.4) between the specimens at +/-45° to the joint. The length l' of the CFRP is related to the lap length l_o by the expression.

$$l' = 0.707(2l_o + G) \qquad [5.1]$$

where G is equal to 6.25 mm, and represents the space between the specimens filled with PowerFix 3.

For the purpose of determining the optimum lap length, a series of lengths were tested. Specifically, the lengths of l_o = 50, 100 and 150 mm were tested. For each length, two sets of specimens were tested to ensure repeatability.

Referring to Figure 5.2, for each test, one end of the specimen was secured to the floor using a length of 15.9 mm threaded rod, and the other end was attached to a hydraulic jack and 44.5 kN (10 kips) load cell. The specimens were then pulled in tension till failure. In all cases examined failure occurred in the flange. Therefore, a 50 mm lap length was adopted for this work.

5.2 Tests of Double Tee Specimens

The testing of the double tee specimens was considerably more involved than the previous lap length test. This section will review the various tests conducted on the double tee specimens, and the specific gauge locations used.

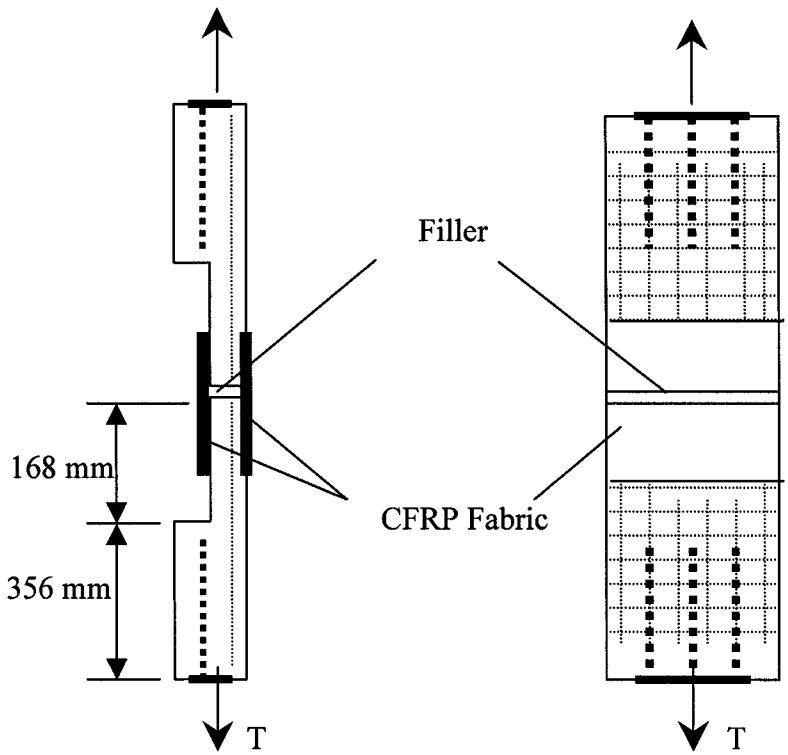

Figure 5.2: Lap Length Specimen Test

Prior to all tests, the bearing plates of the test specimens were welded (over a short length) to the supporting load cells. This weld prevented the specimen from slipping from the supports during any given test.

5.2.1 Individual Double Tee Specimens

Two separate double tee specimens were tested for this phase. In each case, a series of tests were conducted to obtain substantial information about the performance of the individual double tee members. Both dynamic and static tests were conducted on the specimens.

Prior to any testing, gauges of various types were placed on the specimens. For the dynamic test, each of the double tees was gauged with accelerometers under both webs at the midspan location. For the static testing, two displacement transducers (LVDT) were placed at midspan to measure the maximum displacement, and strain gauges were affixed to the top surface of the flange (at the centerline the webs) at a distance of 2100 mm from the end of the specimen. The distance of 2100 mm corresponds to the location of one of the shear connectors cast into the specimens, and is a point of interest in further testing. Figure 5.3 shows a schematic of the gauge locations.

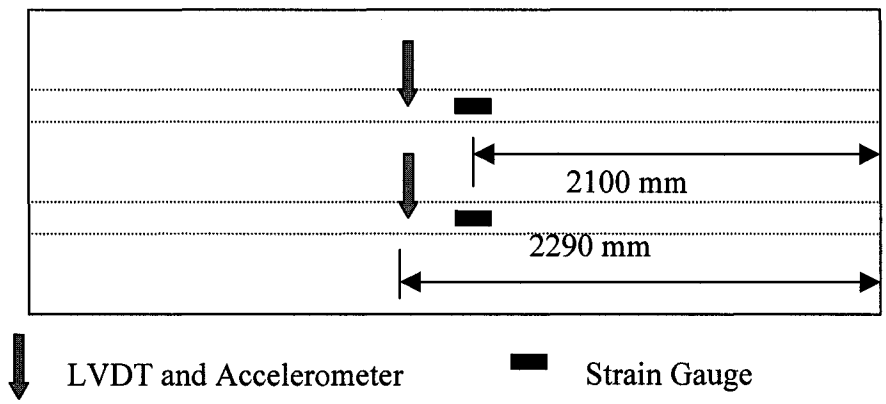

Figure 5.3 Schematic of Gauge Locations for Single Double Tee Tests.

Before any static testing was conducted, a dynamic test (drop test) was performed on the specimens. For this test, a sandbag of 21.1 kg was dropped from two different heights onto the specimen in close proximity to the midspan location. Figure 5.4 shows a photograph of the mechanism used for this drop test. Each test was repeated twice. In total, four sets of data were acquired for each test. These tests were used to provide the dynamic properties of the specimens prior to any damage resulting from the static loading.

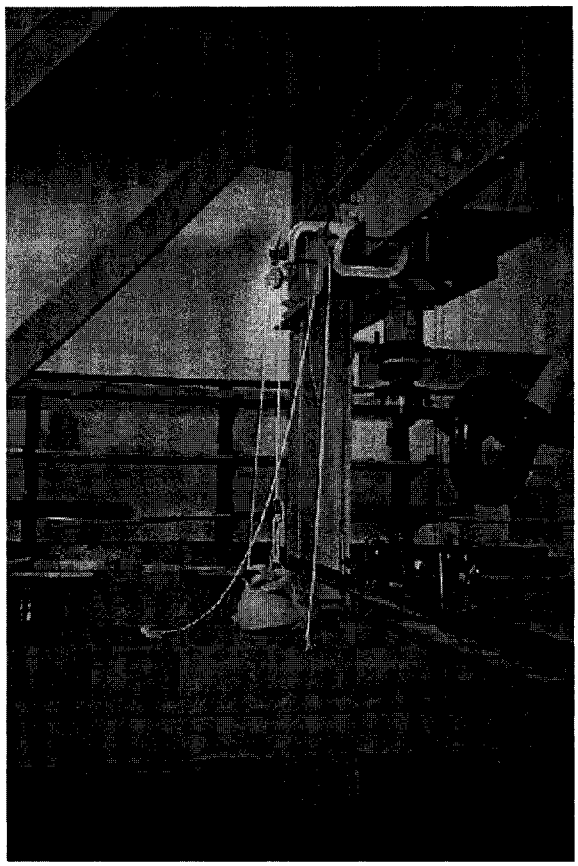

Figure 5.4: Drop Test Setup

Once the initial dynamic tests were completed, a static load test was performed. The static load was applied on the specimens at centerspan in the form of two concentrated loads, one over each web (see Figure 5.5). The load was placed over each of the webs to prevent premature failure of the specimen due to punching of the flange. The load was gradually increased until approximately 33% of the ultimate load, or cracking of the concrete was heard. For this test, centerspan deflection, strains, support reactions, and applied load were recorded. The static load was then removed

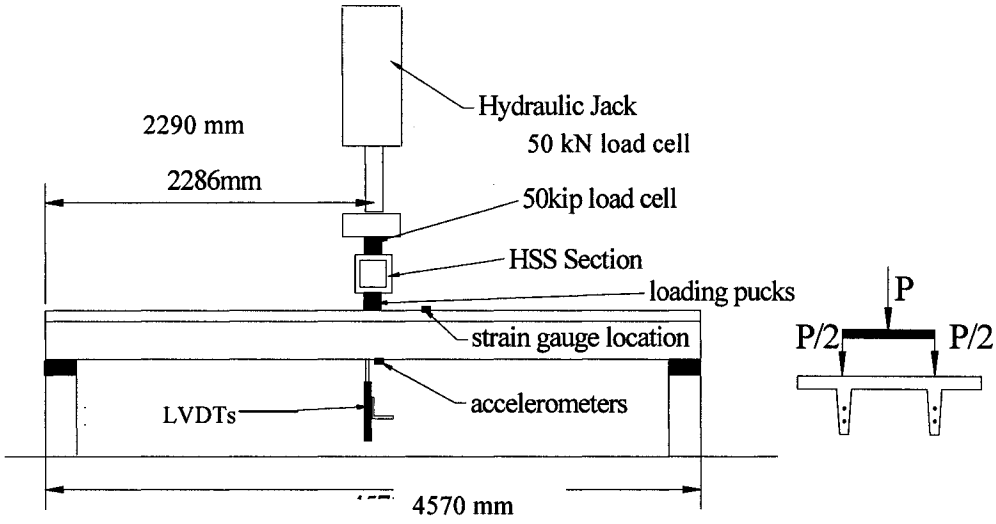

Figure 5.5: Static Loading Arrangement.

from the specimen. Once the static load was completely removed, the Drop test was repeated to monitor changes in dynamic properties. After this dynamic test, the static test was conducted again. Once again displacements, strains, support reactions, and applied loads were measured. The load was allowed to increase past the previous high until further cracking was heard, or approximately 50-66% of the predicted ultimate was reached.

The drop tests and static tests were repeated several times until the ultimate load of the specimens had been reached. Each time the static load test was performed, all measurements were recorded form a zero load to monitor any change in the specimen's performance.

5.2.2 Connected Double Tee specimens

In order to avoid repetition, the writer will first review the various connections examined, and then define the testing procedure, which was common to all tests.

The first connection examined in this study was the standard welded shear connection, employed currently by the precast industry. Two double tee members were aligned next to each other, at the supports, with a spacing of 6.25 mm (1/4 in.) between the two double tees. This spacing is consistent with that used in industry, and allows for a steel plate to be placed between two opposing shear connectors. Referring to Figure 5.6, once connected to the support system, steel plates of similar size to that used when making the shear connector were placed between the specimens at the connections, and arc welded to each member. In total, 12 connections were made between each set of specimens.

The next connection system involved only the use of CFRP and epoxy injection systems. In this system, as was done in the previous system, a 6.25 mm (1/4 in.) space was left between the members. This opening was filled with the PowerFix 3 epoxy to create a solid and continuous link between the members. This epoxy fill was left to dry for 24 hours. After the drying period expired (24 hours), the two layers of CFRP (discussed previously, see Sections 3.3 and 4.1.4) were affixed to the top and bottom sides of the connection. The resins for the CFRP were then allowed to dry prior to testing.

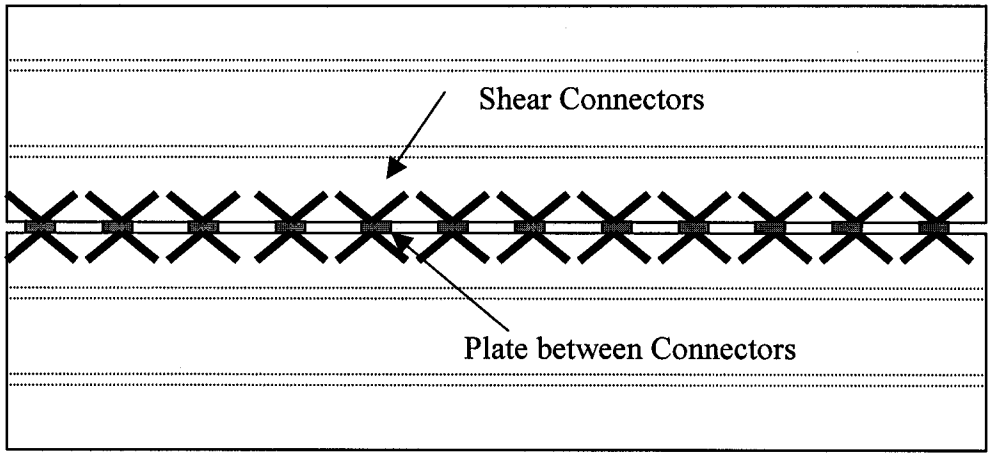

Figure 5.6: Schematic of Double Tee to Double Tee Connection using Welding Only

The final connection system tested involved a combination of the previous two systems. Thus, this connection was first welded, using the same procedure as in the first system, and then the epoxy and CFRP were introduced into the system.

The locations of gauges were the same for all double tee to double tee tests. As was the case with the individual double tee tests, the LVDTs and accelerometers were located at the centerspan of the members. Figure 5.7 shows a schematic of strain gauge locations. As was done by Hofheins et al. (2001), sets of three strain gauges were used to form rosettes at four different locations along the connection. In particular, these rosettes, seen in Figure 5.8, were located so as to measure the strains (both normal and shear) at the connections located close to the end and centerline of the members. Other strain gauges were also located along the same cross-sections as the rosettes, to monitor strains associated with flexure.

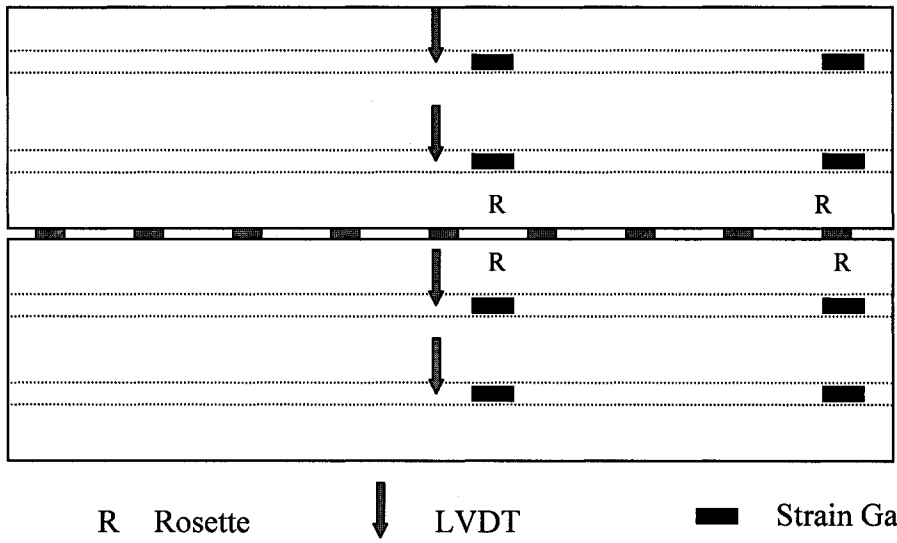

Figure 5.7: Schematic of Gauge Location for Double Tee to Double Tee Testing

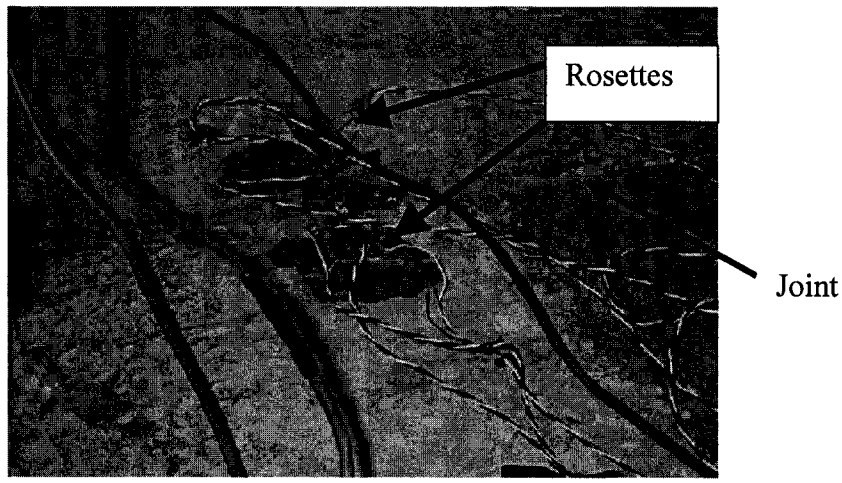

Figure 5.8: Photograph of Strain Rosette Formed from Three Strain Gauges

The testing methods used for all the double tee to double tee experiments were the same, irrespective of connection system. In fact, the methods employed here conformed to the methods used for the individual double tee tests, specifically the static loading and dynamic testing sequence. The only difference was associated with the location of the load and the application of a laterial load at mid-span. In the present case of vertical

loading, the load was applied to one member while the adjacent member was left unloaded. The other significant difference in the testing method, as relates to the single vs. connected double tee studies, was the introduction of a lateral load.

The lateral load was applied at centerspan and involved the application of a quasi-static load, applied to the outer web of the first member. Referring to Figure 5.9, this load was applied using a hydraulic jack, and 22.5 kN (10 kips) load cell attached to a flat plate on a ball and socket connection. This ball and socket connection allowed the plate to rest flat against the web of the member. The load was slowly increased up to approximately 4 kN. This limit of 4 kN load was based on safety concerns and limitations placed on the testing by the laboratory facilities. The focus of this test was to examine the stress distribution as a result of diaphragm action of the connected members.

After the lateral load was removed. An impact load was applied to determine the dynamic properties of the member prior to the application of any vertical load. The specimen was then tested statically and dynamically in the same incremental fashion as the single members.

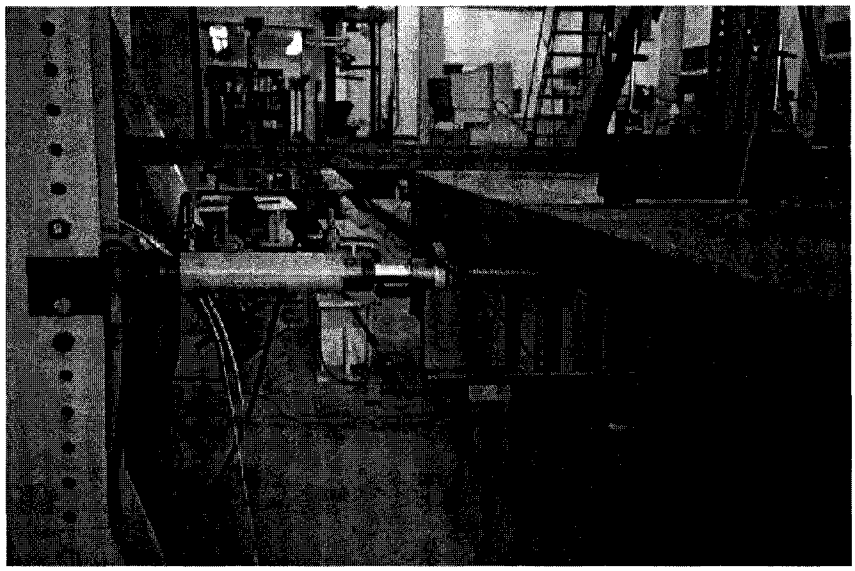

Figure 5.9: Photograph of Lateral Load Set-up

6. Experimental Results and Discussion

The following section provides the results from the experimental phase of this work and discusses its implications. The layout of this chapter is set so as to provide the reader with the ability to make comparisons between the different connection types. Therefore, rather than address each individual connection test separately, the writer has opted to discuss specific test types and measurements together (for example: support reactions for all cases will be presented together). The initial discussion addresses the testing of the individual double tee specimens. Moreover, all results presented here were confirmed via finite element analysis, using ADINA 2004.

6.1 Response of Individual Double Tee Specimens

As mentioned in Section 5.2.1, two individual double tee members were tested during the initial phases of this work. From concrete cylinder testing, it was determined that each member was constructed of concrete with average compressive strengths of 62 MPa +/- 4% (set 1) and 70 MPa +/- 5% (set 2), respectively. Also, the writer determined that the anticipated ultimate load as defined by the Concise Beam design software was P_U =14.3 kN for f'_c = 65 MPa.

As was done for all experiments involving the double tee members, the location and formation of cracks were observed, marked, and recorded by photographs. In the case of both individual members, the test specimens exhibited very few cracks along their length. The cracks that did develop were all consistent with cracking associated with flexural stresses. In both cases, the first crack was not visible until approximately 7-9

kN. Furthermore, these initial cracks appeared to form simultaneously in each web at the centerspan location (under the load). As the load was increased, the initial cracks continued to extend up the cross-section towards the flange. As the load approached the ultimate load, the cracks extended into the flange, see Figure 6.1, causing the web to open up wide enough so that light was seen through the opening.

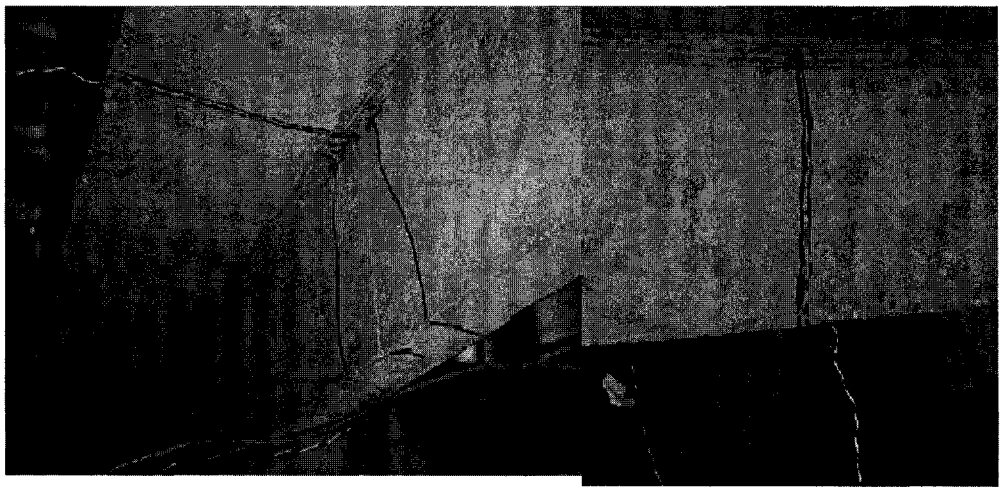

Figure 6.1: Observed Cracking in Individual Double Tee Members

After the formation of the initial cracks, other cracks did form along the length of the member. Yet, as shown in Figure 6.2 the spacing between the cracks was relatively large in comparison with conventional reinforced concrete. Very few cracks formed before the ultimate load was reached, as would be expected of a prestressed member.

Figure 6.2: Crack Spacing for Individual Double Tee Member
(in Region of Mid-Span)

As mentioned earlier, in Section 5.2.1, each member was loaded until failure. These specimens failed under a load (P_U) of 15.9 kN (set 1) and 18.4 kN (set 2), respectively, which tends to agree favourably with the 14.3 kN load predicted by the software "Concise Beam". The variation between the experimental and calculated values can be attributed to the use of resistance factors incorporated into the software.

In the case of both specimens, as shown in Figure 6.3, the deflection response of the system was linear, up to $P \approx 6.75$ kN. Employing the elementary beam theory, the moment corresponding to the cracking moment should have been $M_{cr} = 8.9$ kN-m ($P = 7.8$ kN). As illustrated in Figure 6.3, the specimen's response after this point ceased to be linear. Moreover, the system's response to subsequent loads followed almost identical

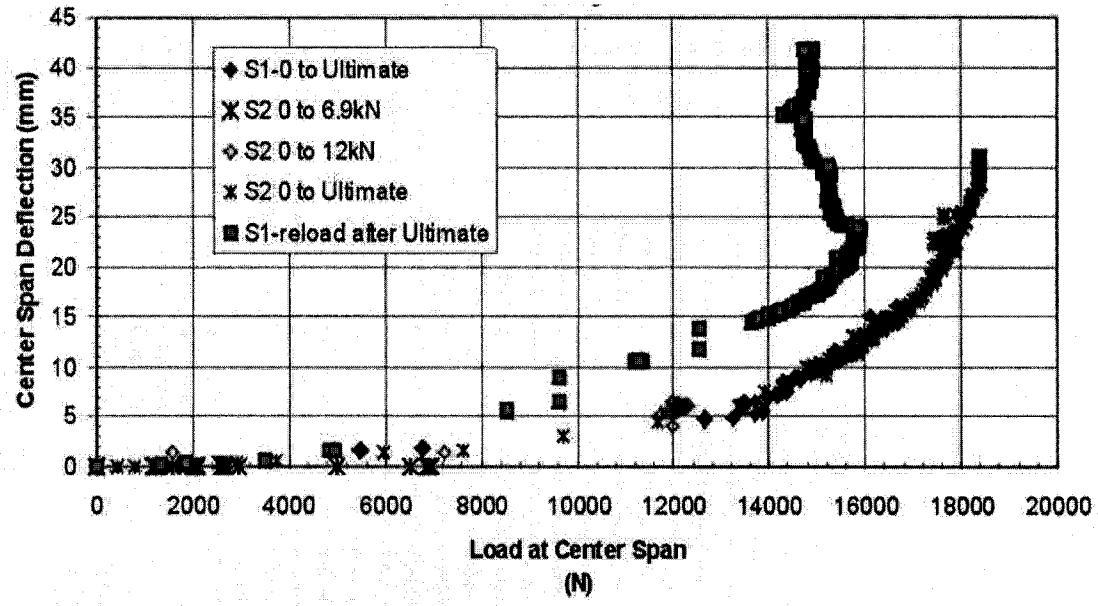

Figure 6.3: Deflection Response of Individual Member

paths for both specimens. The deflection followed the original path until just prior to the ultimate load value, then the curves tended to deviate from one another.

Figure 6.4 displays the average flexural strains developed at the extreme compression fibers for both of the specimens. It can be observed that the strains, which developed in the system, also tended to behave in a linear fashion up to the load associated with the cracking moment. After the cracking moment was reached, the strains were non-linear. In addition, the load-strain curves during loading-unloading-reloading followed a similar path during each loading sequence. Very little variation existed between the paths of subsequent reloading cases.

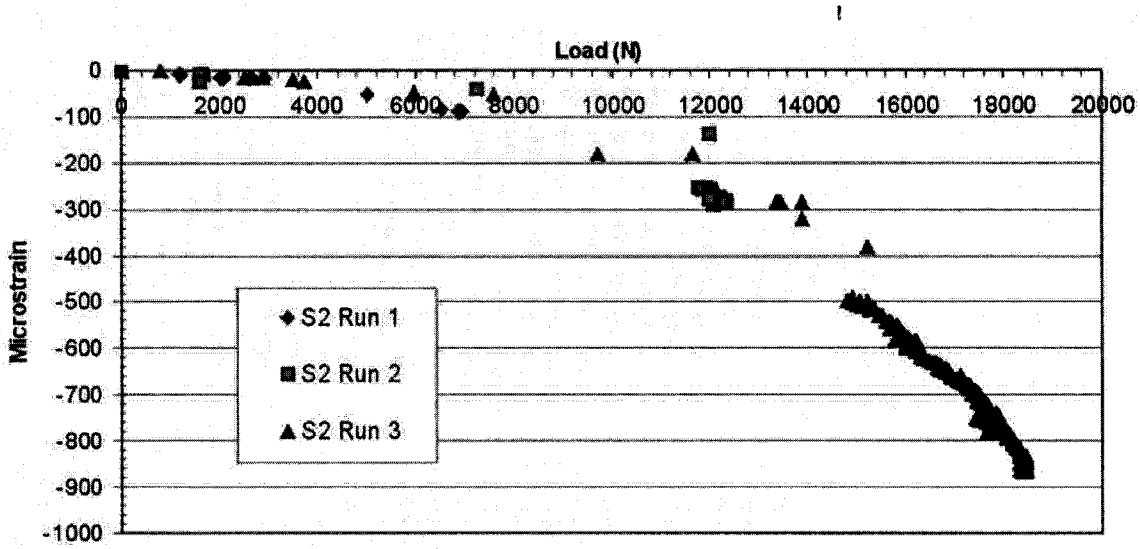

Figure 6.4: Flexural Strain vs. Load

Finally, Figure 6.5 shows a plot of P_{high}/P_u vs the system's natural frequency. It was observed that the natural frequency remained constant at approximately 16.8 Hz, irrespective of the past loading history. This is associated with the dynamic forces being less than that required to open the cracks, thus changing the system's moment of inertia. Figure 6.6 is an example of the dynamic response of the system. The system's response, a short time after the initial impact, clearly followed the expected sine path. From this data, the average wave length, and thus the period of the system, was determined. As would be expected, it was found during a review of the data, that the wave length was constant thoughout the entire response.

6.2 Reponse of Connected Double Tee Specimens

6.2.1 Observed Cracking Behaviour

As noted earlier, during the course of each test, the formation of cracks, due to flexure or shear, was monitored. The response of the connected members, in terms of

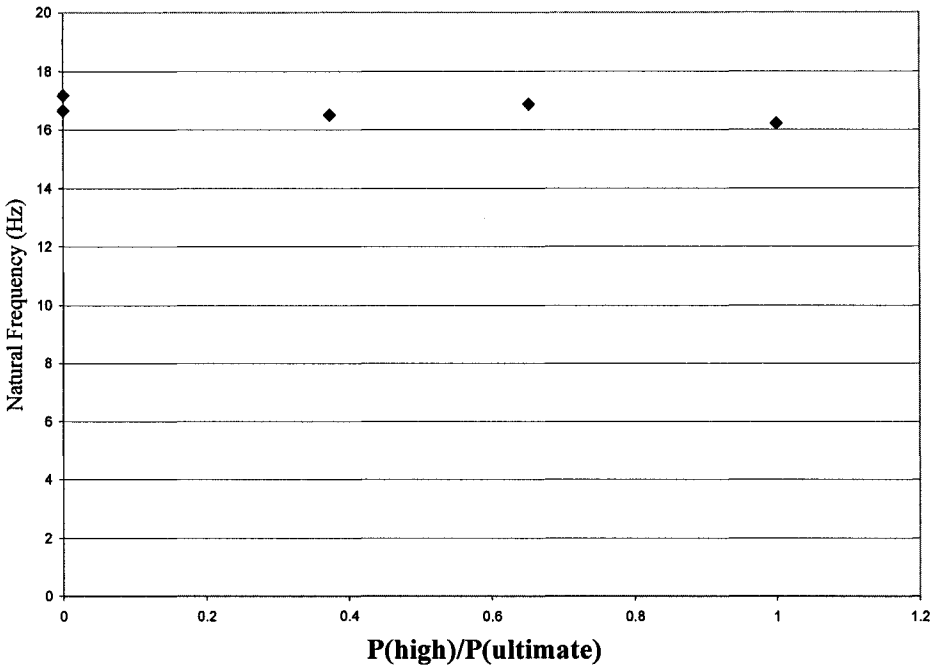

Figure 6.5: P_{high}/P_u vs. Natural Frequency

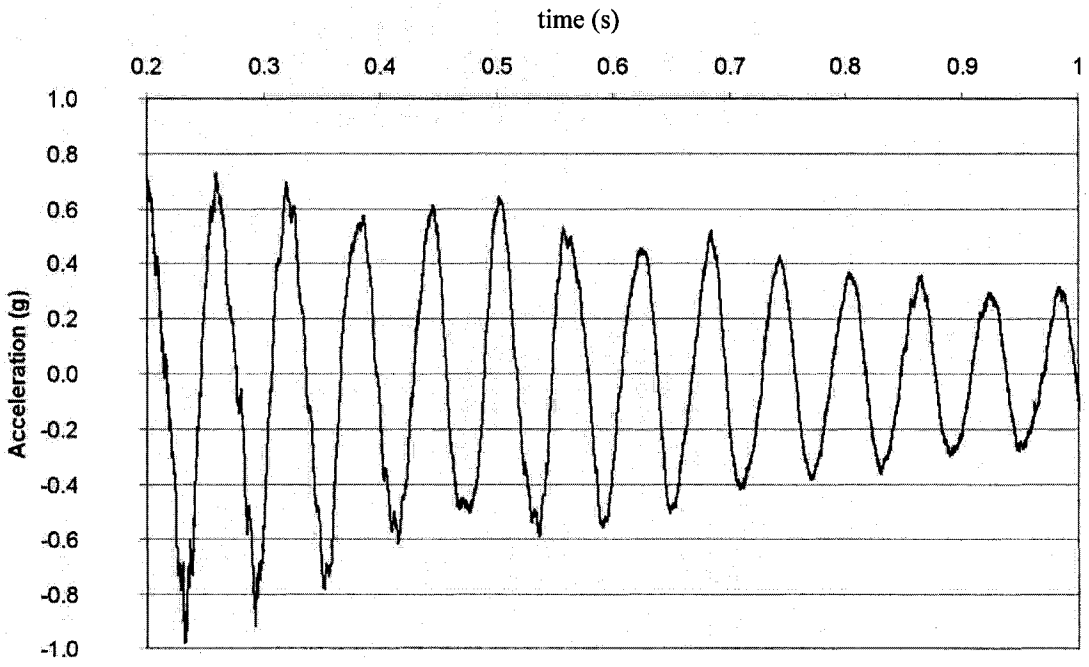

Figure 6.6: Example of Dynamic Response of an Individual Double Tee Member

cracking, did exhibit some interesting results. In fact, the connection type also appeared to play a role in the cracking pattern.

In the case of the welded connection, the initial crack(s) formed at, on average, a load (P) of approximately 17 kN. This initial crack formed, referring to Figure 6.7, in web A at center span, while the other webs remained uncracked. As other small hairline cracks formed along web A, due to increasing load, web B cracked at midspan (at P = 24 kN). As the load was increased, and thus the deflection curve of the cracked webs, webs C and D eventually cracked at mid-span (P = 29 kN and 32 kN, respectively), each cracking at an incrementally higher load than the previous web. It was noted that the loading increment between each subsequent web cracking was substantial. Figure 6.8 shows a close-up photograph taken near centerspan with the web closest in the photograph being web D. Note that while webs A through C exhibit several cracks each, web D exhibits only one small crack in this region. In fact, the complete formation of this crack web D (up to the flange-web intersection), happened only at the ultimate load.

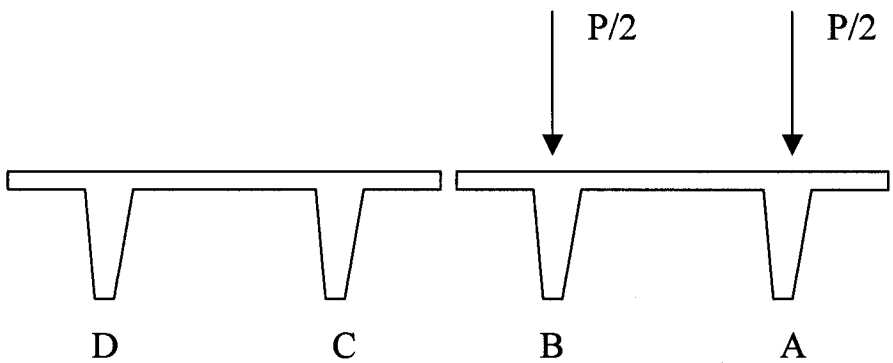

Figure 6.7: Web Identification System

Figure 6.8: Cracking of All Webs for Welded System

For the case associated with the composite connection, the observed cracking pattern differed from that observed during the welded connection tests. Once again, the formation of the initial crack in each web did start at web A, then progressed through B and C and D. The loading increment between the initiation of each "initial web crack" was drastically reduced from that observed during the weld test. Moreover, the initial crack in web A was observed to occur, on average when the load was 20 kN. Figure 6.9 shows a photograph of one of the cracked specimens prior to the application of the ultimate load. This photograph was taken from the side closest to web A, in the region of center span. It can be seen that webs A, B and C all have several cracks formed by this time, while D had only one crack (visible in the photograph). In the case of the CFRP connection, the ultimate load corresponded with the opening of all four centerspan web cracks, as shown in Figure 6.10.

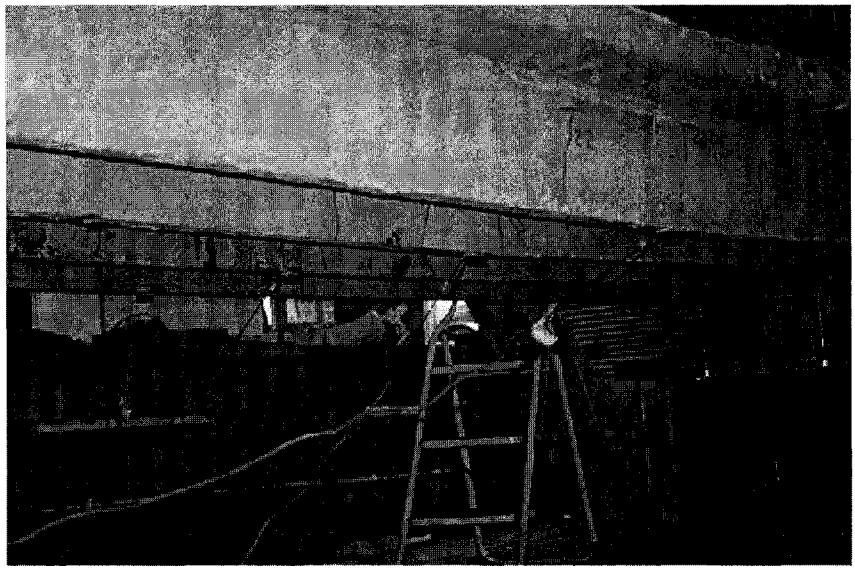

Figure 6.9: Cracking of Composite Joint Connection Prior to Ultimate Load

Figure 6.10: Crack at Mid-Span at the Ultimate Load

For the connection associated with the composite and welded joint, the observed cracking behaviour was consistent with that observed for the CFRP. That is to say, the rate of cracking and number of cracks were all consistent with the CFRP test

observations. The only difference is that the initial crack did not form until approximately 24 kN.

6.2.2 Deflection Response

As noted in Section 5.2.2, the deflection response of all double tee systems was monitored. Specifically, the deflection of the webs at center span was measured. This section will review the results for the three different connection types. For reference purposes, each measurement location was given a different designation. These designations are shown in Figure 6.11.

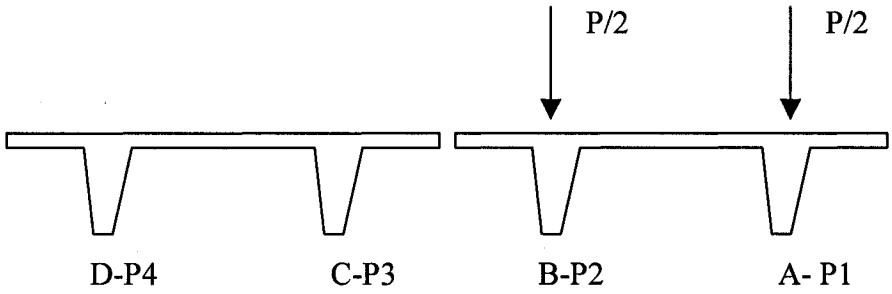

Figure 6.11 Designations for Deflection Measuring locations.

First, the system with the welded connection will be reviewed. Figure 6.12 shows a plot of load versus deflection for all four deflection measuring locations. From this Figure, it was observed that the webs under the load (webs A and B) deflected in an almost identical fashion to each other. It was also observed that the formation of the cracks, specifically at the initial crack value of approximately 17 kN (see Section 6.2.1), drastically affected the rate at which the webs deflected with respect to each other. From Figure 6.12, it was also observed that the deflection of each web followed a linear path up to the load associated with that particular web's first crack. For the case of the welded connection system, the linear range for webs A, B, C and D appears to be up to loads of

approximately 17kN, 18kN, 26kN, and 33kN, respectively. Figure 6.12 also clearly identifies the ultimate load, as the deflection continued to increase with no increase in load carrying capacity.

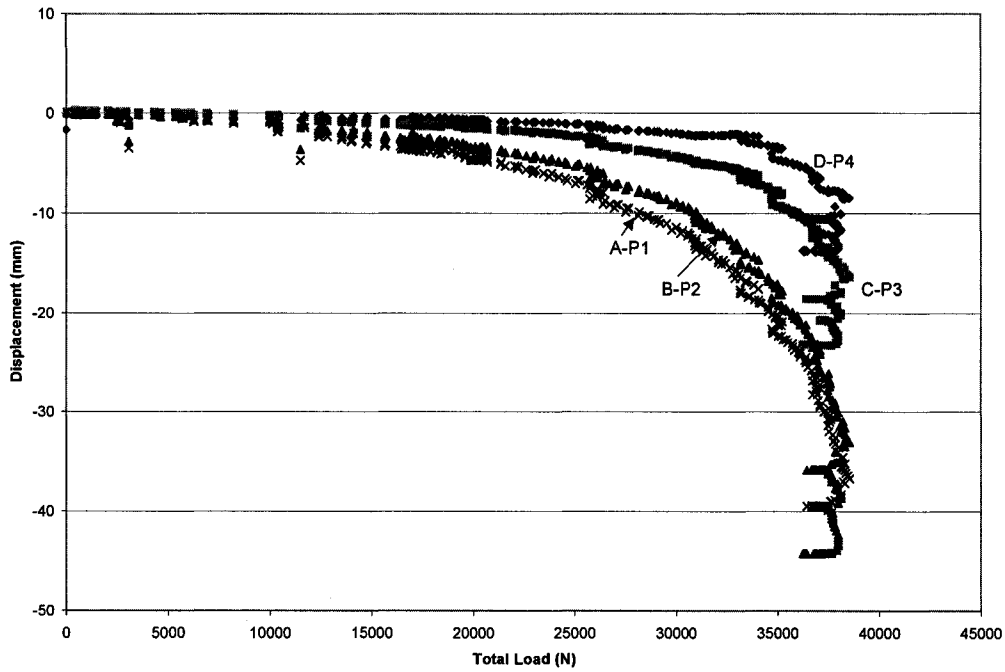

Figure 6.12: Load Deflection Response for Welded Connection System

Some observations are made about the deflection response for a welded connection system. Figure 6.13 shows a photograph of one of the welded systems under load. It was observed that the loaded double tee (refer to Figure 6.11) deflected to form a curved path, as would be expected. The unloaded side of the system exhibited very little visible deflection response. From the photograph on right side of Figure 6.13, the web seen in the background corresponding to web D appears to be straight compared to web A in the foreground of the same photograph. It was also observed that once the ultimate load was reached, the loaded member clearly started to rotate outwards, as shown in Figure 6.14. This could best be seen by looking up from the underside the double tee between the webs.

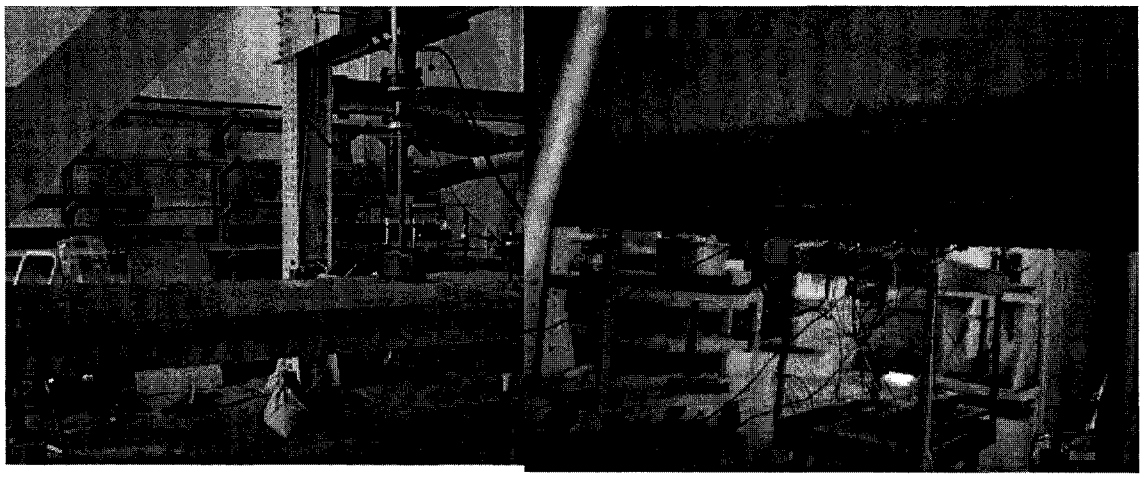

Figure 6.13: Welded System Under Loading

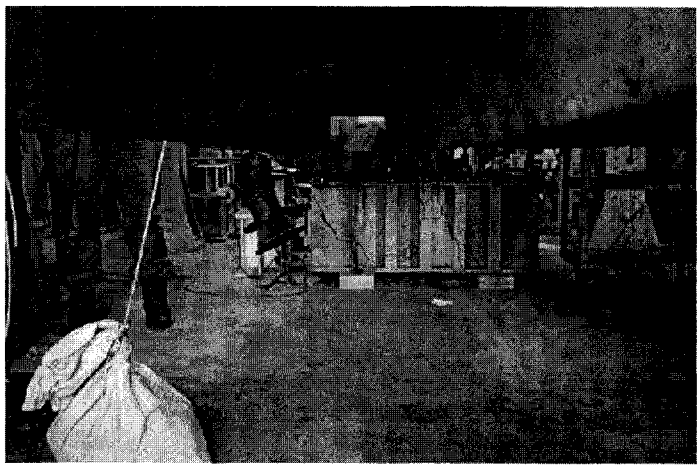

Figure 6.14: Photograph Looking at Webs of Welded System (at Ultimate Load)

The next connection type examined was the composite connection. Generally, this system yielded the best overall performance of all the systems tested, with respect to deflection response. Referring to Figure 6.15, the linear region for each of the measured locations terminated close to each other. As well, they terminated at a higher load than the system with the welded connection. From a review of Figure 6.15, the loads associated with the end of the linear range for webs A, B, C and D are, approximately 20 kN, 20 kN, 22.5 kN, and 24 kN, respectively. It was also noted that webs A and B appear

to have deflected nearly the same amount at all times, with A being only slightly higher than B due to the development of a torsional moment.

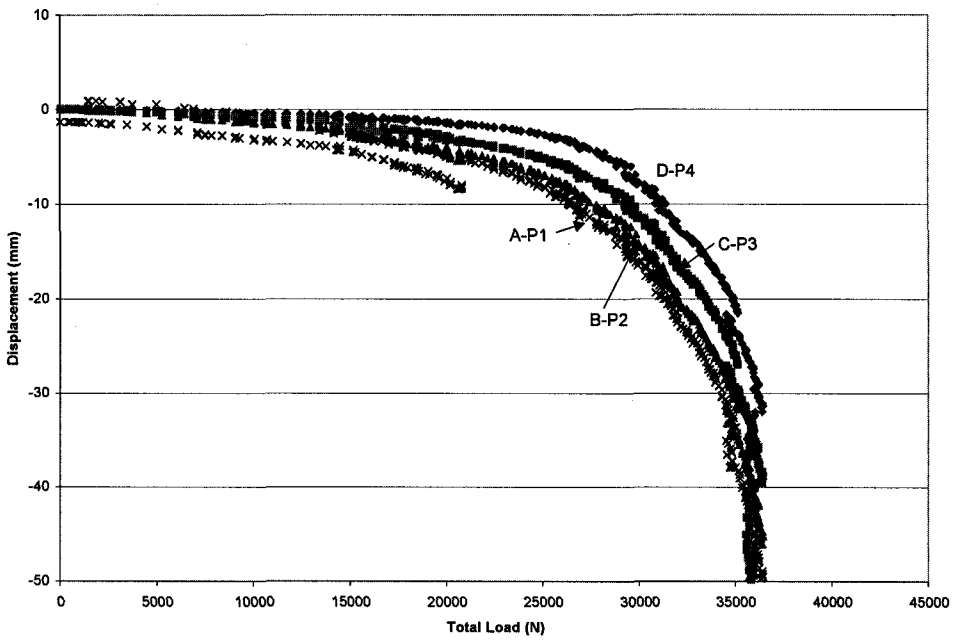

Figure 6.15: Deflection Response of Composite Connection System

When comparing Figures 6.12 and 6.15, the difference between the welded system and the composite system is not clearly visible until the load in the welded system reached the non-linear range. The first significant difference is the composite system continues to act in a linear fashion until a higher load than its welded counterpart. Substantial differences are visible, particularly in the non-linear range. Firstly, for the composite system, the difference in deflection in the non-linear range between the gauges appears to be near constant, until the ultimate load is reached. If attention is now placed on the overall performance of the system, in the non-linear range, it can be noted that the ductility of the system is much higher for the composite than for the welded system. That is to say that the response of the composite system gives ample warning before failure of the system.

From a visual inspection of the composite system during loading, some observations were made. This connection type resulted in deflections that were by far more visible. Figure 6.16 shows a photograph of one of these specimens as it nears the ultimate load. Such a visible deflection was not noted during the welded connection tests. Moreover, referring to Figure 6.17, it was observed that the flange to flange connection appeared to be bending under the applied load. This bending is suggestive of the formation of two-way action in the system, and is characteristic of this connection type, but not of the welded connection. From all of these actions, the overall system appeared to take on a "dish shape", which is to say the performance was characteristic of a loaded two-way slab system.

Figure 6.16 Composite System Under Load

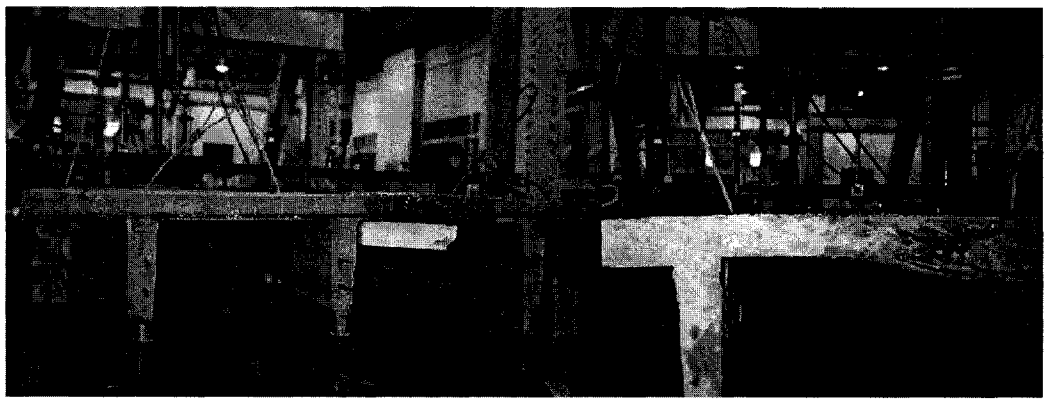

Figure 6.17: Close-up of the Composite System's Joint Under Loading

Finally, the connection associated with both the welding and the use of advanced composite system was examined. This specimen's deflection response, seen in Figure 6.18, demonstrates a combination of both the previous systems. It was first observed that webs A and B demonstrated greater deflection than C and D, as was seen during the welded connection tests. Like the composite system, the linear range of the load-deflection curve extended past that of the welded system. In fact, the loads associated with the intersection of the linear and non-linear ranges for webs A, B, C and D appear to be approximately, 24 kN, 24 kN, 25 kN, and 25 kN respectively.

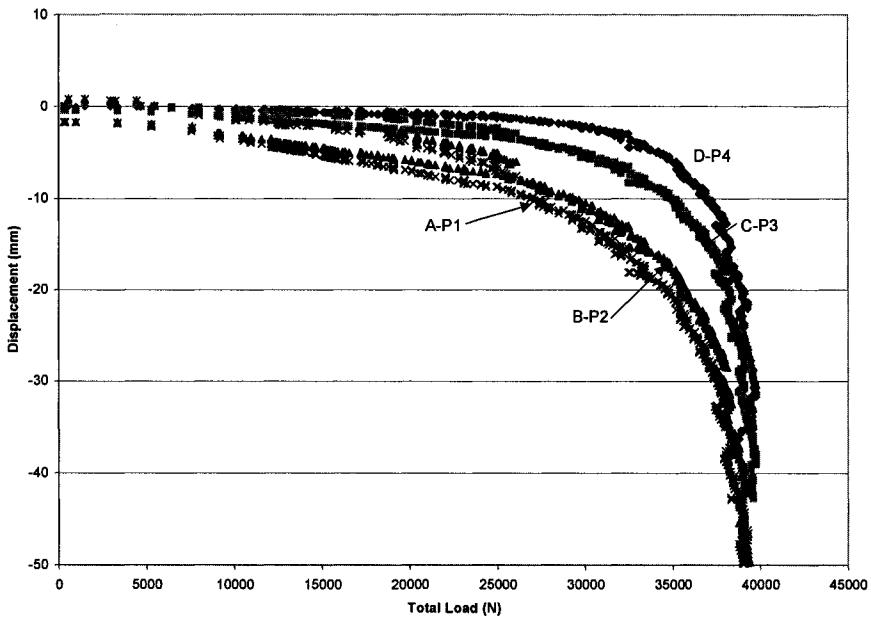

Figure 6.18: Deflection Response of Composite-Weld Connection

The overall performance of the composite-weld connection appears to be a combination of the two individual connections. That is to say, the results shown in Figure 6.18 appear to lie between those of Figures 6.12 and 6.15. Like the composite connection, in the non-linear range, the differences in deflection between the webs appear

to remain near constant. Also, the response near failure is closest to that of the composite connection; the system exhibits a more gradual increase in the load-deflection response.

As already mentioned, the observed deflection response was closest to that of the composite system. This is partly attributed to the fact that the deflection was not visible until the non-linear range was reached. Once again, (see Figure 6.19) the characteristic "dish shape" was observed, which is associated with bending of the flanges.

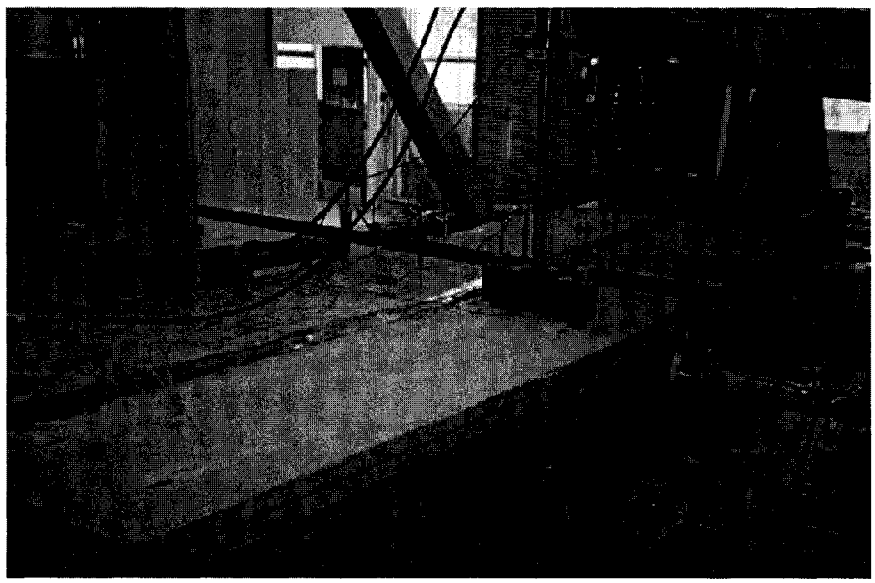

Figure 6.19: Composite-Weld System Under Load

6.2.3 Distribution of Reaction Forces

As mentioned in Sections 4.4.1.2 and 5.2.2, the reaction forces were monitored for all connection types tested. This section will outline the results obtained from these measurements. The results for all three connections are shown in Figure 6.20(a) through (c).

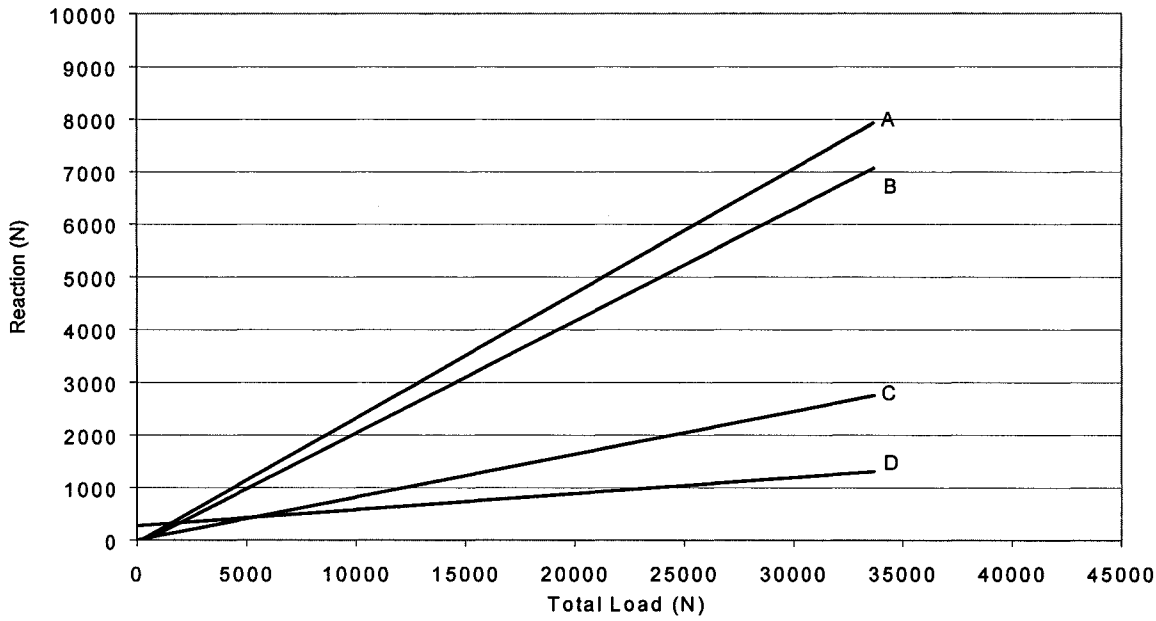

Figure 6.20(a): Reaction Distribution for the Welded Connection

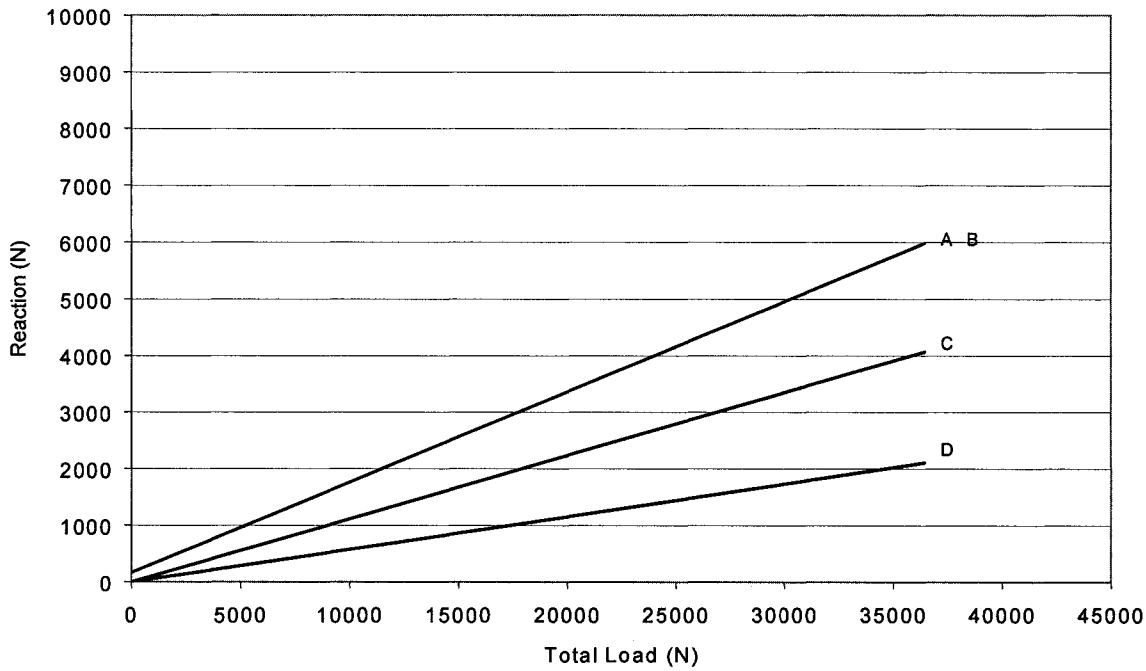

Figure 6.20(b): Reaction Distribution for the Composite Connection

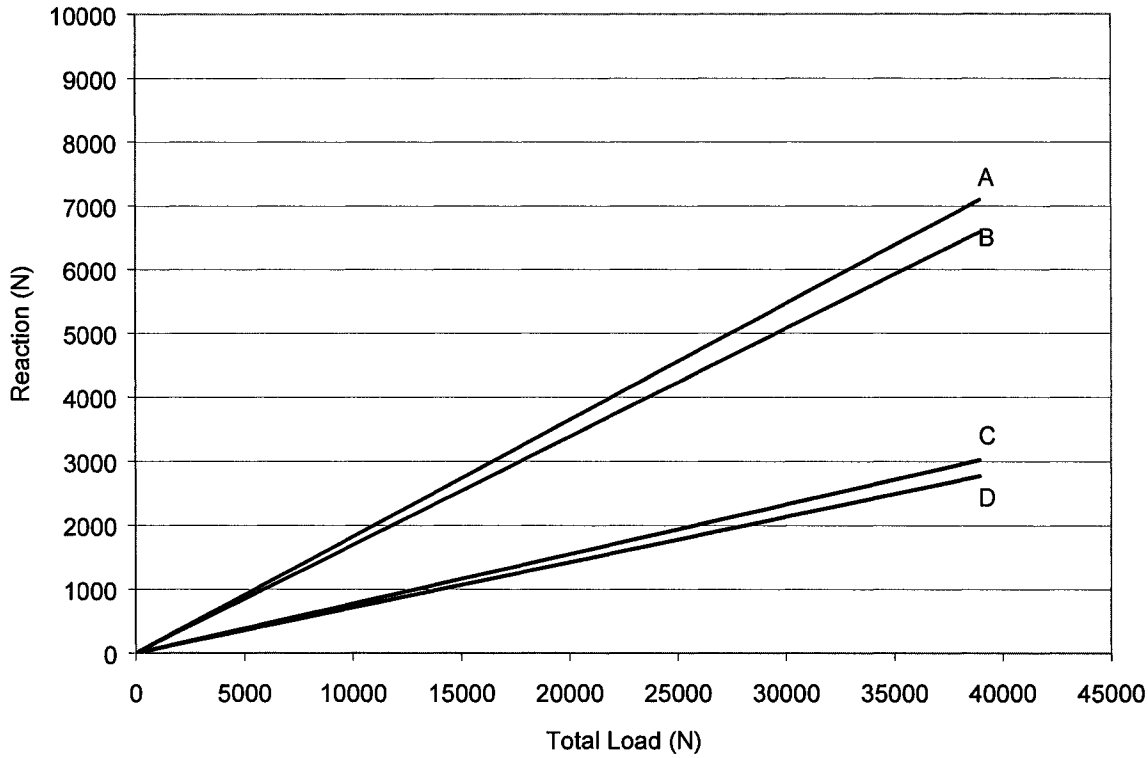

Figure 6.20 (c): Reaction Distribution for the Composite-weld Connection

From Figure 6.20a (welded connection), it can be found that the majority of the load was carried by webs A and B, as would be expected. From this Figure, it appears that web A tends to take a slightly higher load than B. This situation can be attributed to the constraints placed on the system by the connection. Webs C and D appear to take a much lower component of the load than A and B. This reduction in C and D is associated with the contribution of the twisting of the section.

If the reactions for the composite connection are now reviewed, see Figure 6.20(b), some slight differences are observed, when compared to that found in Figure 6.20(a). While webs A and B still carry the majority of the load, webs C and D appear to

be carrying more of the applied load. All webs will not carry the same load because of the applied torsional moment; however, there does appear to be an improved load carrying ability for this case. This connection appears to shift lines A and B down while notably shifting lines C and D up.

Finally, the case of the composite-weld connection's response is shown in Figure 6.20(c). This connection presents the best performance, relating to the load sharing, with webs A and B carrying almost identical loads, and webs C and D also doing the same. This connection appears to exhibit the best load sharing of all the connections tested, as it combines the effects of the two individual connection types.

6.2.4 Longitudinal Strain Response

This section focuses on the longitudinal strains that developed at the 2100 mm location. It was observed that the longitudinal strains, measured above the webs at the end of the specimen, were consistent with the expected values. The writer will only focus on the strains of the top surface of the web at x = 2100 mm, as the longitudinal strain measurements taken near the connection exhibited stress concentrations associated with that connection type. This situation will be addressed in the next section.

For the purpose of clarity, the web identification developed earlier in Figure 6.7 will once again be used. The results from all of the systems are provided in Figure 6.21 (a) through (c).

Referring to Figure 6.21 (a), the data provided is associated with the welded connection system. As can be seen, the measured strains are relatively constant for all gauges. Moreover, as would be expected, web D exhibited the least strains of all four locations for the majority of the loading. It is also noted that the strain vs load curves appear to maintain an almost linear path until just prior to failure. Altogether, this suggests that the connection has little effect on the distribution of the bending stresses in the system; therefore, no stress concentrations formed, in these regions, as a result of the connection.

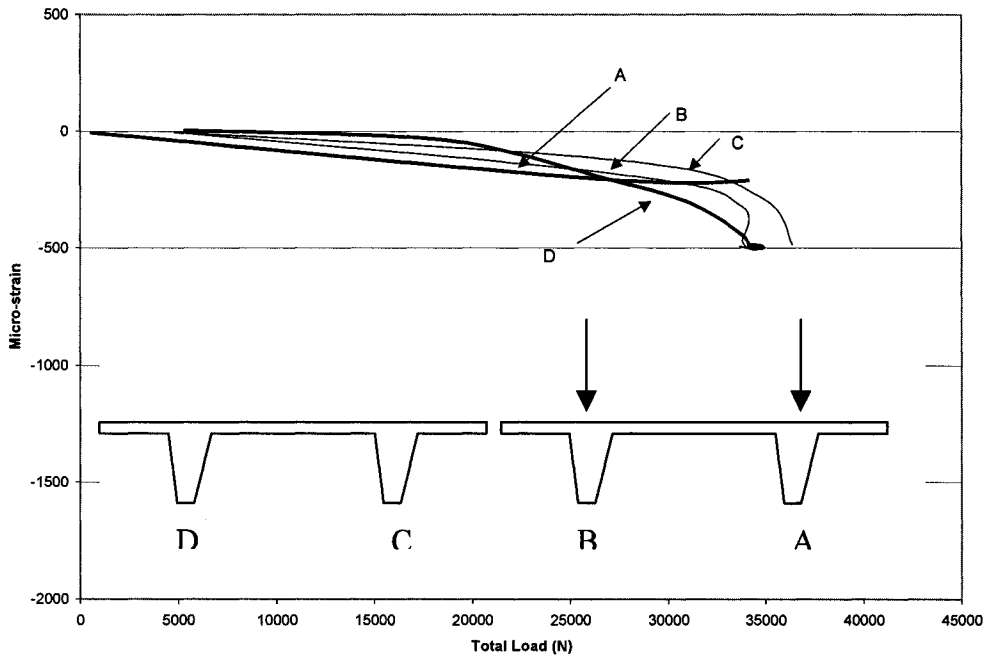

Figure 6.21(a): Longitudinal Strain in the Flange vs. Load for the Welded Connection

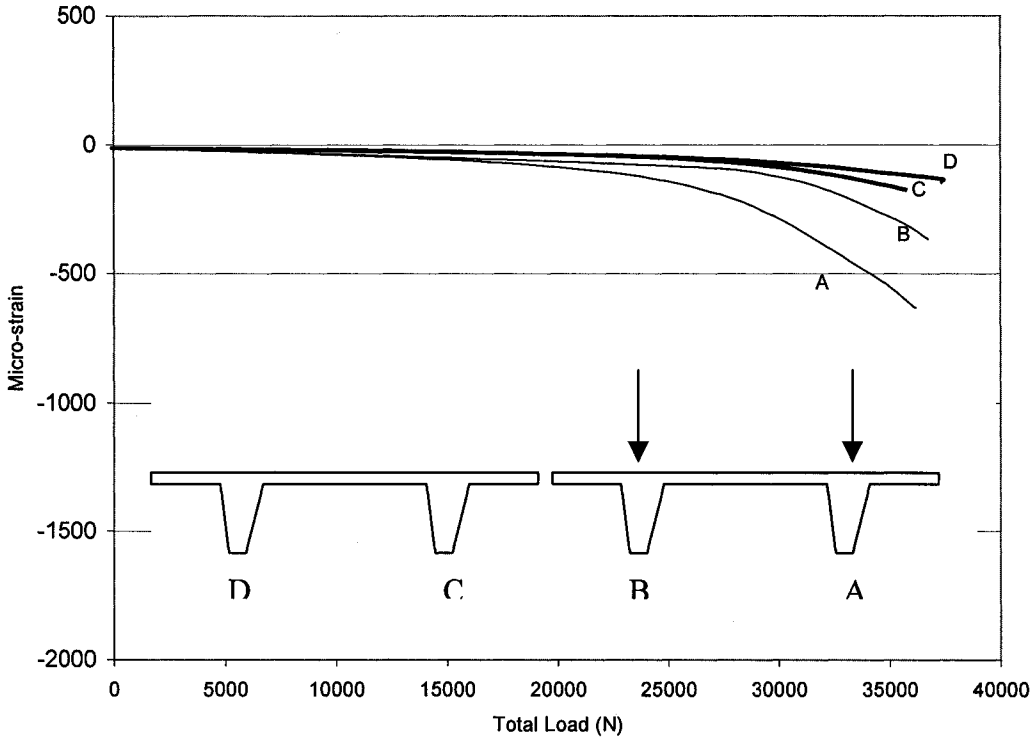

Figure 6.21(b): Longitudinal Strain in the Flange vs. Load for the Composite Connection

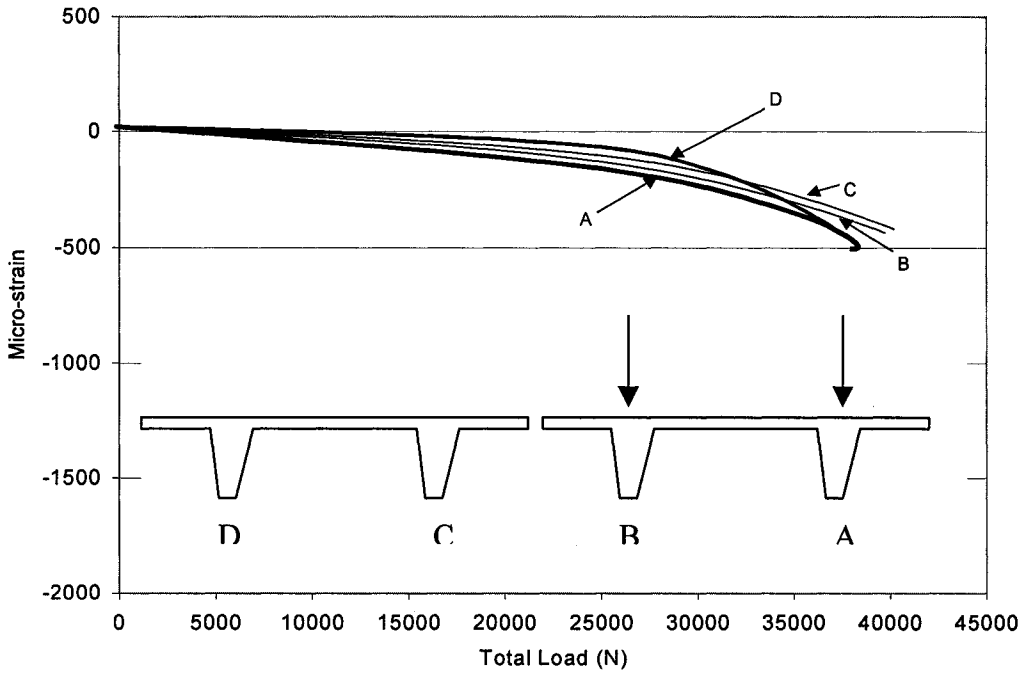

Figure 6.21 (c): Longitudinal Strain in the Flange vs. Load for the Composite-Weld Connection

The next case examined was the system containing the composite connection. This system exhibited some small variation from that of the welded connection, refer to Figure 6.21(b). The strains in webs A and D appear to perform in a similar manner to that of the welded connection. It was also noted that web A, which is directly under the load, exhibits the highest strains at all loading values, as would be expected. If consideration is given to the path for each web, C and D appear to perform in a linear fashion until just prior to failure. The distribution of the strain paths agree favourable with the observed deflection profile. The high strain, which can be related to the largest deflection, occurs at A while the lowest strain and deflection occur at D. Webs B and C lie between A and D suggesting a curved cross-sectional profile during loading.

Finally, consider the case of the composite-weld connection system data shown in Figure 6.21(c). The results of these measurements appear to be consistent with a combination of the two previous cases; however, the overall performance is closer to that of the welded connection. Webs B, C and D all tended to exhibit very similar strains during the entire loading process, while web A exhibited the greatest variation. This combination appears to exhibit the best overall performance in terms of the longitudinal strain distribution.

Overall, the three systems act in a similar fashion to each other. Moreover, the system's performance at any given percentage of the ultimate load (rather than the actual load itself) appears to reveal near identical strains irrespective of the connection type.

For example, the strains at 60% or 90% of the ultimate load revealed near identical strains; however, the corresponding loads for the various systems are different.

6.2.5 Strain Development at Connections

This section will focus on the results of the strain measurements, via strain rosettes, in the region of the connection. It is recalled that rosettes were placed on both sides of the connection at approximately 37.5 mm away from the member's edge, at distances of 190 mm and 2100 mm, from the right end. For the purpose of clarity, the rosettes were numbered as shown in Figure 6.22. Furthermore, the presentation of the results will be given such that the results/trends of the three different connections are shown on the same graph for the purpose of comparison. In addition, the data will be presented as an average weighted trendline due to the volume of recorded data. The definitions of positive and negative normal and shear strains (according to the system used in this work) are given in Figure 6.23.

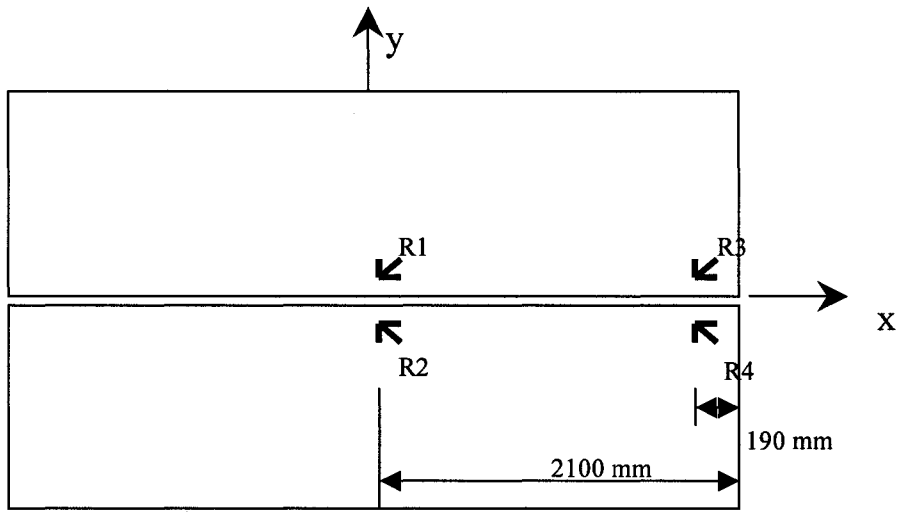

Figure 6.22: Rosette Numbering System

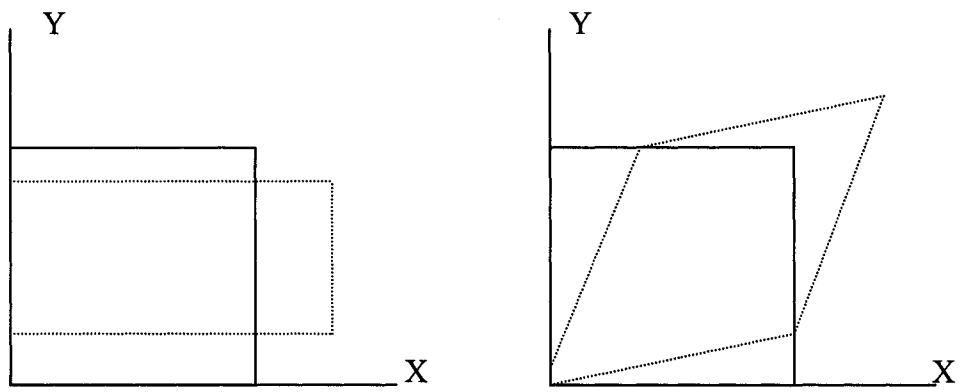

Positive normal strain in the X and negative in the Y

Positive Shear Strain, no normal strain

Figure 6.23: Definition of Sign Convention for Strain

This discussion will begin with a review of the strains measured in the longitudinal direction (ε_x), see Fig 6.24. First, consider the strain transferred across the joint from R1 to R2. At R1 the composite-weld connection appears to perform at a midway between the weld and composite, respectively. If the results of R1 and R2 are compared for the composite and composite-weld systems, it can be found that the paths are near identical, thus the strains are the same on both sides of the connection. For the welded system. The strain jumps substantially as the joint is crossed. Note that on the R2 side of the welded connection, the strain exhibits the highest levels of all three connection methods. This suggests that the presence of the intermittent welded connection tends to introduce substantial stress concentrations into the unloaded side of the system. The responses seen in Figure 6.24 reflects the observed deflected shape. The welded connection exhibits the largest variation in the

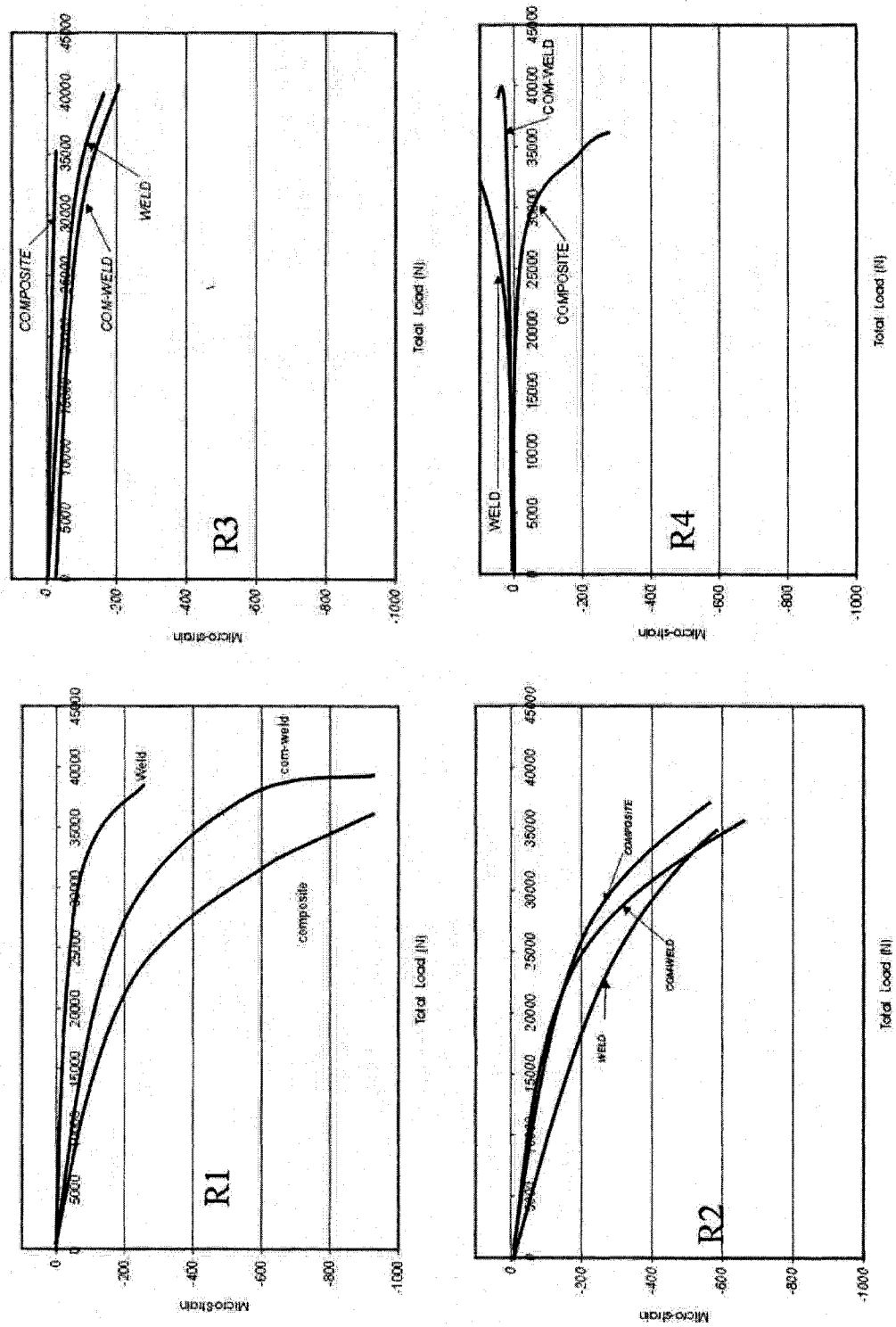

Figure 6.24: Comparison of Strains in the Longitudinal Direction at the Connection

longitudinal strain as the joint is crossed. This suggests that the welded connection tends to induce high strains in the region surrounding the connection.

Referring to the results for gauges R3 and R4 in Figure 6.24, a substantial difference is observed between the performance of the system on either side of the connection. In the case of the composite connection at R3, the measured strain was near zero while, for the other two cases, the strain maintained a relatively low compressive value. It was also noted that the paths of gauges R1 and R3, for the welded system, were very similar in nature, while the composite-weld and composite connections demonstrated greatly reduced stresses, when comparing the same gauges. Once the response at R4 was considered, some significant differences were noted. In particular, the strain in the composite system increased notably and the welded system went from compression on the load side to tension on the unloaded side. Meanwhile, for the combined composite-weld case the strains appear to approach zero at R4.

Continuing the current discussion, the response of the four gauges in the transverse direction (ε_y) will now be considered. The results of this analysis are provided in Figure 6.25. As might be expected, both systems that contained the composite material exhibited tensile strains at R1, which is consistent with the bending of the flange, noted earlier in Section 6.2.4. This tensile strain directly transferred across the joint in both cases; however, the strain levels increased at R2 with respect to R1. Unlike its composite counterpart, the weld exhibited significantly different behavior; in particular,

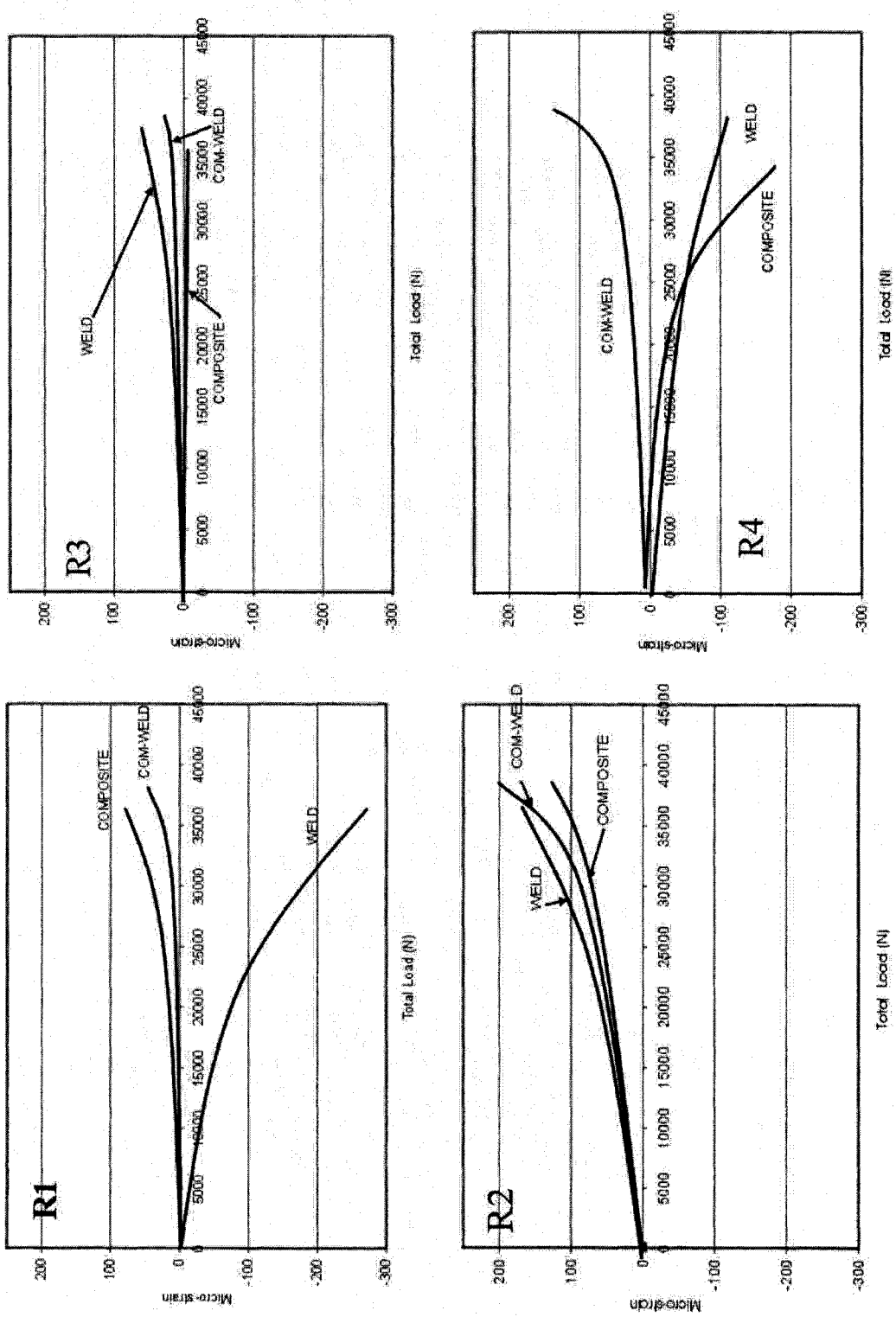

Figure 6.25: Comparison of Strains in the Transverse Direction at the Connection

gauge R1 revealed a compressive strain. Once the joint was crossed, this compressive strain reverted to a tensile strain at R2. These sign changes suggest that the region around the connection is being bent downward in order to maintain a level joint transition. It is also noted that, with respect to R2, all three of the systems tested performed in a very similar fashion to each other, resulting in the trendlines nearly overlapping.

As was the case in the longitudinal direction, the transverse direction strains at gauges R3 and R4 exhibited different tendencies when compared to their R1 and R2 counterparts. At gauge R3, the weld and composite-weld systems both revealed tensile strains, albeit at low values. The composite system appears to carry a slightly compressive strain, if any strain at all. On the unloaded side of the joint at R4, the composite and weld experienced notable compressive strains while the composite-weld experienced an increase in tensile strain. Referring to Figure 6.25, the shift in the weld and the composite system's curves appeared to be similar in nature, when comparing R4 to R3.

Finally, referring to Figure 6.26, consider the response of each system in terms of shear strain. From the load-shear strain relationship for R1 it is clear that the weld case lies between the composite and composite-weld cases. The welded system appears to had high shear strains in the region around the load, while the composite system's shear strain is substantially higher in the same region. When comparing these R1 results to the findings at R2, some observations can be made. What is of interest is

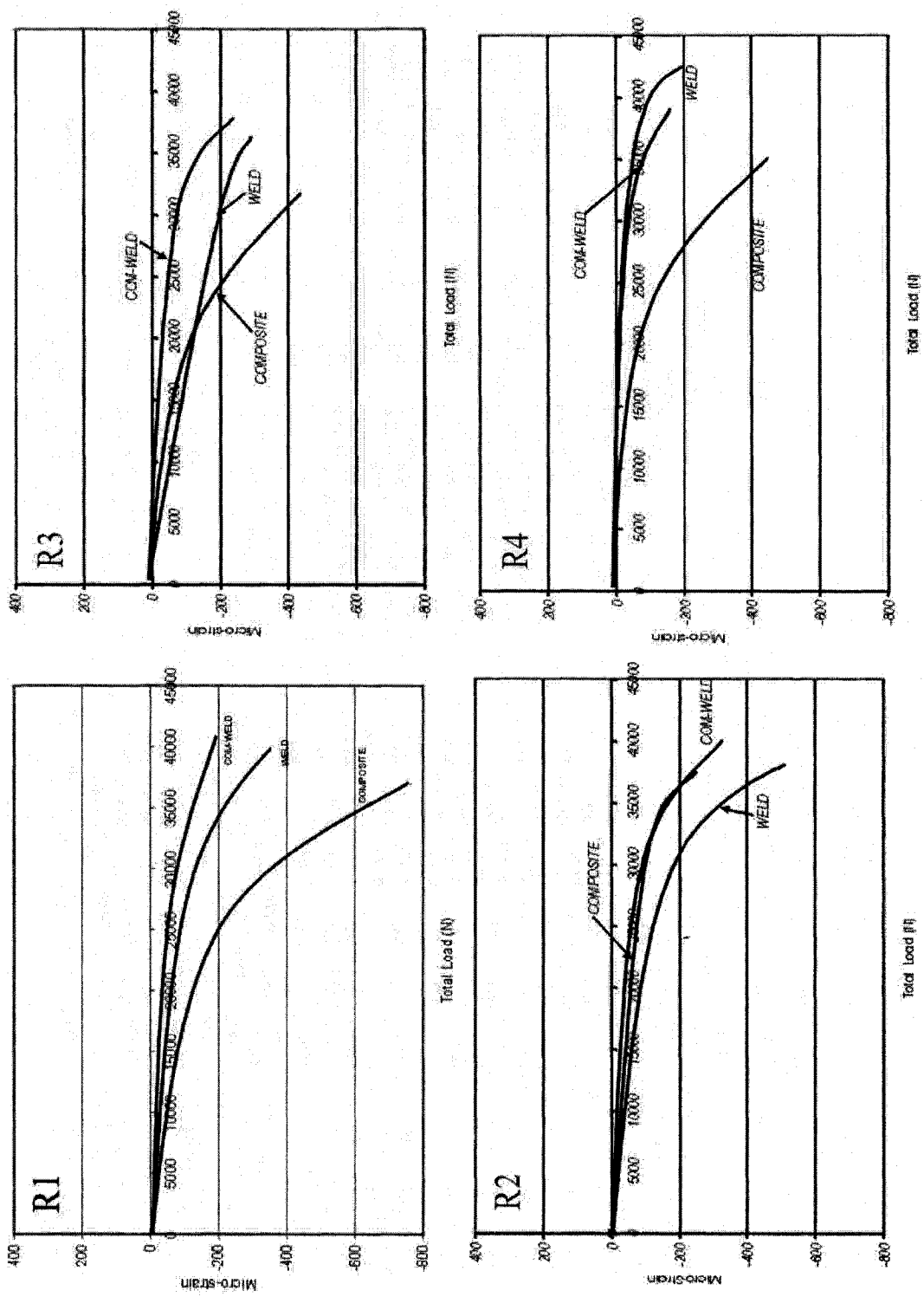

Figure 6.26: Comparison of Shear Strains at the Connection

the welded system and composite-weld system both have very similar behaviour/tendencies on either side of the joint (R1 to R2). In fact, the paths for these systems tend to overlap each other.

Moving to gauges R3 and R4, the performance in this region is notably different from that observed at the R1 and R2 locations. What is of particular interest is the performance of the composite system. Unlike at the 2100 mm location, the shear strain paths at the 190 mm location (R3 and R4) came close to overlapping each other. Meanwhile, the weld and composite-weld systems tended to reverse their signs. In the case of the welded system, the shear strain not only changed from negative to positive, it also increased in terms of absolute maximum value. The composite-weld system manifested a drastic reduction in shear strain, which resulted in near zero readings for the most of the loading time.

The performance of all members reviewed in this section provided results that were agreeable with the laboratory observations. Specifically, the response at each rosette tended to agree with the deflected shape. As there was a noted difference between the deflected shape of the welded system and the composite system the stresses and strains were affected. This effect was more pronounced at the centerspan location than the end locations, due to the restraint present in that region.

6.2.6 Ultimate Load

As mentioned earlier, each system was taken up to its ultimate load. This phase of work yielded some interesting results, which will be discussed here in detail. It is

recalled that the specimens were cast in two separate sets. Therefore, the results of each test are compared with the findings from the individual double tee test, corresponding to that particular set (refer to Section 6.1). As each connection test required two members, each member was taken from the same set to ensure equal strength on both sides of the joint. As mentioned in Section 6.1, the ultimate loads of sets 1 and 2 were 15.9 kN and 18.4 kN, respectively. These loads corresponded to members comprising of concrete, with compressive strengths of 62 MPa and 70 MPa, respectively. It was also observed that all members failed in flexure.

Consider first the case of the welded connection. Both welded connection systems were made of set 2 members. These systems were able to sustain loads of 33.7 kN and 38.5 kN which, when compared with the individual member's value, gave ratios in the order of 1.83 and 2.09, respectively. Taking an average of these numbers would suggest that two welded members yield a system able to take a load equal to twice the individual member's strength. Thus, no extra strength was observed to have come from using this connection type.

Now consider the case of the composite connection. These connection systems were made of set 1 members, and had ultimate load values of 35.8 kN and 36.4 kN. This results in individual to system ratios of 2.25 and 2.29. Therefore, the addition of the composite material appears to create a situation that allows the system to obtain a strength increase of approximately 25 % with respect to an individual member.

Finally, consider the case of the composite-weld connection. These systems were made of set 2 elements, and experienced ultimate loads of 39.3 kN and 40 kN. These

ultimate loads corresponded to 2.14 and 2.17, respectively, times the ultimate strength of the individual member. As was the case in the composite connection, this connection type appears to afford the system an increase in loading capacity, of approximately 14-17 % (of individual member's ultimate load). The combined connection does not yield as favourable results as does the composite material by itself. Thus, the presence of the weld appears to create a situation that reduces the effectiveness of the composites force/stress transfer mechanisms.

It should be pointed out that each member failed in flexure, at approximately midspan. The effect of stress concentrations in this region and, thus the transfer of these forces across the joint, appear to play a significant factor in the member's apparent load carrying capacity. Thus, the effects, seen in the last section at R1 and R2, appear to be of more importance to the current investigation than that of R3 and R4.

6.2.7 Dynamic Response

As mentioned in Section 5.2 a dynamic test was performed on each of the systems, at different stages of loading. Figures 6.27 (a) to (c) show plots of acceleration versus time for the three different connection types. While each of these plots correspond to the highest drop position, it was noted that these findings were in line with those observed for the "low" drop position (refer to Section 5.2.2). It was observed that the type of connection had no notable effect on the system's dynamic response; however, other key observations were made.

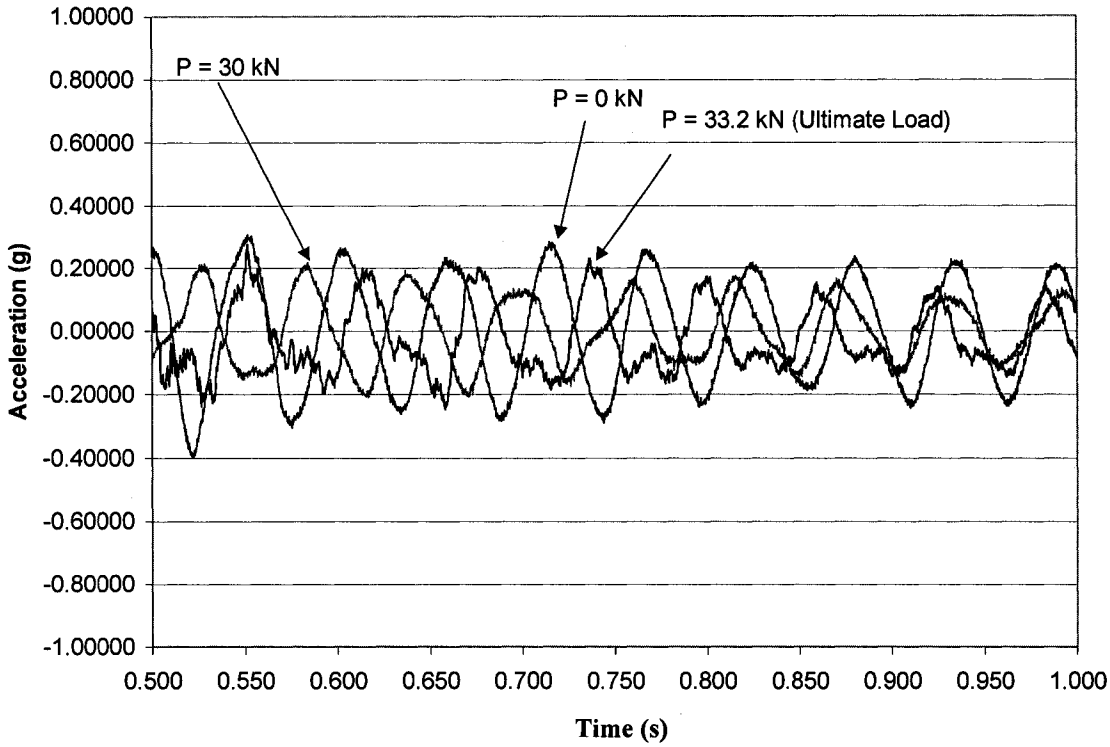

Figure 6.27 (a): Acceleration vs. Time for Dynamic Excitation of the Welded System

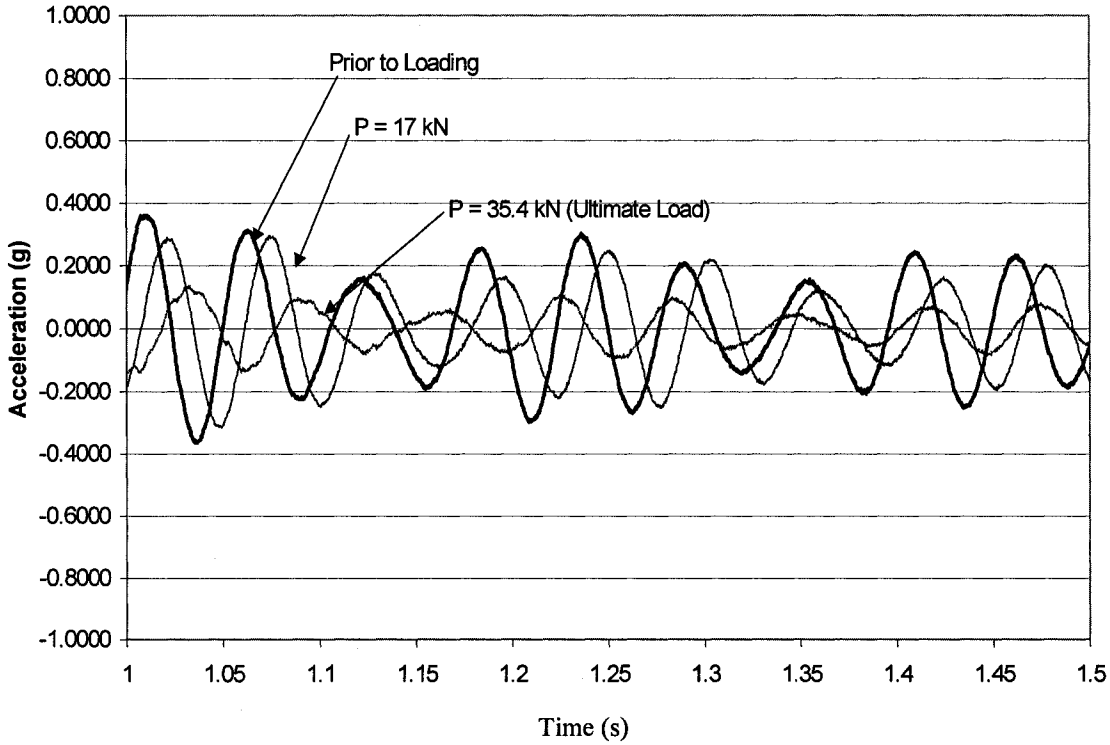

Figure 6.27 (b): Acceleration vs. Time for Dynamic Excitation of the Composite System

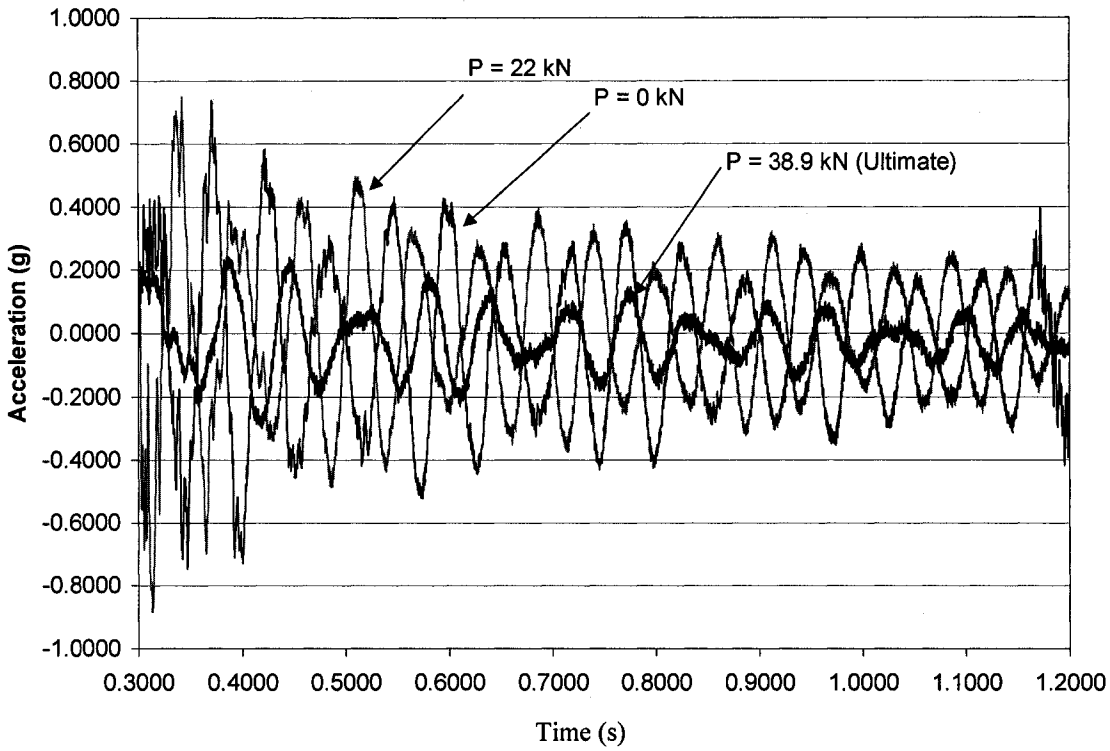

Figure 6.27(c): Acceleration vs. Time for Dynamic Excitation for the Composite-weld System

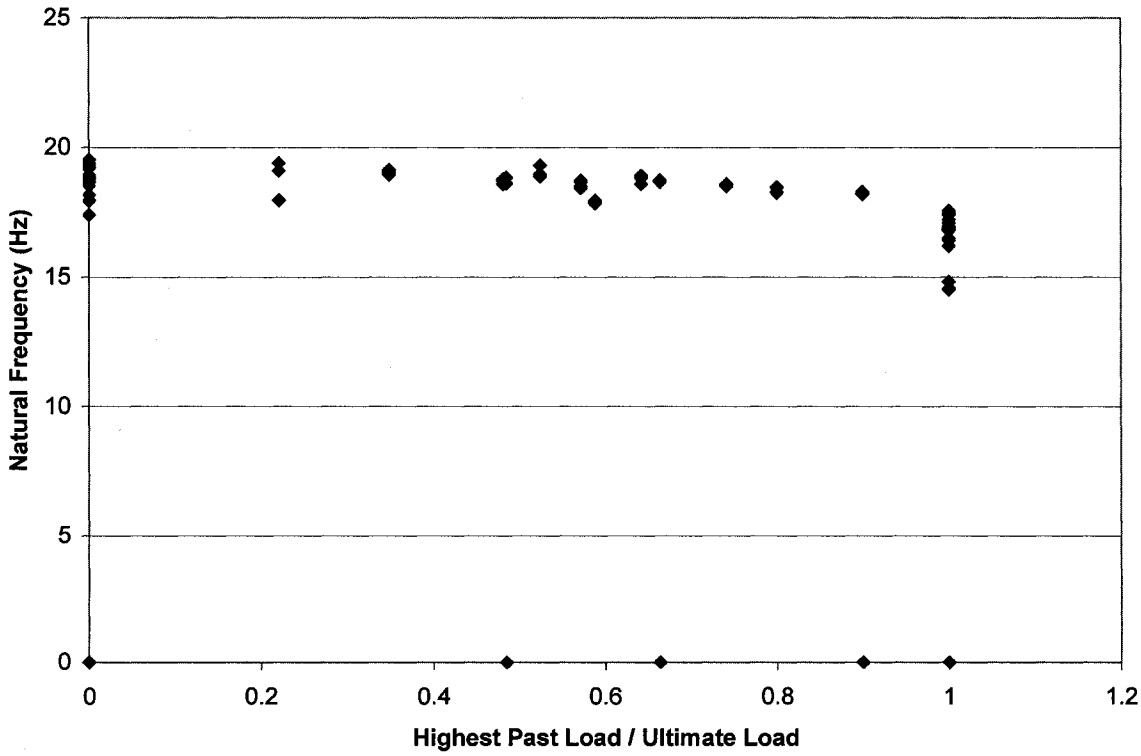

Figure 6.28: Natural Frequency vs Normalized Highest Past Load

The first calculation was to determine the natural frequency of the system. It was of interest to determine the effect that past loading conditions have on the system's response. As shown in Figure 6.28, the presences of the cracks appear to have little or no effect on the system's natural frequency, for the tests conducted. This is not to say that the cracks do not effect the natural frequency but rather this was the case for the magnitude of the impact load provided in the lab. This is supported by the presence of some variation in the natural frequency after the ultimate load is achieved. The ultimate load was accompanied by spalling of the concrete materials around the cracks. These systems also showed an inability to completely close all cracks after the introduction of excess deflection (post ultimate loading). This would suggest that, indeed, the natural frequency does change in the presence of cracks. Unfortunately, this is only true in situations where the formed cracks are unable to completely close or the input force, P(t), generates a system of stresses great enough to open the crack(s).

These systems also exhibited similar damping properties. Specific calculations using known methods, such as Logarithmic decrement, tend not to apply here. This is associated with the complexity of the damping systems at work in the system. As pointed out by Chopra (1995):

> *"In actual structures, however, many other mechanisms also contribute to the energy dissipation. In a vibrating building these include friction at steel connections, opening and closing of microcracks in concrete..."*

Therefore, some general observations are derived from the response of these systems. From Figure 6.27 it is obvious that as the size and number of cracks increase, with increasing high past loads, the system tends to dampen the excitation at a greater rate. The greatest damping occurs in systems that have attained their ultimate load.

6.2.8 Response to Lateral Loading

This section will focus on the results obtained from the lateral load test. The results will be presented in two stages, first the longitudinal strains, associated with bending, as measured above each web will be investigated. The strains at the joints will then be examined.

As stated above, the longitudinal strains, measured in the top flange above each of the webs (at 2100 mm from the end) will be discussed first. The results of this testing can be found in Figure 6.29. Consider first the results from the welded connection system. From the data it is evident that this system is not acting like a single flexural member (webs A and B in compression and C and D in tension). While A and D do tend to demonstrate this characteristic, B and C suggest a rather different mechanism at work. Based on a review of all the data, the connection itself appears to be placing a significant tensile strain into the system along this cross-section. This introduction of tensile strains appears to result in only a small compressive strain developing at C and a very high tensile strains developing at B. This suggests that the connection is not allowing the diaphragm to act as a single beam, however it is preventing the system from acting completely as two separate systems. Therefore, the weld introduces a combination of

these two cases. However, because of the similarity between B and D the system is closer to representing two independent members in bending rather then one system.

The next system involved the composite connection. This system acted drastically different from that of the previous connection. First, referring to Fig 6.29, when compared with the welded connection results, the maximum tensile strains is drastically reduced, thereby suggesting an improved strain/stress distribution. If consideration is given, with respect to the distribution of the strains in all the webs, it is noted that the strains and thus the stresses appear to be representative of a single flexural member in bending. As A and B appear to be mirrored about the "x" axis by C and D, this suggests that the joint represents the location of the neutral axis. Therefore, the composite connection by itself creates a situation whereby the system acts in a monolithic fashion.

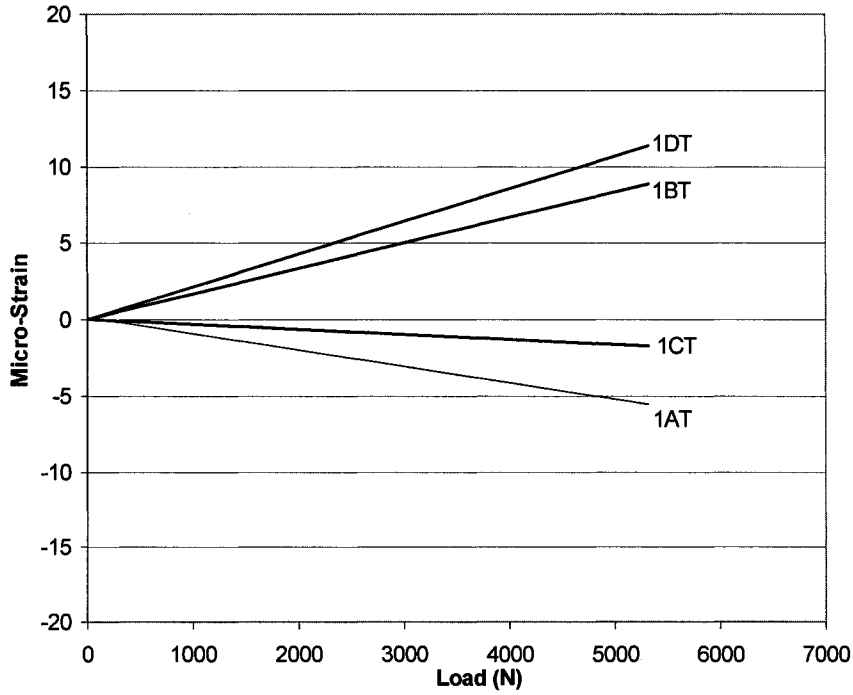

Figure 6.29(a): Longitudinal Strains Developed By Lateral Loading in Welded Connection

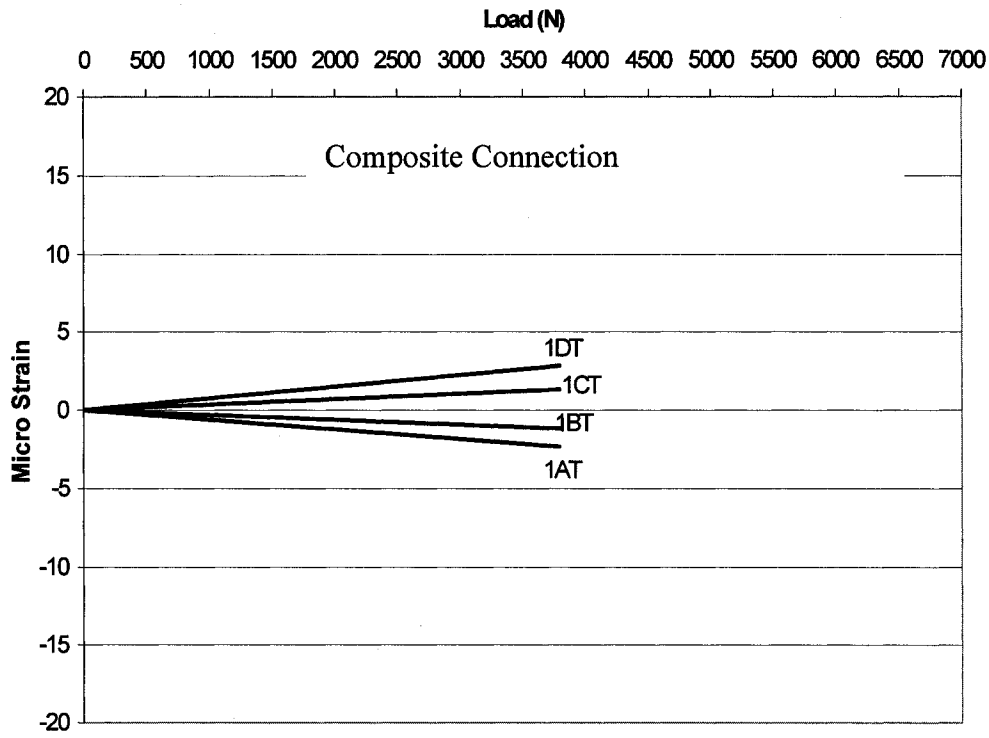

Figure 6.29(b): Longitudinal Strain Developed by Laterial Load in Composite System

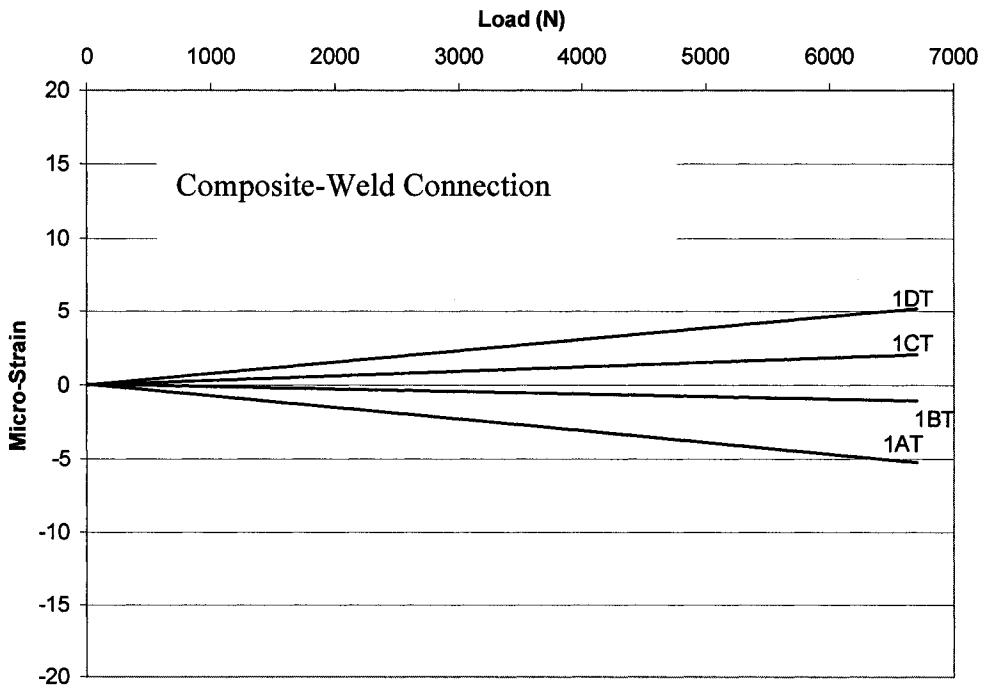

Figure 6.29: Longitudinal Strains Developed By Lateral Loading in Composite-Weld System

Finally, Consider Figure 6.29(c) which provides the results for the composite-weld connection system. As was the case many times before, the combined connection appears to act as combination of the composite, and welded systems acting together. However, the writer does acknowledge that the overall performance of this system is more representative of the composite system. This system suggests that once again the top member (if viewed in plan) acts in compression, while the bottom member acts in tension. This is a situation synonymous with the response of a flexural member. However, as was the case in the welded system, the compressive strains in A and B appear to be small in comparison with C and D. In the welded case this shift, or tendency, was associated with a tensile stress/strain concentration forming at the connection. Indeed it appears from the data that the introduction of the weld appears to have re-introduced this tensile strain concentration, thereby causing an apparent shifting of the neutral axis, away from the joint.

Overall, the only system that acted as a true flexural member, and thus a diaphragm, under lateral loading was the system containing the composite connection. Moreover, this system exhibited the lowest increase in strains and thus the best stress/strain distribution.

The composite-weld connection did exhibit an ability to act as a diaphragm, in comparison to the welded connection. However, the introduction of the welded connections did appear to effect the overall system performance, but not nearly to the extend that was observed in the welded connection system alone.

In support of the above observations and discussion, some more observations were made when investigating the performance of the system near the connections (at the rosette locations). As the investigation associated with the flexural action is most easily observed near the center-span the writer has elected to focus solely on the R1 and R2 locations (see Figure 6.22). The findings from R3 and R4 revealed no new information from that observed at the R1 and R2 locations.

Refer to Figure 6.30 for the results from the welded connection test. As would be expected, for a system acting as two near independent components, the longitudinal strain (x direction) at R1 is a very high tensile value, while R2 exhibits a moderate compressive value. The strains in the transverse (y direction) appear to be constant across the connection. What is of importance to the determination of the overall diaphragm performance is the shear strain, thus the shear stress. For both locations the value of γ_{xy} appears to be near zero, which would be expected at a free edge of a member in bending. In a diaphragm system this number should be near its maximum as the test setup placed the joint in the center (at the neutral axis) of the system.

Consider the results given in Figure 6.31. These results represent the strains in the composite connection system. The results obtained for this system differ extensively from those observed in the previous connection. As would be expected

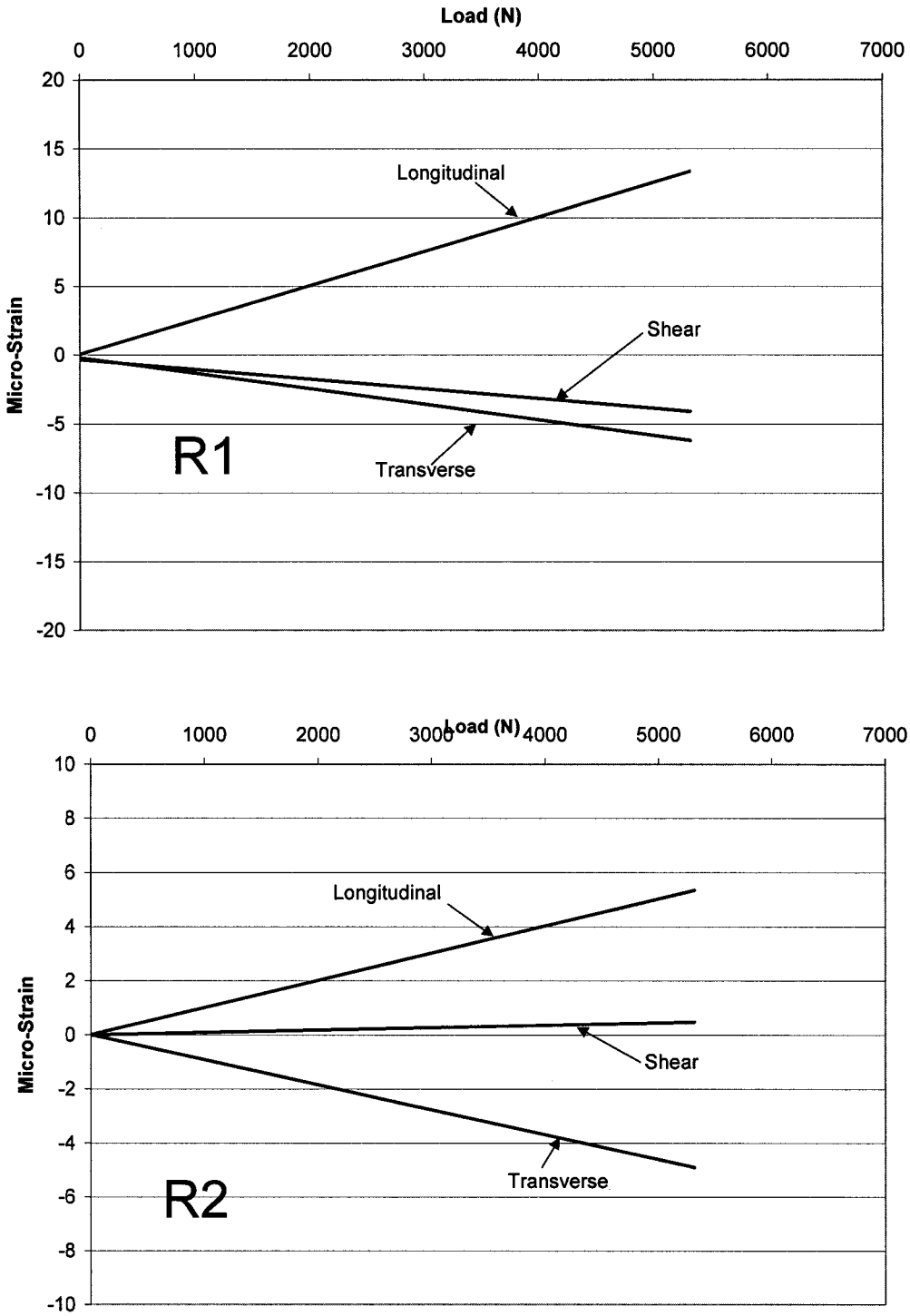

Figure 6.30: Strains Near the Connection for the Weld System Under Lateral Load

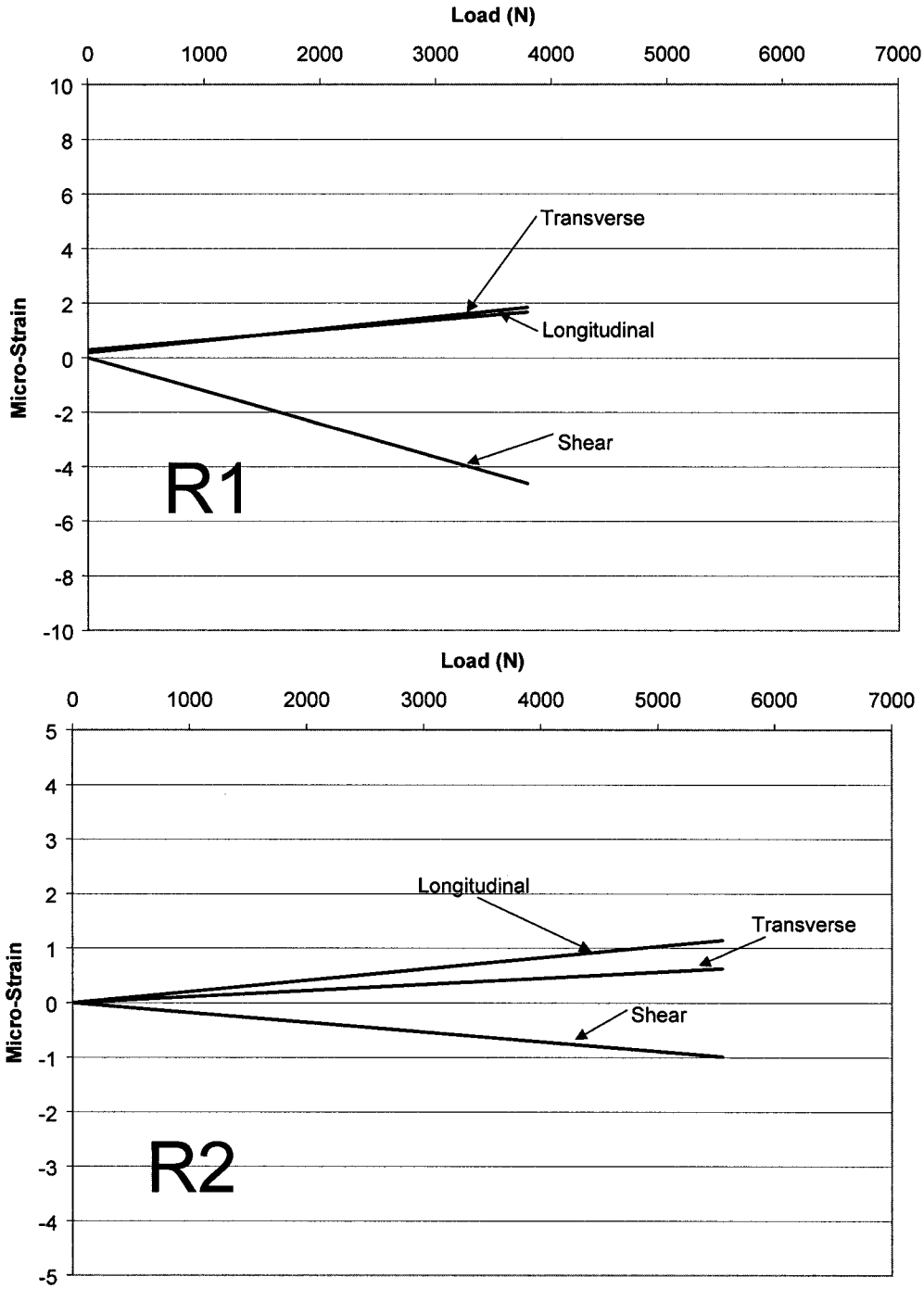

Figure 6.31: Strains Near the Connection for the Composite System Under Lateral Load

of a system that acts as a flexural member/diaphragm the longitudinal strains near the connection, at the rosette locations, are near zero, indicating the neutral axis location in the joint. The strains in the transverse direction appear to experience some decrease as the joint is past. Most significant, is the presence of positive shear strains of near equal values on both side of the joint. This suggested that indeed shear strain and thus shear stress does transfer across the joint. Moreover, the similarity between the R1 and R2 results also support the claim that the neutral axis lies in the joint.

Finally, consider the case of the composite-weld connection, the results for this system type are shown in Figure 6.32. As was pointed out earlier, this combined connection system tends to act in a manor that suggests a combination of the previous two cases. Consider first the longitudinal strains at R1 and R2. These strains exhibit a continued decrease in value as the compressive side of the member is approached. This suggests that the apparent location of the neutral axis is in the top member (as viewed in plan). The response in the transverse direction exhibits similar traits to that seen in the composite connection system. Therefore, these strains appear to diminish as the extreme fiber in tension is approached. Finally, the response of the system, in terms of shear strain suggest that, indeed, shear strains and thus shear stress are able to be transferred across the joint.

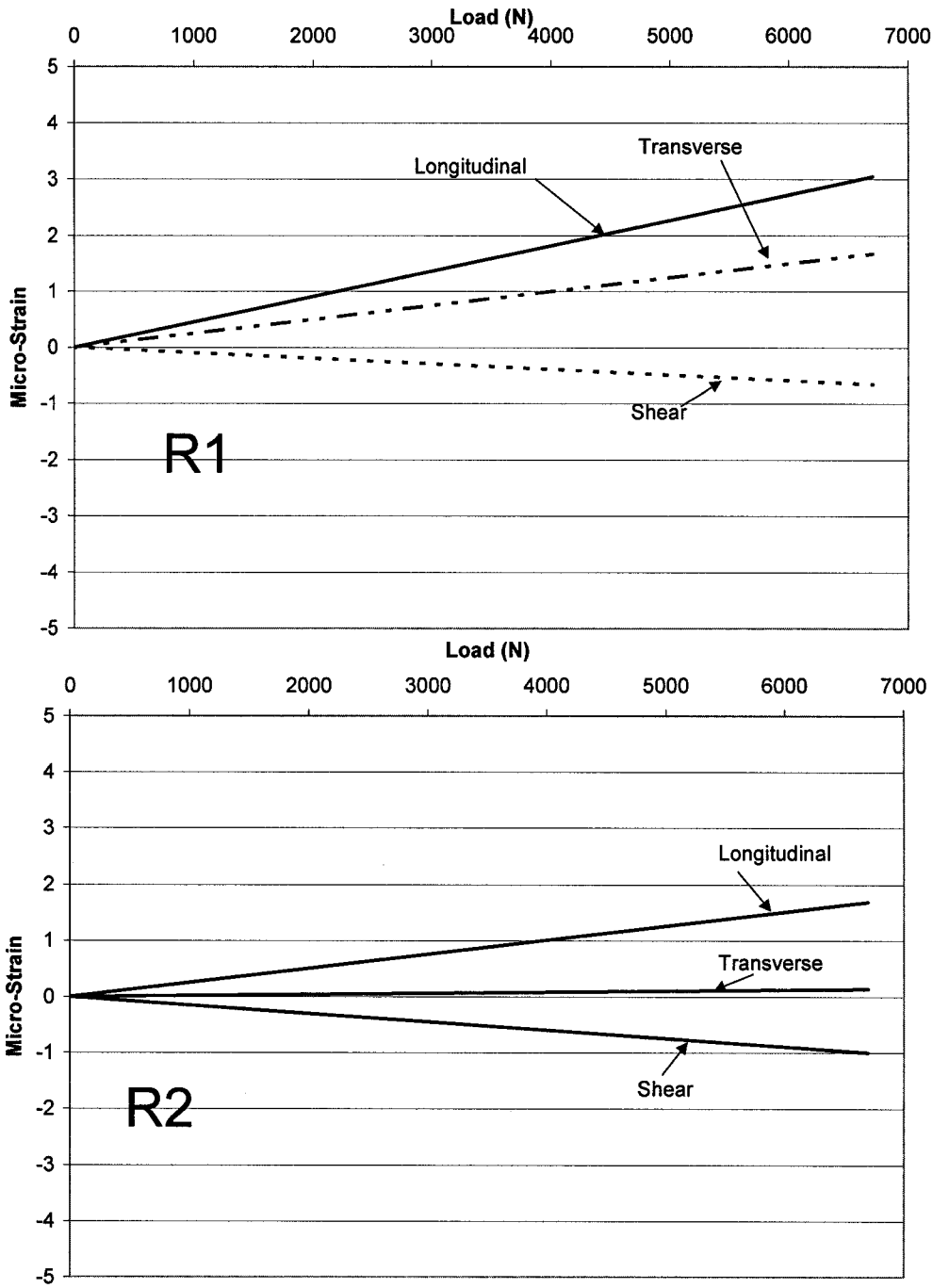

Figure 6.32: Strains Near the Connection for the Composite-Weld System Under Lateral Load

While the lateral loading test was preformed the values obtained may not necessarily be accurate. The strains measured, and presented in this section, are lower than the error tolerance of the strain indicators used. Therefore, from the above information, only qualitative results relating to the general behaviour of the system can be derived.

6.3 Summary of Failure Loads

The final results of all the systems tested are summarized in Table 6.1. Overall, the connections with the composite material performed the best, as additional ductility and load sharing was added into the system.

Table 6.1: Final Results of Experimental Testing

Model ID	Casting Set (1/2)	*f'c* MPa	Ultimate Load (kN)	Ratio to Single (w.r.t. set)	Failure Mode
Single	1	62	15.9		flexural
	2	70	18.4		flexural
Welded Connect.	2	70	33.7	1.83	flexural
	2	70	38.5	2.09	flexural
Composite Connect.	1	62	35.8	2.25	flexural
	1	62	36.4	2.29	flexural
Comp-Weld Connect.	2	70	39.3	2.14	flexural
	2	70	40.0	2.17	flexural

7. Cost Analysis

The following section will detail the cost of each of the proposed connections, with respect to current year (2004) pricing. These prices are based on approximations given by local industry and material suppliers. Moreover, all values are given in Canadian currency unless otherwise noted. An example of the cost for a given structure, with each connection type, will also be presented. Due to the cost of the epoxy injection system it was proposed that a concrete grout be used in place of the epoxy. While the efficiency of concrete grout was not investigated during this work it was used as a variable in this cost analysis for comparative reasons.

7.1 Cost per Unit Connection

In order to identify a unit cost for a given connection the average spacing used for the shear connector will be adopted (1542 mm (5 ft)), the reasoning behind this spacing is given in Chapter 4. Table 7.1 provides a price comparison for each of the cases examined during this work. Based on the required amount of concrete, which is a relatively small portion per 5 ft length, it was found that the cost did not change significantly with changes in the strength of the concrete mix used. For comparative reasons, Table 7.1 also provides a cost comparison ratio with respect to the current industry standard, for the various connection types examined.

The value for the welded connection, found in Table 7.1, of $25 per mechanical connection includes labour costs. The cost of the fillers is based on an assumed quantity of 940 ml. The cost of concrete is taken at $150.00 per cubic meter, and the cost of the

high strength epoxy is $167.55 per liter. The CFRP, with adhesive materials, was taken as $71.00 per square meter. This value is a discounted amount assuming all orders of this type would involve large quantities. The value given in the table for the CFRP assumes four layers of 0.61 m width each (commercial available roll size).

Table 7.1: Cost Comparison for Connection Types Examined

Connection	Cost per 1.5m (5 ft)	Cost as a factor of welding only
Carbon fiber & PowerFix	$422.50	16.9
Carbon Fiber & PowerFix & Weld	447.50	17.9
Carbon Fiber & Concrete	$300	12
Carbon Fiber & Concrete & Welding	$325	13
Carbon Fiber & Weld only	$290	11.6
Carbon Fiber only	$265	10.6
Weld (Existing)	$25	1

7.2 Costing of Structure

The pricing for a double tee member is based on the surface area of the element. This price is, generally, $107.54 per square meter ($10.00 per square foot); however, this price is a function of the size of the project and the building's use. that is, the pricing given above would be reduced for a parking structure as the cost per vehicle would greatly outweigh any other construction method, making precast a less than feasible choice.

7.3 Comparison of Construction Cost to Connection Cost

While the recommended connection is not limited to parking structures and, in fact, it is directed more towards structures that must be designed as post-disaster facilities, the following example will utilize a parking structure system for comparison of construction and connection costs. The parking structure that is used in the comparison employs the floor plan for one of the structures which collapsed in Northridge, refer

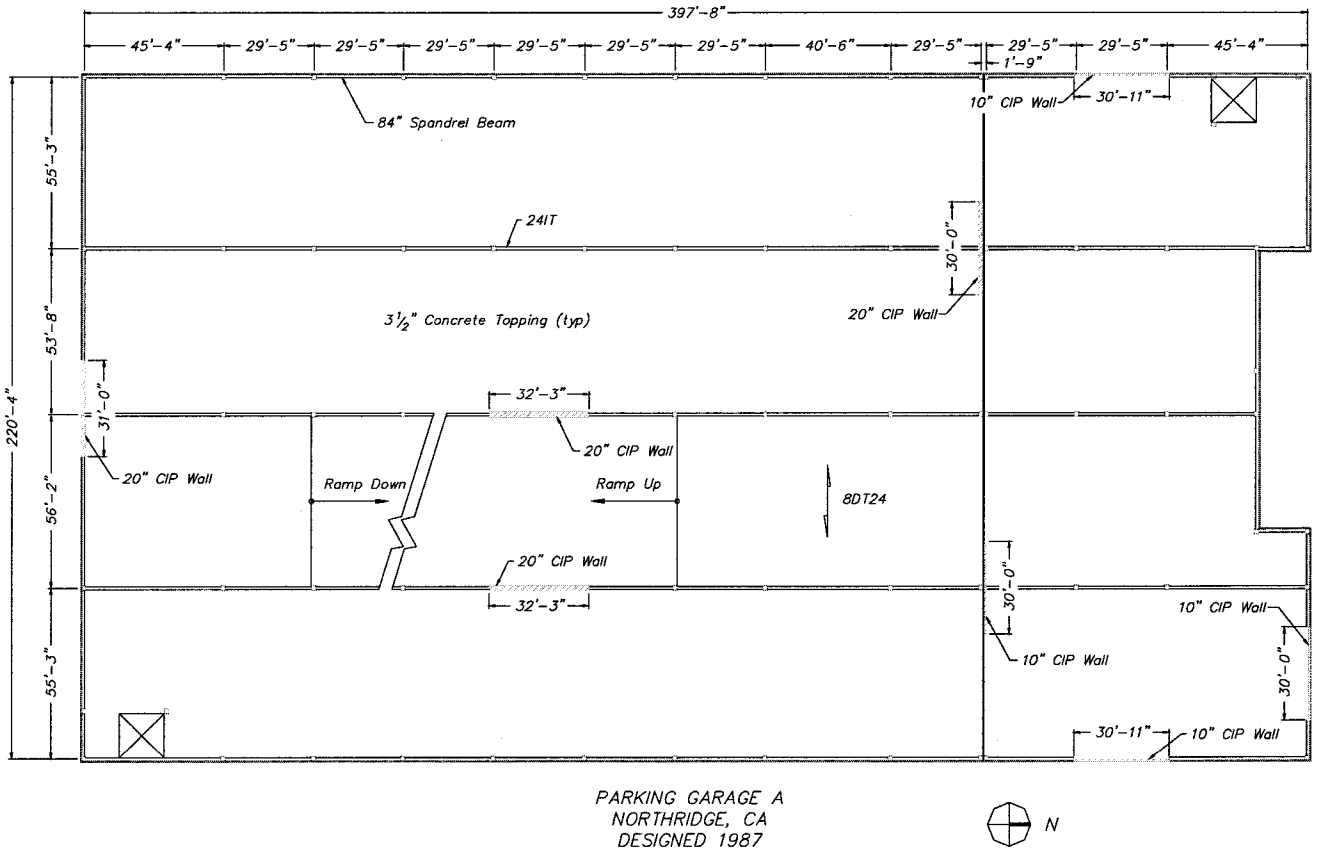

Figure 7.1: Plan of One Level of Parking Structure

to Figure 7.1. The costing will be started by conducting a cost anaylsis for one level (no-ground level, above grade) of the structure. To define the cost of construction, per parking space, for the structure, Table 7.2 will be used; the values give in this table are in US dollars. In order to present all comparisons in terms of Canadian currency an exchange rate of 1.327 (OANDA.COM 2004) will be used. The values given in Table 7.2 assume that the structure is to be built in California, USA.

Table 7.2: Typical Cost per Parking Space for Parking Structures (IPD (2004))

	Small Site 30,000 s.f.		Medium Site 60,000 s.f.		Large Site 90,000 s.f.	
	Customer Parking 350 s.f./car	Employee Parking 320 s.f./car	Customer Parking 335 s.f./car	Employee Parking 300 s.f./car	Customer Parking 325 s.f./car	Employee Parking 290 s.f./car
Surface Parking	$2,048	$1,872	$1,960	$1,755	$1,901	$1,697
Ground + 1 level	$8,088	$7,394	$7,055	$6,318	$6,559	$5,853
Ground + 2 levels	$9,009	$8,237	$7,774	$6,962	$7,225	$6,447
Ground + 3 levels	$9,367	$8,564	$8,035	$7,196	$7,462	$6,659
Ground + 4 levels	$9,746	$8,911	$8,349	$7,476	$7,757	$6,922
Ground + 5 levels	$9,999	$9,142	$8,558	$7,664	$7,954	$7,097
Ground + 6 levels	$10,179	$9,307	$8,707	$7,797	$8,094	$7,222
Ground + 7 levels	$10,314	$9,430	$8,819	$7,898	$8,199	$7,316
Ground + 8 levels	$10,420	$9,526	$8,906	$7,976	$8,281	$7,389

For the structure in question the double tee members had an average width of 2440 mm (8 ft) (e-mail correspondence, July 2004). As noted in Figure 7.1 the double

tee members were orientated such that their longitudinal axis was in an east-west direction. Therefore, using the 2440 mm span, the number of members needed for the outside rows (west and east end of the structure) would be:

$$N_{DT} = \frac{397.67}{8} \approx 50 \qquad [7.1]$$

For the middle two rows, based on scaling of the plan, 48 members would be require for each. Based on the span lengths provided the total length of the double tee to double tee joint would be:

$$l_{tj} = ((50\text{-}1)x55.33)+((48\text{-}1)x53.67)+((48\text{-}1)x56.17)+((50\text{-}1)x55.25)$$

$$=(10{,}581 \text{ ft})/(3.28 \text{ ft/m}) = 3226 \text{ m} \qquad [7.2]$$

This length will be used with the values given in Table 7.1 to determine the corresponding connection cost.

Assuming the structure is for customer parking, and the structure is three stories (average value for the precast systems that failed at Northridge, according to Iverson and Hawkins (1994)) on a large site the number of parking spaces can be determined. The total floor area divided by the area per car (given in Table 7.2) indicates that the total number of parking spaces would be:

$$N_S = \frac{7{,}896m^2\left(84{,}946ft^2\right)}{30.2m^2\left(325ft^2\right)} \approx 260 \text{ spaces} \qquad [7.3]$$

Using the cost, given in Table 7.2, of $1,901. 00 (US currency) and the number of spaces calculated above, the cost of constructing one of the levels (including materials, installation, and welded connections) would be approximately:

$$Cost = 260 \times (1{,}901 \times 1.327) \approx \$655{,}900 \text{ (Canadian currency)}. \quad [7.4]$$

As the above calculations assume three stories the cost of the structure, assuming all levels are the same in terms of plan shape, would be $1,967,700.00, which is the base cost of the structure.

Using the average spacing of mechanical connectors, defined earlier in this dissertation, the number of connections per level would be:

$$\text{Connections per level} = \frac{Total\ \ Length\ \ of.\ \ Joints}{Average\ \ Spacing} = \frac{3226m}{1.524m} = 2116. \quad [7.5]$$

Note that only two of the three levels would require connections, as the first level is a ground level. Thus, the total number of welded connections for the structure would be 4,232. Using the cost of $25.00 per connection, given in Table 7.1, the connections account for $105,800.00 (5 %) of the total cost. Therefore, in the absence of any connection the structure, in today's dollars, would cost $1,861,900.00

The following will use the values provided in Table 7.1 to define the cost of the current structure using alternative connection methods. Table 7.3 provides the cost associated with all connection methods for this particular structure, provide cost per level, cost of the entire structure, and the new total cost as a ratio of the existing construction cost (welded connection only).

Table 7.3: Cost Comparison for Various Connections for Sample Structure

Connection	(1) ♣	(2) ♣	(3) ♣	(4) ratio
Carbon fiber & PowerFix	894	1,788	3,650	1.86
Carbon Fiber & PowerFix & Weld	945	1,894	3,756	1.91
Carbon Fiber & Concrete	635	1,270	3,132	1.59
Carbon Fiber & Concrete & Welding	688	1,375	3,237	1.65
Carbon Fiber & Weld only	614	1,227	3,089	1.57
Carbon Fiber only	561	1,121	2,983	1.52
Weld only	53	106	1,968	1.00

♣ defines a column associated with values in terms of thousand dollar units
(1) cost of connection for one level
(2) cost of connection for entire structure
(3) total cost of structure with given connection
(4) =((3)/ $1,967,600.00)

7.4 Economic Considerations

From a review of Tables 7.1 and 7.3 it is noted that the proposed connections can drastically increase a structure's cost. In terms of only the construction cost these connections fail to provide any economic benefit; however, if other factors are considered a higher initial capital cost maybe outweighed. When considering the total cost of a structure other factors should be considered. These factors include the structure's importance and a risk assessment of the potential losses associated with failure. Both these areas can be expanded to encompass many factors; for example, the structure's importance in terms of its need as a post-disaster structure. While the above example of a parking structure does not qualify under this designation, other institutions such as hospitals, evacuation routes, and schools do fall under this categorization. In each of these cases a failure would have disastrous effects in both the long and short term. As relates to potential losses, a parking structure has a minimal value as the occupancy of such structures in generally low, therefore properties losses will govern. If, however, a

collapse was to occur in a mall or school, the human losses may greatly outweigh the additional construction cost.

Another factor that must be considered when selecting the connection method is the potential risk to the structure. Consideration of the regional conditions, in terms of required design loads, should be given. Therefore, an analysis should be conducted into the potential for a system experiencing overloading, due to gravity or lateral loading, during its service life.

8. *Conclusions, and Recommendations for Design and Future Work*

This chapter contains the final conclusions derived from this work. A design philosophy and a set of recommendations for future work are also presented.

8.1 Conclusions

From the present investigation, the following conclusions can be drawn with respect to the objectives outlined in Chapter 1. It should be noted that these conclusions relate only to the short-term as long-term environmental impacts on the connection have not been studied. For a schematic of the proposed connection refer to Figure 1.4.

1. The introduction of a grouting material into, and the placement of CFRP fabrics across the joint, ensures that the precast system performs in a monolithic fashion, thereby enhancing the system's ability to better distribute the load. By improving the load distribution (or load sharing) the system is able to carry a higher load.
2. The proposed joint (grout and CFRP) enhances the system's stiffness resulting in a better performance during seismic and/or lateral loading. Therefore, the introduction of these materials improves the system's performance in terms of diaphragm action.
3. The introduction of the proposed connection improves the system's deflection response. This system appears to provide a more gradual transition across the connection, in comparison to the existing welded system.
4. The CFRP fabric's resistance appears to provide significant enhancement of the system during a seismic event, when compared to the existing connection system.

5. The proposed connection eliminates stress concentrations along the joint. In the case of a retrofit of an existing connection, it reduces stress concentrations. This was observed most clearly from the FEA modelling.
6. The introduction of the proposed connection improves the stress distribution in the flanges of adjoining connected double tee members, subject to combined loading (refer to Figure 8.22 of Section 8.6)
7. The proposed connection provides the best performance with respect to earthquake response due to the enhancement of the diaphragm system. Moreover, the use of the high strength material (PowerFix 3) plays an active role in further enhancing this performance.
8. While cost is prohibitive in some cases, the proposed connection has great advantages in enhancing existing and new structures that are of critical importance during an unforeseen event (i.e. large magnitude earthquake).
9. The current connection method can result in high stress/strain concentrations in the regions surrounding the connections .

The current work provides a new design method for enhancing the load carrying capacity, and seismic response for precast double tee systems. Moreover, this work provides a new application for advanced composite materials.

8.2 Design Recommendations

The proposed connection must be designed for each specific case, and the type of composite material used. This section will outline the key considerations when using this connection type.

1. Due to the current cost of this connection, consideration of the structure's importance (ie hospital, main bridge span along an emergency or escape route etc.) should be undertaken prior to any design. Moreover, the designer should consider the likelihood of the system ever being subjected to a critical loading case (ie. earthquake or high wind potential).
2. The required cross-sectional area of fabric used should ensure that a sufficient amount of CFRP crosses the joint, such that the joint exhibits a higher tensile strength than the adjacent flanges. Therefore, the calculated resistance of the composites should be greater than the calculated resistance of the flange.
3. The adhesive used for the project should be selected such that the glass transition temperature is sufficiently high, such that the structure's performance will not be affected for the remainder of the service life of the connections.
4. The fabric should be placed such that it crosses the joint at a positive and negative 45^{o} angle. This ensures sufficient resistance irrespective of the direction of loading. Moreover, this fabric should be placed across the joint both on the top and bottom surfaces of the flange, see Figure 1.4.
5. During installation, some welded connections are suggested. This is to ensure that the system does not shift while the epoxy and grouting systems cure. In the case of a connection retrofit, this step is not required if the system is already welded.

6. For a retrofitted system, the concrete surfaces must be cleaned of any and all debris. Any concrete toppings should be removed prior to installation. This will ensure the concrete materials do not experience premature delamination during a critical situation.
7. Once the top surface is cured (based on the curing time provide by the manufacturer), exposed composite material should be covered with a concrete material or asphalt to prevent damage of the strengthening materials.

8.3 Recommendations for Future Work

As noted earlier, the present work is an initial investigation into the short-term performance of a new application for advanced composites. This work was focused at providing a new, or repair methods for systems in need of strengthening. The following are a few recommendations for future work in this area.

The writer recommends a closer examination of the use of concrete grouts with this connection type. Such work should be conducted experimentally and numerically.

It is recommended that experimental testing be conducted on the flange to flange connection for further verification of the FEA models; refer to the work of Pincheira et al. (1998). This experimental work should focus on the connection's resistance to tensile forces, shearing forces, and combinations thereof. Moreover, the system's response to cyclic loading should also be investigated.

As the current work is an initial work, and focuses on the connection of two members (as is the case in some bridge spans); the writer feels that further investigations should be conducted to consider the effectiveness of this joint in larger systems consisting of "n" double tee members. It is believed that such a situation should reveal that the proposed connection would greatly enhance the system's diaphragm action in all directions of loading.

As the introduction of the grout appears to have played a significant role in improving the system's load distribution/sharing abilities, further investigation into its role should be undertaken.

As mentioned earlier, it has been suggested that the PowerFix epoxy system be replaced with a concrete grout. While a connection consisting of a concrete grouting compound, rather than the proposed PowerFix 3 (or equivalent) may tended to perform the same, the writer feels that this more than likely would not be the case. When cast, precast double tee members tend to have very smooth finishes along the flange edge; this is generally due to the method used to form the member. Therefore, some concern arises over the grouting material's ability to adhere to the smooth finish of the precast element. This particular concern is not observed when using PowerFix 3 due to its bonding properties. Thus, some work should be conducted, experimentally, to determine the performance of the concrete grout, with respect to its ability to bond to a smooth concrete product.

References

1. Abdelrahman, A., 2001: *Strengthening of RC flat slab using CFRP strips*. Port Said Engineering Research Journal, Vol. 5, No. 1., March, Egypt

2. ACI, 318-89 – American Concrete Institute: *Building Code Requirements for Structural Concrete.*, Farmington Hills, MI

3. ACI, 318-99 – American Concrete Institute: *Building Code Requirements for Structural Concrete.*, Farmington Hills, MI

4. Adamo & Associates Structural Engineers 2003: Available at: URL:http://www.adamoassociates.com, accessed Jan. 2004

5. ADINA 2004 – Automatic Dynamic Incremental Non-Linear Analysis, ADINA R & D Inc., Watertown, MA., USA, Copyright 1994-2002

6. Antonopoulos, C.P., Triantafillou, T.C., and Papanicolaou, C.G. 2001: *Experimental investigation of FRP strengthened RC beam-column joints*, FRPRCS-5, University of Cambridge, Thomas Telford

7. Arockiasamy, M., Badve, A.P., Rao, B.V., and Reddy, D.V., 1991: *Fatique strength of joints in a precast prestressed concrete double tee bridge*. PCI Journal, Vol. 36, No. 1., Jan-Feb.

8. Aswad, A., and Burnley, G., 1991: *Point load tests of double tee flanges*. PCI Journal, Vol. 36, No. 4., July-Aug.

9. Aswad, A., Burnley, G., Cleland, N., Orndorff, D., and Wynings, C., 2004: *Load testing of precast concrete double tees without web reinforcement*. PCI Journal, Vol. 49, No. 2., March-April

10. Bakht, B., and Mufti, A., 2001: *Load Distribution in shear-connected concrete plank bridges*, CSCE, Conference of the Canadian Society of Civil Engineering, Victoria, British Columbia

11. Bakht, B., Mufti, A., and Sargent, D., 2001: *Assessment of stresses in welds of shear-connected concrete plank bridges*. CSCE, Conference of the Canadian Society of Civil Engineering, Victoria, British Columbia

12. Black Mint Software: *Concise Beam*, 2004: Available at URL://http://www.blackmint.com, accessed May 2003.

13. Campbell, T.I., 2000: *Hybrid FRP/stainless steel reinforcements for pretensioned concrete beams*. Advanced Composite Materials in Bridges and Structures, CSCE, Ottawa, Ontario

14. CAN/CSA A23.3-94, 1994: *Design of Concrete Structures*, Canadian Standards Association, Toronto, Ontario, Canada

15. Chopra, A., 1995: *Dynamics of Structures Theory and Applications to Earthquake Engineering*. Prentice Hall, New Jersey

16. CPCI, 2004 - Canadian Precast Prestressed Concrete Institute: Available at: http://www.cpci.ca, accessed Jan. 2004.

17. Csagoly, P.F., Bollman, H.T., and Nickas, W.N., 1986: *Cracking shear capacity of prestressed concrete beams*. 3rd Annual International Bridge Conference, Pittsburgh, PA, 1986

18. Elliott, K., and Davies, G., 2001: *Analysis of floor joints between precast concrete hollow core units in a floor diaphragm*. Available at: URL: http://www.civeng.nottingham.ac.uk, access Nov. 2003.

19. Fleischman, R., and Farrow, K., 2003(a):*Effect of dimension and detail on the capacity of precast concrete parking structure diaphragms*. PCI Journal, Vol. 48, No. 5., Sept-Oct.

20. Fleischman, R., and Farrow, K., 2003(b):*Seismic design recommendations for precast concrete diaphragms in long floor span construction*. PCI Journal, Vol. 48, No. 6., Nov.-Dec.

21. Fleischman, R., Sause, R., Pessiki, S., and Rhodes, A., 1998: *Seismic behaviour of precast parking structure diaphragms*. PCI Journal, Vol. 43, No. 1., Jan-Feb

22. Ghosh, S. K., 1987: *Shear reinforcement requirements for precast prestressed double-tee members*. ACI Structural Journal, Vol. 84, No. 4., July-Aug

23. Ghosh, S. K., 2000: *Seismic design provisions for precst concrete structures,* Impact of the seismic design provisions of the international building code, S.K. Ghosh Associates Inc., Chicago, USA

24. Grace, N.F. 2000: *Transfer length of CFRP/CFCC strands for double-T girders. PCI Journal.*, Vol. 45, No. 5

25. Grace. N.F., and Abdel-Sayed, G., 1996: *Double tee and CFRP/GFRP bridge system.* Concrete International, Vol. 18, No. 2., Feb.

26. Hamada, H., and Fukute, T., 1992: *Bending behaviour of unbonded prestressed concrete beams prestressed with CFRP rods.* Proceedings of the International Symposium of Fibre Reinforced Cement and Concrete, Sheffield, England

27. Hofheins, C., Reaveley, L., and Pantelides, C., 2002: *Behaviour of welded plate connections in precast concrete panels under simulated seismic loads.* PCI Journal, Vol, 47. No. 4., July-Aug.

28. Holmes, T.A., and Burnley, G., 1997: *New mega tee passes load testing.* PCI Journal, Vol. 42, No. 2., Mar-Apr.

29. Hu, C., and Ye, G., 2001: *Prestressing test and static test on T-shaped concrete beam in the highway bridge.* Yanshilixue Uy Gongcheng Xuebao, Vol. 20, Oct.

30. IPD (2004) – International Parking Design: Available at: URL://http// /www.ipd-global.com/, accessed July 2004

31. Issa, M., Patton, T., Abdalla, H., Yousif, A., and Issa, M., 2003: *Performance of transverse joint grout materials in full-depth precast concrete bridge deck systems.* PCI Jounal, Vol. 48, No. 4, July-Aug.

32. Iverson, J., and Hawkins, N., 1994: *Performance of Precast/Prestressed Concrete Building Structures During Northridge Earthquake.* PCI Journal, Vol. 39, No. 2., March-April

33. Kanakudo, T., Furuta, T., and Fukuyama, H, 2001: *The effect of stiffness of externally bonded FRP in RC beams subjected to shear*, FRPRCS-5, University of Cambridge, Thomas Telford

34. MacGregor, J., and Bartlett, M., 2000: *Reinforced Concrete: mechanics and design*, Prentice Hall, Scarborough

35. Mohsen E., 1990: *Feasibility study of transversely prestressed double tee bridges.* PCI Journal, Vol. 35, No. 5, Sept-Oct.

36. NBCC, 2001: Federal Publications Inc., *National Building Code of Canada*, Toronto, Ontario

37. NCBC, 2004 - National Concrete Bridge Council: Available at: URL: http://*www.nationalconcretebridge.org/* , accessed Feb. 2004.

38. NGDC 2004 - National Geophysical Data Center: Available at: *URL:http://www.ngdc.noaa.gov*. accessed March 2004.

39. OANDA.COM 2004: *The currency site*, Available at: URL: http://www.oanda.com/convert/classic, accessed July 2004

40. Pantazopoulou, S.J., and French, C.W., 2001: *Slab participation in practical earthquake design of reinforced concrete frames*, ACI Structural Journal, Vol. 98, No. 4, July-Aug.

41. PCI Committee Report, 1998: *Standard Precast Connections, PCI Journal*, Vol. 43, No. 4, July-Aug.

42. PCI Design Manual, 1996: *Design Manual Precast and Prestressed Concrete.* CPCI, Canada

43. PEER Strong Motion Database, 2004, Available at: URL: http://peer.berkeley.edu, accessed April 2004.

44. Peterman, R.J., Ramirez, J.A., Julio A., and Olek, J., 2000: *Influence of flexure-shear cracking on strand development length in prestressed concrete members.* PCI Journal, Vol. 45, No. 5, Sept.

45. Pincheira, J., Oliva, M., and Kusumo-Rahardjo, F., 1998: *Tests on double tee flange connectors subjected to monotonic and cyclic loading.* PCI Journal, Vol. 43, No. 3., May-June

46. Prota, A., Nanni, A., Manfredi, G., Cosenza, E., 2001:*Seismic upgrade of beam-column joints with FRP reinforcement.* FRPRCS-5, University of Cambridge, Thomas Telford

47. PSI, 2004 - Prestressed Systems Inc.: Available at: URL://http://www.psi-hci.com, accessed May 2004.

48. Savage, J.M., Tadros, M.K., Arumgasamy, P., and Fischer, L.G., 1996: *Behavior and design of double tees with web openings.* PCI Journal, Vol. 41, No. 1, Jan-Feb.

49. Shahawy, M.A., Beitelman, T., Arockiasamy, M., and Sowrirajan, 1996: *Experimental investigation of structural repair and strengthening of damaged prestressed concrete slabs utilizing externally bonded carbon laminates.* Structural Composites in Infrastructures, Proceedings of the 1995 2nd International conference for Composites Engineering, New Orleans, LA, Elsevier Science Ltd., Oxford

50. Shehata, I.A.E.M., Cerqueira, E.C., Pinto, C.T.M., and Shehata, L.C.D., 2001: *Strengthening of R.C. beams in flexure and shear using CFRP laminate*, FRPRCS-5, University of Cambridge, Thomas Telford

51. Sika Canada, 2003: *Sika CarboDur composite strengthening system Engineering guidelines for design and application*, Toronto, Ontario, Canada

52. Soudki, K.A., 1997: *Transfer length of carbon fiber rods in precast pretensioned concrete beams.* PCI Journal, Vol. 42, No. 5, Sept.-Oct.

53. Strigel, R.M., Pincheira, J.A., and Oliva, M.G., 2000: *Reliability of 3/8 in. Stud-Welded Deformed Bar Anchors Subject to Tensile Loads*. PCI Journal, Vol. 45, No. 6., Nov.-Dec.

54. Tabsh, S.W., and Nowak, A.S., 1991: *Reliability of highway girder bridges*. ASCE, Journal of Structural Engineering, Vol. 117, No. 8, Aug.

55. Tai, J., Kulka, F., 1977: *An anatomy of diaphragms*. Workshop on ERCBC, University of California, Berkeley, July 11-15

56. Tan, K., 2000: *Punching shear strength of RC slabs bonded with FRP systems.* Advanced Composite Materials in Bridges and Structures, CSCE, Ottawa, Ontario

57. Teng, J.G., Chen, J.F., and Smith, S.T. 2001: *Debonding failures in FRP-strengthened RC beams: failure modes, existing research, and future challenges*.ASCE Composites in Construction: A Reality, Proceedings of the International Workshop, Capri, Italy, July 20-21

58. Venuti, W.J., 1970: *Diaphragm Shear Connectors Between Flanges of Prestressed Concrete T-Beams*. PCI Journal, Feb.

59. Vingenuity Inc, 2004: *Earthquake ground database*. Available at: URL: http:// http://www.eresonant.com/pages/motions, accessed April 2004.

60. Wood, S., Stanton, J., and Hawkins, N., 2000: *New seismic design provisions for diaphragms in precast concrete parking structures*. PCI Journal, Vol. 45, No. 1, Jan.

61. Wood, S., Stanton, J. and Hawkins, N., 1996: *Performance of precast parking garages in the Northridge earthquake: Lessons learned.* Structural Congress – Proceedings, Vol. 2, Building an International Community of Structural Engineers

62. Zheng, W. and Oliva, M.G., 2003 "Practical Method to Estimate Deformation of Precast Untopped Double-tee Diaphragms." Paper accepted by PCI Journal for publication

63. Zureick, A., Deaver, R., and Summers, B., 2003: *Repairs with high-performance materials make bridges stronger, last longer: Georgia researchers test carbon fiber composites*. National Research Council, TR News, No. 226, May/June

64. Zureick, A., and Kahn, L., 2001: *Rehabilitation of Reinforced Concrete Structures Using Fiber-Reinforced Polymer Composites*. ASM Handbook, Vol. 21, Materials Park, OH, USA

Appendix A

(from Concise Beam V4.01, Black Mint 2004)

Concise Beam (TM), Version 4.16, (c) 2003 Black Mint Software, Inc
Licensed to: 4082030522, Dr. M. Madugula, University of Windsor - FOR EDUCATIONAL USE ONLY
Project:
Problem:

SUMMARY REPORT

Design Code Used: CSA A23.3-94

CONCRETE MATERIAL PROPERTIES

		Precast Beam	
Concrete Density	Wt =	2400	kg/m^3
Compressive Strength	f'c =	65.0	MPa
Modulus of Elasticity	Ec =	35714	MPa
Strength at Transfer	f'ci =	42.3	MPa
Modulus of Elast. at Transfer	Eci =	30219	MPa

Cement Content = 410 kg/m3
Air Content = 5.00 %
Slump = 50 mm
Aggregate Mix = 0.40 (ratio fine to total aggregate)

Curing
Curing Method = Moist
Humidity = 70 %
Age at Erection = 40 days

BEAM LAYOUT

Segment/Length No	From mm	To mm	Offset Z mm	Offset Y mm	Section Identification Folder	Section	Topping Parameters t1 mm	b1 mm	t2 mm	b2 mm
1	0	4572	0	0	DoubleTee	research				

Total Beam Length = 4572 mm, Left Support @ 0 mm, Right Support @ 4572 mm

PRECAST SECTION PROPERTIES (NON-COMPOSITE) *

Seg. No.	A mm^2	I mm^4	yb mm	Sb mm^3	St mm^3	V/S mm	bw mm	h mm
1	26455	90.673E+6	144	631793	1.519E+6	15	51	203

* These properties do not include the transformed area of any reinforcing or prestressing steel.
See the Transformed Section Properties text report for properties that include the area of steel.

PRESTRESSING STEEL TENDONS

Prestressing Strand Details

ID	Qty	Material	Section	Offsets x mm	Offsets y mm	Debonded Length * Left mm	Debonded Length * Right mm	Tendon Area mm^2	Jacking Force Pj N	%fpu
1	2	fpu=1860 MPa	#5	0	50	0	0	40.2	52340	0.70
		Ep= 190000 MPa		4572	50					
2	2	fpu=1860 MPa	#5	0	100	0	0	40.2	52340	0.70
		Ep= 190000 MPa		4572	100					

notes: * A suffix 'D' on the debond length indicates that the strand is fully developed at that end.
Prestressing steel is low relaxation strand.
Calculated Losses: Initial = 3.4 %, Final = 14.2 %
Total Prestress Forces: Pj(jacking) = 104681 N,
Pi(initial) = 101150 N,
Pe(effective) = 89866 N @ x = 2286 mm

Prestressing Strand Transfer and Development Lengths (mm)

ID	Strand Diameter	Left End of Strand Debond	Left End of Strand Transfer	Left End of Strand Development	Right End of Strand Debond	Right End of Strand Transfer	Right End of Strand Development
1	5	0	265	790	0	265	790
2	5	0	265	790	0	265	790

notes: Transfer and development length calculation used: fpr = 1822.8 MPa,
fse = 1098.2 MPa at x = 2286 mm

BEAM AND TOPPING SELF-WEIGHT

Concise Beam (TM), Version 4.16, (c) 2003 Black Mint Software, Inc
Licensed to: 4082030522, Dr. M. Madugula, University of Windsor - FOR EDUCATIONAL USE ONLY
Project:
Problem:

Segment/Length No.	From mm	To mm	Linear Weight Beam N/mm	Topping N/mm
1	0	4572	0.62	

EXTERNALLY APPLIED LOADS

Load Case	Load Label	Load Type	Load Intensity (*) Left	Load Intensity (*) Right	Offset (mm) Left	Offset (mm) Right

* point loads = N, line loads = N/mm, point moment/torsion = Nmm, line torsion = Nmm/mm

Load Combinations
Factored Combination 1 = 1.25 D + 1.5 L
Factored Combination 2 = 1.25 D + 1.25 W
Factored Combination 3 = 1.25 D + 1.25 T
Factored Combination 4 = 1.25 D + 1.05 L + 1.05 W
Factored Combination 5 = 1.25 D + 1.05 L + 0.875 T
Factored Combination 6 = 1.25 D + 1.05 W + 0.875 T
Factored Combination 7 = 1.25 D + 0.9 L + 0.9 W + 0.75 T
(The use of T is not yet implemented)

SHEAR AND TORSION INPUT PARAMETERS

Seg. No.	Folder	Stirrup Grade MPa	Aoh mm^2	Ph mm
1	default	400	0	0

Aoh is the area enclosed by the torsion stirrups to the outside of the stirrups.
Ph is the perimeter of Aoh.

ANALYSIS RESULTS SUMMARY - TOTAL FACTORED EFFECTS

x (mm)	Shear (N) Max.	Shear (N) Min.	Moment (Nmm) Max.	Moment (Nmm) Min.	Torsion (Nmm) Max.	Torsion (Nmm) Min.
0	1779	0	0	0	0	0
457	1423	0	732062	0	0	0
914	1067	0	1.301E+6	0	0	0
1372	712	0	1.708E+6	0	0	0
1829	356	0	1.952E+6	0	0	0
2286	0	0	2.034E+6	0	0	0
2743	0	-356	1.952E+6	0	0	0
3200	0	-712	1.708E+6	0	0	0
3658	0	-1067	1.301E+6	0	0	0
4115	0	-1423	732062	0	0	0
4572	0	-1779	0	0	0	0

SUPPORT REACTIONS (N)

Load Case	Unfactored Support Reactions Left	Right
Beam Wgt	1423	1423
SDL BT	0	0
Topping Wgt	0	0
SDL AT	0	0
LL Sustain	0	0
Live Load	0	0
Roof Load	0	0
Fluid Wgt	0	0
Vert.Wind	0	0
Strain Load	0	0

Load Combo.	Left	Right

Project:
Problem:

Sust. Total	1423	1423
Total	1423	1423
Factor Max.	1779	1779

CONCRETE STRESS RESULTS
(+ve = compression, -ve = tension)

Location	x mm	Stress MPa	Limit MPa		Overstress Notice	
STRESSES AT TRANSFER						
Maximum Compression						
Top of Beam	2286	0.4	25.4		0 %	
Bottom of Beam	274	13.7	25.4		0 %	
						Longitudinal Tensile Rebar Needed (mm^2)
Maximum Tension						Required / Provided / Additional
Top of Beam	274	-0.5	-3.3		0 %	
Bottom of Beam	0	0.0	-3.3		0 %	
STRESSES IN SERVICE						
Maximum Compression						
Top of Beam	2286	0.4	39.0		0 %	
Bottom of Beam	274	12.0	39.0		0 %	
Top of Topping	0	0.0	0.0		0 %	
Maximum Tension						
Top of Beam	274	-0.4	-4.0	*	0 %	Not cracked
Bottom of Beam	0	0.0	-4.0	*	0 %	Not cracked
Top of Topping	0	0.0	0.0	*	0 %	
STRESSES IN SERVICE (SUSTAINED LOADS ONLY)						
Maximum Compression						
Top of Beam	2286	0.4	29.3		0 %	
Bottom of Beam	274	12.0	29.3		0 %	

* Halve this tensile limit for corrosive environments.

Minimum Transfer Strength, f'ci = 22.8 MPa
Modulus of Rupture, fr = -4.8 MPa

CRACK CONTROL

Beam Not Cracked

DEFLECTION/CAMBER ESTIMATE RESULTS (mm)
(-ve = deflection, +ve = camber)

Maximum Camber Under All Final Loads at x = 2286 mm

Load Case	Instantaneous Deflections	@ Transfer	Mult.	@ Erection	@ Completion	Mult.	@ Final	DL Growth since Completion + LL
Prestressing	6.4	6.4	1.80	11.5	11.5	2.45	15.7	4.2
Beam Weight	-1.3	-1.3	1.85	-2.3	-2.3	2.70	-3.4	-1.1
SDL (BT)	0.0	0.0	1.00	0.0	0.0	2.70	0.0	0.0
Topping Wght	0.0	0.0	1.00	0.0	0.0	2.30	0.0	0.0
SDL (AT)	0.0	0.0	1.00	0.0	0.0	3.00	0.0	0.0
Live Load	0.0						0.0	0.0
Net Deflect.		5.1		9.2			12.2	3.1
Net Deflect. (sustained loads)							12.2	

Note: Live Load includes all live load cases, including sustained live load.

Span/deflection : DL Growth + LL = L / 1484 < L/480 OK for non-structural attachments
< L/240 OK otherwise

FLEXURAL DESIGN CHECK

Project:
Problem:

Design Code Used: CSA A23.3-94
Beta Used: 0.81
Alpha Used: 0.75

x mm	Factored Moment Mf Nmm	Moment Resistance Mr Nmm	Minimum Resistance 1.2Mcr Nmm	Depth in Compression c mm	Conformance Notes
0	0	0	3.765E+6	-	
457	732062	13.022E+6	13.556E+6	-	
914	1.301E+6	16.370E+6	13.605E+6	9	
1372	1.708E+6	16.370E+6	13.639E+6	9	
1829	1.952E+6	16.370E+6	13.660E+6	9	
2286	2.034E+6	16.370E+6	13.667E+6	9	
2743	1.952E+6	16.370E+6	13.660E+6	9	
3200	1.708E+6	16.370E+6	13.639E+6	9	
3658	1.301E+6	16.370E+6	13.605E+6	9	
4115	732062	13.022E+6	13.556E+6	-	
4572	0	0	3.765E+6	-	
Points of Maximum and Minimum Factored Moment					
2286	2.034E+6	16.370E+6	13.667E+6	9	
0	0	0	-8.865E+6	-	

SHEAR AND TORSION DESIGN CHECK

Design Code Used: CSA A23.3-94

x mm	Applied Shear Vf N	Shear Depth d mm	Prestress Component Vp N	Concrete Resistance Vc N	Stirrup Resistance Vs N	Applied Torsion Tf Nmm	Threshold Torsion Tcr/4 Nmm	Conformance Notes
0	1779	163	0	17409	0	0	0	
457	1423	163	0	20854	0	0	0	
914	1067	163	0	10337	0	0	0	
1372	712	163	0	7399	0	0	0	
1829	356	163	0	7399	0	0	0	
2286	0	163	0	7399	0	0	0	
2743	-356	163	0	-7399	0	0	0	
3200	-712	163	0	-7399	0	0	0	
3658	-1067	163	0	-10337	0	0	0	
4115	-1423	163	0	-20854	0	0	0	
4572	-1779	163	0	-17409	0	0	0	

x mm	Required Shear Stirrups Av/s mm^2/mm	Torsion 2At/s mm^2/mm	Maximum Spacing s mm	Additional Long. Steel Al * mm^2	Allow. Reduction in Al in Compress. Zone mm^2
0	0.000	0.000	0	0	0
457	0.000	0.000	0	0	0
914	0.000	0.000	0	0	0
1372	0.000	0.000	0	0	0
1829	0.000	0.000	0	0	0
2286	0.000	0.000	0	0	0
2743	0.000	0.000	0	0	0
3200	0.000	0.000	0	0	0
3658	0.000	0.000	0	0	0
4115	0.000	0.000	0	0	0
4572	0.000	0.000	0	0	0

* based on maximum stirrup spacing.

Appendix B

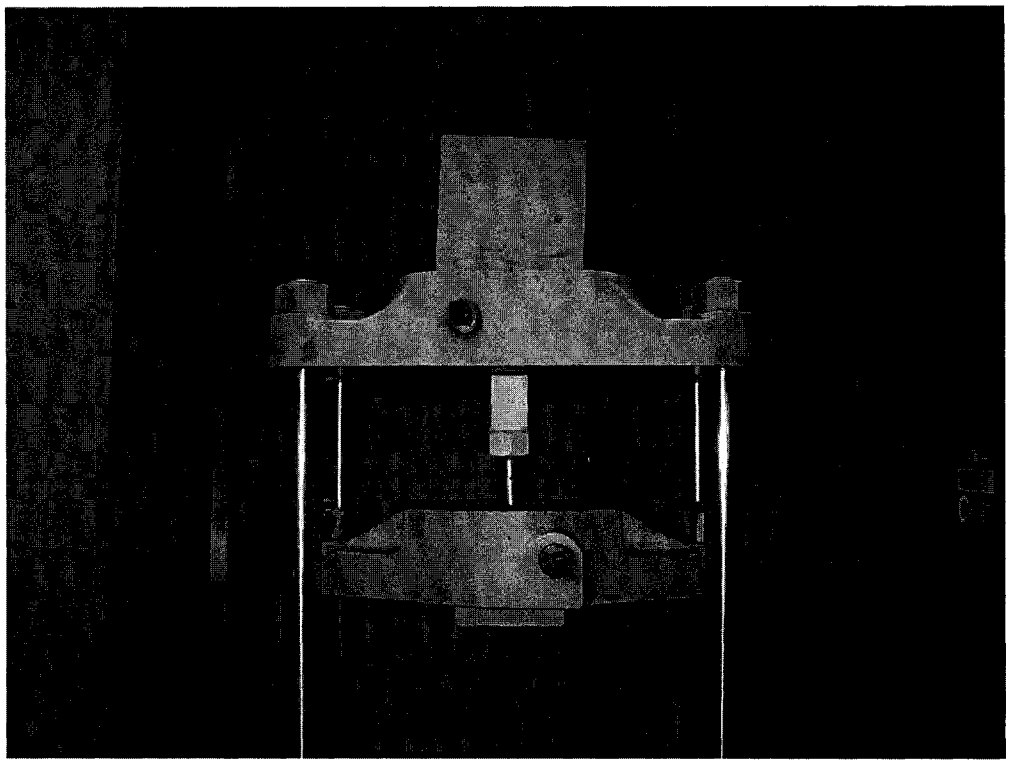

Figure B.1: Bearing Specimen in Testing Machine

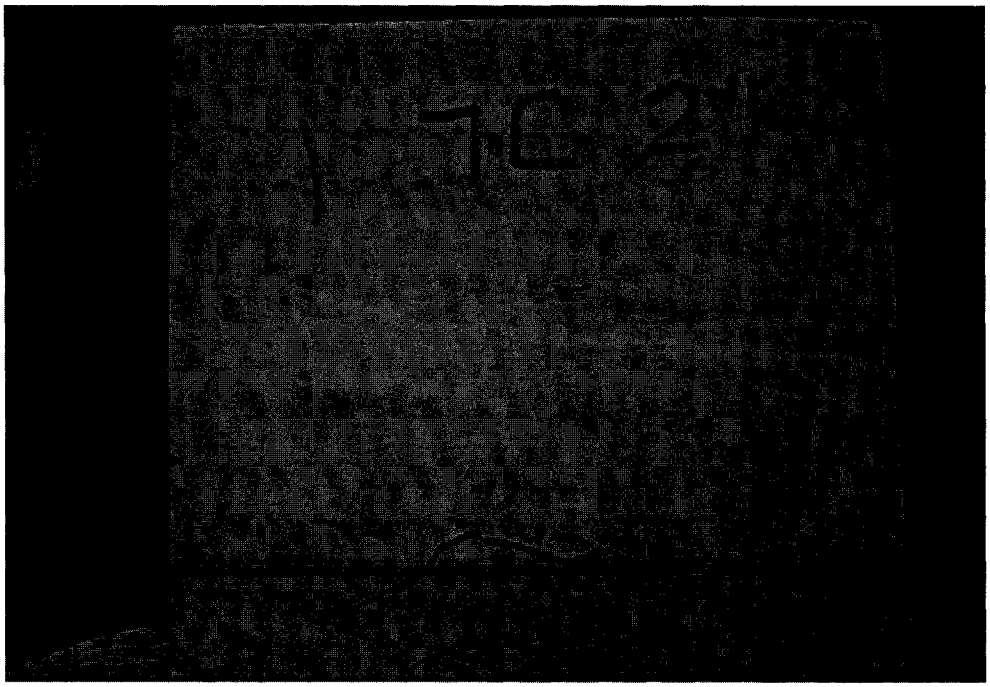

Figure B.2: Failure Observed in One of the Bearing Assembly Tests

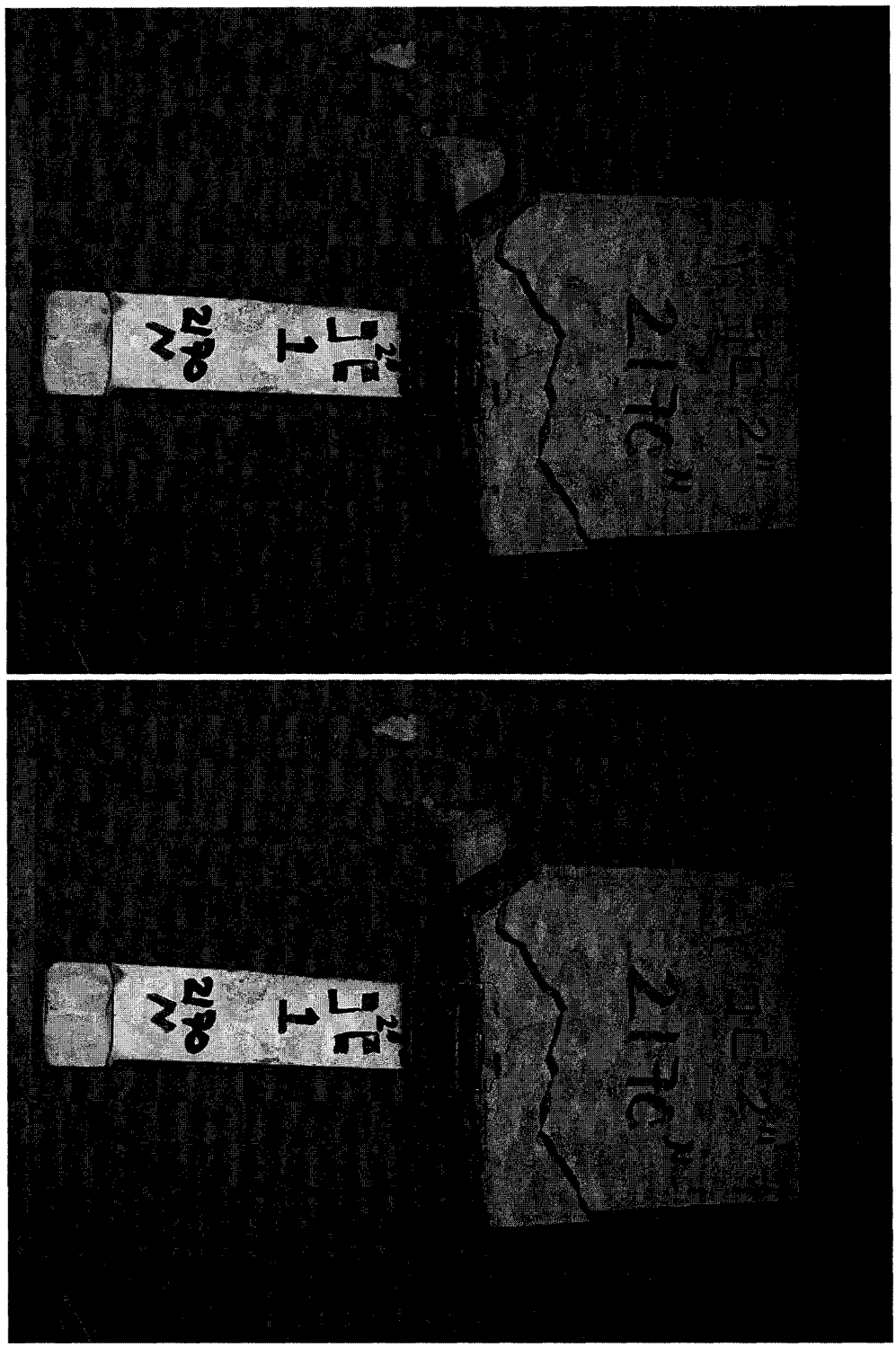

Figure B.3: Photographs of Failed Specimens

Appendix C

Table C.1 Calibration Factors for Load Cells

Load Cell	Calibration Factor	Corresponding Units
50,000 lb	27.61476	N
10,000 lb	5.540784	N

Table C.2 Support Load Cell Calibration Data

Designation	Calibration Factor (Provides output in N)
1	161.367
2	156.424
3	161.601
4	157.999
5	170.708
6	174.953
7	163.180
8	161.387

Table C.3: Calibration values for LVDTs

LVDTs Designation	Calibration Factor (CF) [(CF)(mV)=(mm)]
1	0.01211
2	0.01213
3	0.01215
4	0.01209

VITA AUCTORIS

WILLIAM TAPE, M.A.Sc., P.Eng.

EDUCATION

2001-Present	University of Windsor, Windsor, ON Preparation of Dissertation Civil Engineering, Structures/Soil Mechanics
1999-2001	University of Windsor, Windsor, ON Master of Applied Science Civil Engineering, Water Resources
1995-1999	University of Windsor, Windsor, ON Honours Bachelors of Applied Science Civil Engineering

AWARDS

- Natural Sciences and Engineering Research Council Graduate Scholarship (2000-2004)
- University of Windsor Tuition Scholarship (1999-Present)
- Ontario Graduate Scholarship for Science and Technology